Universidad de Concepción
Dirección de Postgrado
Facultad de Ciencias Naturales y Oceanográfica
Programa de Magíster en Ciencias con Mención en Pesquerías

EVALUACIÓN DEL DESEMPEÑO DEL MODELO DE ESTIMACIÓN PARA EL MANEJO DE MERLUZA DE COLA (*Macruronus magellanicus*) CON CAMBIOS INTERDECADALES EN EL RECLUTAMIENTO

Tesis para optar al grado de Magíster en Ciencias con Mención en Pesquerías

SANDRA EDULIA CURIN OSORIO
CONCEPCIÓN-CHILE
2014

Profesor Guía: Luis Cubillos Santander
Depto. de Oceanografía
Facultad de Ciencias Naturales y Oceanográficas
Universidad de Concepción

UNIVERSIDAD DE CONCEPCIÓN

La presente tesis se realizó en el Departamento de Oceanografía de la Facultad de Ciencias Naturales y Oceanográficas de la Universidad de Concepción y ha sido aprobada por la siguiente Comisión Evaluadora.

Profesor Guía

Dr. Luis Antonio Cubillos Santander
Departamento de Oceanografía
Universidad de Concepción

Comisión Evaluadora

M.Sc. Juan Carlos Quiroz Espinosa
Instituto de Fomento Pesquero

M.ET. Cristian Canales Ramírez
Instituto de Fomento Pesquero

Director de Programa

Dr. Leonardo Castro Cifuentes
Departamento de Oceanografía
Universidad de Concepción

Dedicada a toda la gente especial de mi vida.
Nicolas Contreras, Mori, Claudio Castillo Jordan, Polillita (Paulina Contreras), Jaqueline Curin, Papa (Jorque Daveggio), Mamá (Nancy Farias), Tíos (Laura Carreño, Marcelo), Gabriel Montes, a la Segunda Familia (Luis Cubillos, Viviana Rivera, Andres Cubillos, Zicri y Trini), Cristian Parra, Colegas de EPOMAR y Aquilito (q.e.p.d).

RESUMEN

La variabilidad interdecadal en el reclutamiento de los stocks de peces afecta la productividad de las pesquerías, y por ende a la estructura, dimensión y dinámica de la pesca. Aunque las causas de la variabilidad del reclutamiento están siendo estudiadas en todo el mundo, es importante analizar sus consecuencias en el manejo pesquero, sobre todo cuando el reclutamiento puede variar a escala decadal. En Chile, la merluza de cola (*Macruronus magellanicus*) es un recurso importante. El reclutamiento promedio de la merluza de cola cambió a un nivel bajo desde el 2000, lo que puede ser reflejo de fluctuaciones decadales. Actualmente, el estado de la merluza de cola es de sobrexplotación por lo que es necesario un plan de recuperación de la biomasa del stock desovante.

En esta tesis, un modelo operativo estructurado por edad y multi-flota permitió evaluar el desempeño del modelo de evaluación y la recuperación potencial del stock bajo variabilidad decadal del reclutamiento. Los escenario de reclutamiento para evaluar recuperación potencial fueron: a) nivel de reclutamiento bajo, modulado por la relación stock-recluta (SR); b) nivel de reclutamiento alto, modulado por un cambio de régimen en la relación SR; y c) variabilidad decadal del reclutamiento modulado por con cambios cíclicos con amplitud y fase constante. Para todos los casos, la variabilidad interanual del reclutamiento consideró errores distribuidos log-normal. La hipótesis de trabajo considera que el desempeño del modelo de evaluación de stock y la estrategia de explotación objetivo son robustos a la variabilidad interdecadal del reclutamiento de merluza de cola. Los resultados mostraron que el modelo de evaluación sobreestimó el reclutamiento durante la fase de reclutamientos bajos y subestimó el reclutamiento cuando cambió a niveles altos, ya sea cuando el reclutamiento fue cíclico o escalonado. En términos de precisión, el mejor desempeño del modelo de evaluación ocurrió cuando el reclutamiento fue cíclico y con errores de proceso y de observación. El MARE fue de 5,7% para la biomasa desovante, 6,15% para la biomasa total y de 0,25% para el reclutamiento. La peor precisión del modelo de evaluación ocurrió cuando hubo un cambio de régimen escalonado en el reclutamiento, con errores de proceso y de observación, y mediante la aplicación de la tasa de explotación objetivo. El MARE fue de 13,9% para el reclutamiento, 14,24% para la biomasa de reproductores y 15,96% para la biomasa total. Sin embargo, la serie de tiempo del error

relativo medio mostró sesgos importante en la estimación del reclutamiento, que fueron canalizados a la biomasa del stock reproductor y biomasa total durante la transición en que el reclutamiento cambia de un nivel bajo a otro alto.

Para el caso del análisis de la recuperación potencial, cuando la gestión pasa por alto el cambio de reclutamiento y la población se mantiene en el nivel de reclutamiento bajo, el stock no fue capaz de recuperarse bajo la tasa de explotación objetivo. Sin embargo, cuando se simuló un cambio en el reclutamiento de un nivel bajo a otro alto dentro de 10 años, el stock mostró una probabilidad de recuperación mayor a 50% después de 2035. Debido a que la recuperación depende de un cambio en el reclutamiento, la recuperación es incierto y se sugiere ajustar la tasa de explotación objetivo durante el régimen actual de reclutamientos bajos de la merluza de cola. Además, es recomendable incorporar un índice de reclutamiento para el modelo de evaluación con el objetivo de rastrear con menos sesgo los cambios en el reclutamiento. En cuanto a la recuperación, es aconsejable diseñar un plan de recuperación de efectivo para el stock de la merluza de cola.

Palabras claves: Desempeño, reclutamiento, cambio de régimen, depleción, recuperación

ABSTRACT

The interdecadal variability in recruitment of fish stocks affects the fisheries productivity, and hence the structure, size and dynamics of fisheries. Although the causes of recruitment variability are being studied worldwide, it is important to analyze their consequences for fisheries management, especially when recruitment can vary on the decadal scale. In Chile, the Patagonian grenadier (*Macruronus magellanicus*) is an important fish resource. The recruitment of the Patagonian grenadier shifted to a low level since 2000, which would be associated to decadal fluctuations. At present, the status of the Patagonian grenadier is of overexploitation and a recovery plan of the spawning stock biomass required.

In this thesis, an age-structured multi-fleet operative model permitted to evaluate the performance of an age-structured stock assessment model and the potential recovery of the Patagonian grenadier stock under decadal recruitment variability. The recruitment scenarios to evaluate potential recovery were: a) low recruitment level, modulated by the stock-recruitment (SR) relationship; b) high recruitment level, modulated by a regime shift in the SR relationship; c) decadal variability in recruitment modulated by cyclical changes with constant amplitude and phase. In all the cases, the interannual variability of recruitment considered an error with log-normal distribution. The hypothesis considered that the performance of the SAM and the target exploitation rate are robust to decadal variability in the recruitment of the Patagonian grenadier. The results showed that the SAM overestimated the recruitment during the low recruitment level and underestimated the recruitment during the high recruitment regime, either when the recruitment was cyclical or step-like. In terms of precision, the better performance of the SAM was under cyclical recruitment with process and observation errors. The MARE was 5.7% for the spawning stock biomass, 6.15% for total biomass and 0.25% for recruitment. The worst precision of the SAM was under step-like recruitment shift with both process and observation errors, and by applying the target harvest rate. The MARE was 13.9% for recruitment, 14.24% for the spawning stock biomass and 15.96% for the total biomass. However, the time series of the mean relative error showed important biases in the estimation of recruitment, which

were channelized to the total biomass and spawning stock biomass when the recruitment changed from a low to a high level.

For the case of the potential recovery analysis, when the management ignores the recruitment shift and the stock remained in the low recruitment level, the stock was not able to recover under the target exploitation rate. However, when a recruitment shift from low to high level occurred within 10 years, the stock showed a probability of greater than 50% after 2035. Because the recovery depends of a shift in recruitment, the recovery is uncertain and it is suggested to adjust the target exploitation rate during the current low recruitment regime of the Patagonian grenadier. In addition, it is recommendable to incorporate a recruitment index to the stock assessment model with the aim of tracking with less bias the changes in recruitment. In terms of potential recovery, it is advisable to design an effective recovery plan for the Patagonian grenadier stock.

Keywork: Performance, recruitment, change, regime change, depletion, recovery

INDICE

RESUMEN 4

INTRODUCCIÓN 15

OBJETIVO GENERAL 19

OBJETIVO ESPECÍFICO 19

HIPÓTESIS 20

METODOLOGIA 21

Área de estudio y base de datos 21

Análisis de cambio de régimen 22

Modelo de estimación 23

CAPITULO I 26

Abstract 27

Introduction 27

Materials and methods 29

Results 36

Discussion 45

References 49

CAPITULO II 55

Abstract 56

Introduction 57

Materials and methods 58

Results 64

Reference 73

DISCUSION GENERAL 76

ANEXO 1 90

ANEXO 2 98

ANEXO 3 101

ANEXO 4 107

INDICE DE FIGURAS

Figura 1: Unidad de pesquería norte (UPCS: 32°10´23”- 43°44’17”S) y Unidad de pesquería sur (UPS: 43°44’17” – 57°00’00” S), indicando los límites de las sub-áreas norte exterior y sur exterior de la merluza de cola (Macruronus magellanicus) 21

Figura 2. Model of two recruitment regimes in the stock-recruitment relationship of the P. grenadier, which was used to simulate projections according to either the low or the high recruitment. The points are the data for the period 1980-2010. 34

Figura 3. Recruitment deviations applying the original SAM (solid line, without explicit recruitment regimes) as compared with a SAMR that incorporates two regimes in the stock-recruitment relationship (discontinuous line). 38

Figura 4. Total catch (Ytotal) and partial catch per fishing fleets (Yst: southern bottom trawl fishery, Yct: central bottom trawl fishery, Yps: purse-seine fishery). Total biomass (Bt) and spawning stock biomass (SSB). Recruitment and predicted recruitment obtained by the S-R model. Total exploitation rate (Utot), and partial exploitation rates per fishing fleets (Ust: southern bottom trawl fishery, Uct: central bottom trawl fishery, Ups: purse-seine fishery), for model with two regimes (SAMR). 40

Figura 5. Performance of the ration between the projected spawning stock biomass and the unexploited spawning stock biomass (S_t/S_0) by considering three exploitation rates, and according to: a) upper: the persistence of the low recruitment regime, b) middle: high recruitment shift after 10 ±5 years, and c) lower: cyclical recruitment. The black line indicates the threshold for recovery $S_t/S_0>0.4$, and the dashed line defines depletion when $S_t/S_0<0.2$. 41

Figura 6. The stochastic decision-making framework for assessing the recovery of the Patagonian grenadier stock. The top plot shows the cumulative empirical probability of St in 2010, and for the years indicated by applying μ=18%. The bottom plot shows the probability profile specifying the $Pr[S_t>S_{2010}]$ for different levels of decision confidence. 43

Figura 7: General approach used to evaluate the performance of the stock assessment model of Patagonian grenadier under interdecadal fluctuations in recruitment. 59

Figura 8. Model of two recruitment regimes in the stock-recruitment relationship of the Patagonian grenadier. The segmented line represents the replacement line of the S-R, and the points are the data of recruitment and spawning stock biomass for the period 1980-2010, according to results of the SAM of Payá and Canales (2012). 62

Figura 9: Example of a realization during a 40-year projection of recruitment, spawning stock biomass, and total biomass of Patagonian grenadier. The dots represent quantities coming from the operating model and the lines represent estimates obtained with the stock assessment model. Case E8 (cyclical recruitment, with both process and observation errors)..... 66

Figura 10. Frequency distribution of the relative error for recruitment (R), spawning stock biomass (SSB) and total biomass (BT) for scenario E8 (cyclical recruitment, with both process and observation errors). 66

Figura 11. Time series for the relative error of recruitment (R), spawning stock biomass (SSB) and total biomass (BT), escenario E8. The dark region represents confidence intervals of 75% and the lighter region confidence intervals of 90%, the black line represents the average relative error. 67

Figura 12. Example of a realization during a 40-year projection of recruitment, spawning stock biomass, and total biomass of Patagonian grenadier. The dots represent quantities coming from the operating model and the lines represent estimates obtained with the stock assessment model. Case E1 (step-like recruitment, with both process and observation errors)..... 68

Figura 13. Frequency distribution of the relative error for recruitment (R), spawning stock biomass (SSB) and total biomass (BT) for scenario E1 (with both process and observation errors).....68

Figura 14. Time series for the relative error of recruitment (R), spawning stock biomass (SSB) and total biomass (BT), escenario E1. The dark region represents confidence intervals of 75% and the lighter region confidence intervals of 90%, the black line represents the average relative error. 69

Figura 15: Probabilidad de encontrar un cambio régimen en el escenario (E1), en escala logarítmica. La grafica inferior representa la probabilidad posteriori de cambio de Barry and Hartigan's.....92

Figura 16: Probabilidad de encontrar un cambio régimen en el escenario (E2), en escala logarítmica. La grafica inferior representa la probabilidad posteriori de cambio de Barry and Hartigan's.....92

Figura 17: Probabilidad de encontrar un cambio régimen en el escenario (E3), en escala logarítmica. La grafica inferior representa la probabilidad posteriori de cambio de Barry and Hartigan's.....93

Figura 18: Probabilidad de encontrar un cambio régimen en el escenario (E4), en escala logarítmica. La grafica inferior representa la probabilidad posteriori de cambio de Barry and Hartigan's.....93

Figura 19: Probabilidad de encontrar un cambio régimen en el escenario (E5), en escala logarítmica. La grafica inferior representa la probabilidad posteriori de cambio de Barry and Hartigan's.....94

Figura 20: Probabilidad de encontrar un cambio régimen en el escenario (E6), en escala logarítmica. La grafica inferior representa la probabilidad posteriori de cambio de Barry and Hartigan's.....94

Figura 21: Probabilidad de encontrar un cambio régimen en el escenario (E7), en escala logarítmica. La grafica inferior representa la probabilidad posteriori de cambio de Barry and Hartigan's.....95

Figura 22: Probabilidad de encontrar un cambio régimen en el escenario (E8), en escala logarítmica. La grafica inferior representa la probabilidad posteriori de cambio de Barry and Hartigan's.....95

Figura 23: Probabilidad de encontrar un cambio régimen en el escenario (E9), en escala logarítmica. La grafica inferior representa la probabilidad posteriori de cambio de Barry and Hartigan's.....96

Figura 24: Probabilidad de encontrar un cambio régimen en el escenario (10), en escala logarítmica. La grafica inferior representa la probabilidad posteriori de cambio de Barry and Hartigan's.....96

Figura 25: Probabilidad de encontrar un cambio régimen en el escenario (11), en escala logarítmica. La grafica inferior representa la probabilidad posteriori de cambio de Barry and Hartigan's.....97

Figura 26: Probabilidad de encontrar un cambio régimen en el escenario (12), en escala logarítmica. La grafica inferior representa la probabilidad posteriori de cambio de Barry and Hartigan's.....97

Figura 27: Variabilidad de la biomasa desovante (1000's de ton) de merluza de cola aplicando diferentes valores de coeficiente de variación en la biomasa hidroacústica.....99

Figura 28: Variabilidad de la biomasa total (1000's ton) de merluza de cola aplicando diferentes valores de coeficiente de variación en la biomasa hidroacústica.....100

Figura 29: Variabilidad del reclutamientos (millones de ton) de merluza de cola aplicando diferentes valores de coeficiente de variación en la biomasa hidroacústica.....100

INDICE TABLAS

Tabla 1: Escenarios plausibles de valores de coeficiente de variación (Cv) para la captura por unidad de esfuerzo de la pesquería sur austral (CPUEst), relación stock-recluta (S_R) y biomasa hisdroacustica (B-H). 22

Tabla 2. Data used in the age-structured stock assessment model of P. grenadier, showing the period covered for each one. 30

Tabla 3: Sensitivity of the current stock assessment model according to changes in the coefficient of variations (CV) of the abundance indices and the recruitment deviations (CV_R) of Patagonian grenadier. The abundance indices are the catch per unit effort of the southern trawl fishery (CV_CPUEst) and the hydroacoustic biomass (CV_HB). The Escenario E2 is the base case representing the results obtained by Payá and Canales (2012). The asterisc represents the CV for two block of time periods of the CPUE, being equal to 0.4 for the period before 1990. 32

Tabla 4. Detection of regime shifts in the recruitment time series of P. grenadier according to different values for the coefficient of variation for the abundance indices (CPUE and Acoustic survey) and deviations of recruitment in the current stock assessment model (SAM). 37

Tabla 5. Value for the parameters estimate of model without regime and model with two regime 38

Tabla 6. Status of Patagonian grenadier at some years of the projected period. The probability of depletion ($Pr[S_t/S_0<0.2]$) and the probability of recovery ($Pr[S_t/S_0>0.4]$) were calculated, as well as the expected catch for three exploitation rate levels (μ) that remained constant during the projected period. 44

Tabla 7. Data used in the age-structured stock assessment model of Patagonian grenadier, showing the period covered for each one. 61

Table 8: Scenarios to evaluate the performance of the stock assessment model of the Patagonian grenadier under interdecadal recruitment fluctuations (1: step-like recruitment shift, 2: cyclical recruitment), considering process error in recruitment (1: with process error, 2: without process error), and observation error (1: without observation error, 2: with observation error). 64

Table 9: Performance of the stock assessment model of Patagonian grenadier through the mean of the absolute relative error (MARE) under different exploitation rates (μ) for recruitment (R), spawning stock biomass (SSB) and total biomass (B_t)..... 65

Tabla 10: Análisis de sensibilidad para la CPUE de la pesquería sur austral (CPUEst), Biomasa acústica (HB) y relación stock recluta (S-R), donde E_n son los escenarios plausible..... 91

Tabla 11: Detección de cambio de régimen en la abundancia de los reclutas a distintos escenarios (E_n) 91

Tabla 12: Escenario plausible de la Biomasa Hidroacustica de merluza de cola. Donde CPUEst es captura por unidad de esfuerzo de la pesquería arrastre sur austral, CPUEps pesquería de cerco centro-sur, HB Biomasa acústica y Yct captura zona centro sur (arrastre)..... 99

INTRODUCCIÓN

El impacto de los cambios climáticos de gran escala en la producción pesquera es una aspecto relevante desde un punto de vista científico y económico, debido a que las pesquerías presentan variaciones en fase con las oscilaciones climáticas, las cuales se observan a escalas decadales e interdecadales (Hollowed et al., 2001; Mantua y Hare, 2002). Mucho estudios indican que las fluctuciones del ambiente tienen un efecto directo sobre la productividad y abundancia en las poblaciones (Mantua y Hare, 2002, Rodionov and Overland 2005, Espino M. 2013).

Ver-pret *et al.* (2013), muestra en un estudio la importancia de incorporar los cambios de régimen en la evaluación de stock de 230 poblaciones. En dicho estudio se evaluó la variabilidad de la productividad de los stock, y se propuso cuatro hipótesis, i) hipótesis de la abundancia, donde la producción está siempre relacionada con abundancia de la población; ii) hipótesis de regímenes, donde la producción se desplaza irregularmente entre regímenes que no están relacionados con la abundancia; iii) hipótesis mixta, donde a pesar de que la producción está relacionada con la abundancia de la población, hay cambios irregulares en esta relación; y iv) hipótesis aleatoria, donde la producción es aleatoria de año en año. Se encontró que la hipótesis de regímenes y mixta explican el 69,1% la variabilidad de la productividad y la abundancia de las poblaciones, sin embargo a pesar que las poblaciones de peces exhiben cambios de régimen interdecadales no son considerados en el manejo.

En los ultimo años los cambio de régimen en las poblaciones marinas han sido de gran interés ya que podría tener importante consecuencia en la productividad y por lo tanto en el manejo pesquero cuando se encuentra reducida la abundancia de peces jóvenes como maduros, es sabido que la sustentabilidad y abundancia de los stock de peces se debe al reclutamiento, el cual es altamente variable y tienen un efecto decisivo en la estrategia de explotación (Csirke, 1989). Existen evidencias en varias de las principales especies explotadas en el mundo, *Strangomera bentincki* y *Engraulis ringens* (Cubillos *et al.,* 2002), *Gadus morhua* (Pörtner *et al.,* 2001; Helle *et al.,* 2002; Planque *et al.,* 2003, Stein & Borokov, 2004), *Merluccius merluccius* (Sanchez & Gil, 2000; Sanchez *et al.,* 2002),

salmón (Mantua *et al.,* 1997) de que la fuerza anual de una clase anual depende fuertemente de las condiciones oceanográficas, y de que la variabilidad regional de las condiciones oceanográficas pueden estar determinada por fenomenos climáticos de gran escala (Namias & Cayan, 1981; Hurrell & van Loon, 1997; Visbeck *et al.,* 2003).

El papel que juega la presión ambiental por fenomenos a gran escala en la variabilidad del reclutamiento interanual ha sido explorada para varios de los stock de *Merluccius* en el mundo, ya sea a través de estudios empíricos (Myers, 1998) como a través de modelos estocásticos del reclutamiento (Fogarty *et al.,* 1991; Fogarty 1993).

En el Océano Pacífico, se han documentado variaciones significativas, interanuales y estacionales de la intensidad del reclutamiento para *Merluccius gayi* (Payá, 2006; Parada *et al.,* 2013), *Macruronus magellanicus* (Cubillos *et al*., 2014), y en el Oceáno Atlántico para *Merluccius hubbsi* (Sabatini 2004), en el Cantábrico (Sanchez & Gil, 2000) y Mediterráneo (Goñi *et al.,* 2004; Abella *et al.,* 2005) para *M. Merluccius*. Asimismo, se conoce que el stock parental tiene un grado de explicación en la variabilidad del reclutamiento, y que los aspectos relevantes de la variabilidad a macro escala del reclutamiento modulada por factores ambientales de frecuencia interdecadales también juegan un rol trascedental en la evaluación de stock. Esta variabilidad no forma parte de los modelos de evaluación, y por lo tanto, no son considerados de manera formal en la decisión de las estrategias de explotación. Sin embargo los cambios decadales han sido incluidos en otras evaluaciones de stock para otras especies de peces tales como *Theragra chalcogramm* (A'mar *et al*., 2009) y *Nemadactylus macropterus* (Wayte, 2013).

La variabilidad interdecadal en el reclutamiento puede ser de utilidad para evaluar los cambios en la productividad, analizar la relación entre éstas con las condiciones ambientales y realizar predicciones a escala interdecadal. Además, podría ser de utilidad para evaluar las mejores estrategias de explotación de la merluza de cola *Macruronus magellanicus* (Lönnberg, 1907).

La merluza de cola, *Macruronus magellanicus*, es actualmente la principal pesquería de la zona austral chilena (Lillo *et al.,* 1997, Giussi *et al.,* 2002, Tascheri *et al.,* 2010) y opera sobre la plataforma continental en Chile central (34ºS-42ºS) y en la Patagonia (42ºS-57ºS). Se distribuye en el cono sur de Sudamérica, desde 37ºS en el Océano Atlántico, hasta los 27º03'S en el Océano Pacífico, pero la mayor abundancia está localizada en la Patagonia de

Chile, entre los 41º40' a 52ºS (Tascheri *et al.,* 2010). En la costa Argentina está asociada a profundidades de 20 a 800 m (Angelescu *et al.,* 1958, Chesheva, 1992), y desde los 20 a 700 m en la costa chilena (Arana, 1970; Avilés *et al.,* 1979, Cohen *et al.,* 1990). A pesar de ser un pez principalmente demersal la merluza de cola y el hoki tienen un reclutamiento altamente variable (D`Amato & Cravalho, 2005; Ernst *et al.,* 2005).

En 2000, bajo la ley 19713/01 LMCA[1] fueron declaradas dos unidades de pesquería: i) Unidad de pesquería centro-sur (UPCS), comprendida entre el límite norte de la Región de Valparaíso (32º10'23''S) y el límite sur de la Región de Los Lagos (43º44'17S); y ii) Unidad de pesquería sur-austral (UPSA), comprendida entre el límite norte de la Región de Los Lagos (41º28,6'S) y el límite sur de la Región de Magallanes (57º00'S). Estas pesquerías se encuentran declaradas en régimen de plena explotación y sometidas a la medida de administración LMCA, y por ende esta sujeta a cuotas anuales de capturas según se indica en el artículo 3 de la ley 19.713. En la pesquería demersal austral, la merluza de cola se captura mediante el sistema de pesca de arrastre, así como también en la zona centro-sur. No obstante, en la pesquería de la zona centro-sur también operó una flota con sistema de pesca de cerco entre 1978 y 2002.

La merluza de cola, ha presentado alta variabilidad enteranual e interdecadal en el reclutamiento, mostrando un cambio significativo entre 1980 y 2010. Entre 1980 y 1999 se observó claramente un período de reclutamientos altos y entre 2000 y 2010 un período de reclutamientos bajos. Además, presentó dos cambios significativos en la biomasa reproductora (SSB), uno en 1997 y otro en 2004 en estos mismos períodos se observaron dos cambios significativos en las anomalías de la temperatura superficial del mar (SSTA), uno en 1996 y otro en 1999. El cambio en las SSTA ocurrido en 1999 afectó a la parte norte del área de estudio (40º a 43ºS), mientras que un cambio importante se produjo en 1996 para las latitudes del sur, donde se han identificado las principales áreas de desove (44º a 46ºS). Por lo que, el cambio en el reclutamiento registrado en 1999 podría estar relacionado ya sea con el cambio en la SSB en 1997, o con el cambio en las SSTA en 1999 (Cubillos *et al*., 2014).

Al 2010, la merluza de cola se encontraba en un estado de baja abundancia y con tasas de explotación altas (Payá y Canales 2012). Según Paya *et al.* (2005), el stock de merluza de

[1] LMCA: Límite Máximo de Captura por Armador

cola ingresó al área de sobrepesca durante los noventa, y fue entre 1999 y 2000 que la biomasa desovante disminuyó a niveles aun recomendados (SSBt/SSBo<0,4), pero desde el 2003 al 2005 la biomasa desovante disminuye rápidamente e ingreso a la zona de sobrexplotación (SSBt/SSBo<0,2). En la actualidad el estatus de este recurso indica un agotamiento del stock desovante, por dos causas que han actuado simultáneamente: i) un cambio de regímen en el reclutamiento a niveles bajos después de 1999, y ii) sobreexplotación.

Dado los antecedentes, este estudio tiene como objetivo generar un modelo operativo que permita realizar proyecciones de la abundancia del stock con fluctuaciones interdecadales del reclutamiento de merluza de cola, evaluar el desempeño del modelo de evaluación de stock y la estrategia de explotación actual del recurso, asi como la probabilidad de recupracion y depleción aplicando cambios de productividad. La importancia del estudio radica en el soporte técnico para la evaluacion de stock y manejo de merluza de cola considerando escenarios plausibles de niveles de reclutamiento.

OBJETIVO GENERAL

- Implementar un modelo operativo que incluya escenarios de cambios interdecadales del reclutamiento de merluza de cola y evaluar el desempeño del modelo de evaluación de stock y la estrategia de explotación que se aplica en la actualidad en la nueva ley de pesca (LGPA).

OBJETIVO ESPECÍFICO

- Acondicionar un modelo operativo estructurado por edad con escenarios plausibles de variabilidad interdecadal en el reclutamiento.

- Evaluar fuente de incertidumbre en la evaluación según escenarios plausibles de fluctuaciones interanuales e interdecadal del reclutamiento de merluza de cola, y error de observación

- Evaluar la robustes del estimador actual de merluza de cola en función de los escenarios plausibles de variabilidad interdecadal en el reclutamiento de la merluza de cola.

- Evaluar a traves de tecnicas estadisticas la existencia de un cambio de regimen en la serie de tiempo para merluza de cola.

- Evaluar la probabilidad de recuperación y colapso del stock de merluza de cola incorporando el cambio de regimen en el modelo de evaluación de stock.

HIPÓTESIS

El desempeño del modelo de evaluación y la estrategia de manejo actual son robustos a escenarios de fluctuaciones interdecadales futuras del reclutamiento de merluza de cola (*Macruronus magellanicus*) en la zona sur austral de Chile.

METODOLOGIA

Área de estudio y base de datos

El área del estudio está comprendida entre 41º40´y 52ºS (Fig 1). Se utilizó datos e información que permiten la evaluación del stock en el período 1980-2010, tales como: i) capturas anuales de merluza de cola, por tipo de flota (arrastre centro-sur, arrastre sur, y cerco), ii) composición por edad y pesos promedio en las capturas de cada arte; iii) índices de abundancia (acústica, y captura por unidad de esfuerzo), cuyo detalle se encuentran documentados en Canales y Payá (2012).

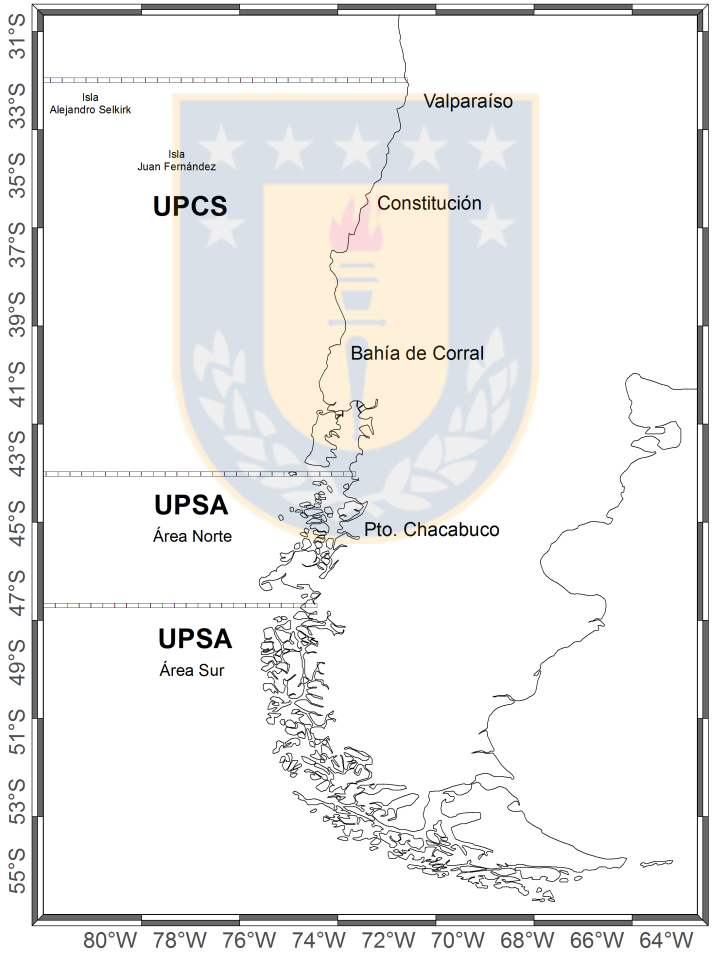

Figura 1: Unidad de pesquería norte (UPCS: 32°10´23”- 43°44’17”S) y Unidad de pesquería sur (UPS: 43°44’17” – 57°00’00” S), indicando los límites de las sub-áreas norte exterior y sur exterior de la merluza de cola (*Macruronus magellanicus)*

Análisis de cambio de régimen

Con el objetivo de determinar si el cambio de régimen no fue espurio en la serie de tiempo de merluza de cola, se planteó doce esenarios con diferentes valores de coeficiente de variación en la captura por unidad de esfuerzo, biomasa hidroacústica y relación stock-recluta (Tabla 1). Se aplicó dos aproximaciones estadísticas: i) Método secuencial para detectar cambio de régimen en el promedio y varianza (Rodionov,); y ii) Metodo Bayesiano (Kim and Cheon 2009). El detalle de los escenarios es el siguiente:

Tabla 1: Escenarios plausibles de valores de coeficiente de variación (Cv) para la captura por unidad de esfuerzo de la pesquería sur austral (CPUEst), relación stock-recluta (S_R) y biomasa hisdroacustica (B-H).

Escenario	Cv_CPUEst	Cv_S-R	Cv_B-H
E1	0.4-0.2	0.6	0.05
E2	0.4-0.3	0.6	0.05
E3	0.4-0.4	0.6	0.05
E4	0.4-0.5	0.6	0.05
E5	0.4-0.3	0.3	0.05
E6	0.4-0.3	0.4	0.05
E7	0.4-0.3	0.5	0.05
E8	0.4-0.3	0.8	0.05
E9	0.4-0.3	0.6	0.1
E10	0.4-0.3	0.6	0.15
E11	0.4-0.3	0.6	0.2
E12	0.4-0.3	0.6	0.3

E2:caso Base

Modelo de estimación

Se utilizó el modelo de evaluación de stock edad-structurado descrito por Payá y Canales (2012), a partir del cual se realizaron proyecciones a 40 años (2011-2050), aplicando una tasa de explotación objetivo y simulando: a) la permanencia del actual regimen con reclutamiento bajo; b) la ocurrencia de un cambio de regímen favorable para el reclutamiento dentro de un período de 10 años más (±5 años), modulado por la relación S-R; y c) varibilidad interdecadal del reclutamiento modulado por un cambio cíclico con amplitud y fase constante. La variabilidad interanual del reclutamiento fue modeloda con una función de distribución de error log-normal. Para esto se realizó una proyección bajo incertidumbre hasta el año 2050, a través del método Monte Carlo de la Cadena de Markov (MCMC) en AD Model builder (Fournier *et al.* 2012), tanto para el capitulo I (Modelo de estimacion) como para el capitulo II (modelo simulación-estimación). Para esto se utilizó 1000 muestras MCMC, provenientes de un muestreo sistemático de 100.000 muestras MCMC.

La proyección se realizó cosiderando una la relación stock recluta de Beverton-Holt (1957) para caracterizar un período favorable y desfavorable del reclutamiento mediante la siguiente ecuación:

Régimen alto

$$\alpha_1 = \left(\frac{1-h}{4h}\right)\left(\frac{S_1}{\bar{R}_1}\right) \quad (1)$$

Regimen Bajo

$$\beta_1 = \left(\frac{5h-1}{4h\bar{R}_1}\right) \quad (2)$$

$\alpha_2 = \alpha_1$ donde h es el parametro de escarpamiento o steepness (h=0.75), de la curva stock-recluta, $\overline{R}_1$ corresponde al reclutamiento promedio del regímen favorable (1980-1999), y $\overline{R}_2$ al reclutamiento promedio del regímen desfavorable (2000-2010).

En la proyección, el reclutamiento con un cambio de régimen se modeló según la siguiente expresión:

$$R_t = \begin{cases} \frac{SSB_t}{\alpha+\beta_1 SSB_1}, & t \leq yfav \\ \frac{SSB_t}{\alpha+\beta_2 SSB_1}, & t > yfav \end{cases} \quad (3)$$

donde SSB_t es la biomasa desovante proyectada en el año t. Y la varibilidad interdecadal del reclutamiento modulado por un cambio cíclico con amplitud y fase variable fue modelada como:

$$R_t = [\overline{R} + A * \cos(\pi * t * n - \phi) \exp(\varepsilon_t)] \quad (4)$$

donde *A* es la amplitud, *n* y ϕ son la fase de una curva seno coseno.

En el Capitulo I, para evaluar si el stock se recupera, la proyección se realizó utilizando la tasa de explotación constante objetivo asociado al 40% de la producción huevo por recluta (PHPR, μ_{ref}=0.18) y se comparó con una tasa de explotacion baja (μ=0,10). La función de desempeño consistió en la razón entre la biomasa desovante proyectada y la biomasa desovante virginal (SSBt/SSBo). Además, se calculó la probabilidad de recuperación, i.e. Pr[SSBt/SSBo>0.4]; la probabilidad que el stock permanezca en su situación actual deagotamiento i.e. Pr[SSBt/SSBo<0.2]. En cada escenario, se calculó además la captura promedio y la desviación estándar como medida de variabilidad.

En el Capitulo II, el desempeño del modelo se evaluó midiendo el sesgo y la precisión del modelo de estimación siguiendo la metodología de Punt (2003), Johnson et al., (2014), Kotaro Ono et al., (2014) y que consiste en calcular el error relativo medio (ERM) y el error relativo absoluto medio (MARE) para las cantidades de interese para el manejo (reclutamiento, biomasa desovante (SSB), biomasa total y mortalidad total), el ERM se define como:

$$E_t^{i,j} = 100 * \frac{\hat{Q}_t^{i,j} - Q_t^{i,j}}{Q_t^{i,j}} \quad (5)$$

donde $E_t^{i,j}$ es el error relativo para la medida *i* durante el año *t* en la simulación *j*, $\hat{Q}_t^{i,j}$ es el modelo operativo (verdad), para medida *i* durante el año *t* para simulación *j*, y $Q_t^{i,j}$ es el modelo estimado de medida *i* durante año *t* para simulación *j*.

Cada replica obtenida se comparó con los valores reales de OM y se calculó los intervalos de confianza de 90% y 75% de los errores relativos, con el objetivo de evaluar la precisión del los modelos. Los cambios en el modelo desempeño entre los escenarios se evalúa por la comparación directa de los valores de ERM y MARE. El detalles metodológico se encuentran descritas en cada capitulo de esta tesis

CAPITULO I

Potential stock recovery of Patagonia grenadier (*Macruronus magellanicus)* under recruitment shifts scenarios.

S. Curin-Osorio[1,3], Luis A. Cubillos[2,3]

[1]Programa de Magíster en Ciencias con mención en Pesquerías, Universidad de Concepción, Chile, Programa COPAS Sur-Austral, Departamento de Oceanografía, Universidad de Concepción, Chile. [3]Laboratorio de Evaluación de Poblaciones Marinas (EPOMAR), Departamento de Oceanografía, Facultad de Ciencias Naturales y Oceanográficas, Universidad de Concepción, Casilla 160-C, Concepción, Chile.

Artículo enviado: Fisheries Research

Abstract

The stock of Patagonian grenadier was depleted due to both intensive fishing and a possible regime shift in recruitment, from higher to lower levels after 1999. Considering that the stock recovery could never occur if the low recruitment regime remains in the future, potential stock recovery was evaluated by simulation under recruitment shifts scenarios. An age-structured population was projected over 40 years (2011-2050) under constant harvest rates, and three scenarios: a) low recruitment regime, b) high recruitment regime after 10 years, and c) cyclical recruitment. The recovery was feasible only under a high recruitment regime or when recruitment was cyclical. Time of recovery was close to 2030 under harvest rate (m) of 10%, and close to 2040 at m =18%. Time of recovery was faster under cyclical recruitment, but the stock would decline again by 2035, and below the target. Regarding the status in 2010, at 80% decision-confidence level the stock becomes recovered by 2025 under regime shifts scenarios, but decadal variability is still uncertain. It is necessary to start an effective recovery plan by monitoring the recruitment, adjusting the target exploitation rate and permitting greater reproductive potential.

Keywords: Depletion, Recovery, Recruitment, regime productivity, stock assessment.

Introduction

An understanding of the dynamics of the fish stocks at very low population levels is imperative when considering the opportunities for stock recovery from the collapse. Although many stocks have had notable collapses (Hutching et al., 2010), some stocks have recovered, e.g. North Sea herring (*Clupea harengus*) (Nichols 2001; Simmonds 2007), North Sea and Northwest Atlantic cod (*Gadus morhua*) (Cook 1998, ICES 2006a, Shelton et al., 2006). In many cases, extremely high exploitation levels are the principal cause for the reductions in population size, and the maintenance of overexploitation is the main cause of failure to recover. Compounding this, depleted stocks are also sensitive to environmental changes (Perry et al., 2010), and often the unfavorable environmental conditions, and consequent impacts on productivity, can hinder proper recovery of fish populations.

Examples include, the additional influence of El Niño on the collapse of the Peruvian anchoveta (*Engraulis ringens*) (Glantz and Feingold 1992, Yañez et al., 2001, Ñiquen and Bouchon 2004). The regime change in the Pacific sardine off Japan (Watanabe 2007), and the shift in environmental conditions after the collapse of the Norwegian spring spawning herring (Toresen and Ostvedt 2000, Fiksen and Slotte 2002). The interaction between exploitation, a reduction in stock productivity, and influences of environmental changes are key factors in stock recovery (Kell et al., 2005, Shelton et al., 2006), and important for stock assessment. Wayte (2013) showed the importance of modelling recruitment regime change into stock assessment models.

Vert-pre et al., (2013) evaluated four hypotheses to test the frequency and intensity of productivity regime shifts: i) the abundance hypothesis, where production is always a function of population abundance; ii) the regimen hypothesis, where production shifts irregularly between regimes that are unrelated to abundance; iii) the mixed hypothesis, where even though production is related to population abundance, there are irregular changes in this relationship, and iv) the random hypothesis, where production is random from year to year. Both the regime and mixed hypotheses explained 69.1% of marine fish stocks (Vert-pret et al., 2013). The authors suggested that irregular changes in productivity are common; therefore, fishery management targets may need to be adjusted whenever productivity changes.

Although exploited stocks may exhibit regime changes in recruitment, it is often ignored into the stock assessment or recovery scenarios. This seems to be the case of the Patagonian grenadier, stock off Chile, which is believed to be overexploited due to intensive fishing and also because of the apparent occurrence of a sudden recruitment change after 1999 (Cubillos et al., 2014). According to Cubillos et al. (2014), the recruitment of Patagonian grenadier showed interannual to interdecadal variability between 1980 and 2010, with a shift from a high recruitment period (1980-1999) to a low recruitment regime between 2000 and 2010. The recruitment change coincides with a large-scale change in sea temperature (Cubillos et al., 2014), a condition that probably is still occurring in the southern Humboldt Current System. According to Payá and Canales (2012), the Patagonian grenadier was in a state of low abundance and high exploitation rates in 2010. The stock is estimated to have been overfished during the 1990s. By 1999 and 2000 the spawning stock biomass (S)

declined under the target ($S_t/S_0<0.4$), and from 2003 to 2005 the *S* diminished under the limit reference point ($S_t/S_0<0.2$).

The objective of this paper is to analyze the potential recovery of the spawning stock biomass of Patagonian grenadier by considering the current status of a low productivity regime and plausible occurrence of a favorable condition for higher productivity in the future, according with three exploitation rates. The first one was a very low exploitation rate ($\mu=0.001$) that allowing to have a reference for unexploited conditions. The second one was an exploitation rate of 10% ($\mu=0.1$), and the third one was the current exploitation rate ($\mu=0.18$). The latter is associated with a reduction of 40% of the reproductive potential (Payá and Canales, 2012). The reduction of 40% is considered a proxy for the spawning biomass at maximum sustainable yield. The hypothesis considers that the spawning stock biomass of Patagonian grenadier will exhibit a significant recovery under the current exploitation rate only when a favorable change in recruitment might occur in the near future.

Materials and methods

Distribution and data

The study area considered the distribution of the Patagonian grenadier fishery along the Chilean coast, from 33ºS (northern Valparaíso) to 52ºS (Magellan's strait). The data and information covered the period 1980-2010 and was used as input to an age-structured stock assessment model described by Payá and Canales (2012). Annual catch and catch-at-age data were from three fishing fleets (Table 1). The bottom trawl fleet of the central zone covered the period from 2003 to 2010, operating mainly on the continental shelf off central Chile (33ºS-41º40'S). The purse-seine fleet operated on surface waters off central Chile from 1980 to 2003, while the bottom trawl fleet fishing operating along the continental shelf of Patagonian waters (42ºS-52ºS) covered the period 1980-2010. Weight at age data by fishing fleets covered the same periods previously described. The indices of abundance consisted of acoustic biomass from 2000 to 2010 (including the age composition of the survey), catch-per-unit-effort (CPUE) from the purse-seine fleet (1980-2003) and CPUE

the southern bottom trawl fleet (1980-2010). Payá and Canales (2012) documented details of the data used for the stock assessment, as well methodological aspects.

Tabla 2. Data used in the age-structured stock assessment model of P. grenadier, showing the period covered for each one.

Areas	Fleets	Catch (t)	Catch at age	Acoustic Biomass (t)	CPUE
Central	Purse-seine	1987-2005	1997-2001	-	1988-2002
(33ºS-41º40'S)	Bottom trawl	2001-2010	2003-2009	-	-
Southern	Bottom trawl	1980-2010	1988-2009	2000-2010	1980-2009
(41º40'S-57ºS)					

The current stock assessment model (SAM)

The SAM of Payá and Canales (2012) is an age-structured model, which assumes a homogeneous stock unit in the southern Pacific Ocean off Chile. The model is parameterized to account for the main factors affecting the abundance of the population, and considering discrete dynamics with known catch per fleets. Natural mortality (M=0.35) is assumed to be known and to remain constant across ages and year. Catchability and selectivity is modeled for each fishing fleet. For the southern trawl fleet a dome-shape model described the exploitation pattern before 1990, and a logistic model described the selectivity between 1991 and 2010. The survey selectivity was logistic and considered constant.

The recruitment in a given year (R_t) is estimated according to:

$$R_t = \bar{R} * \exp(\varepsilon_t) \quad (6)$$

where:

$$\varepsilon_t \approx N(0, \sigma_R^2) \quad (7)$$

$\bar{R}$ is the average recruitment for the whole assessment period (1980-2010) and ε_t are the recruitment annual deviations ($\sigma_R^2 = 0.6$). In addition, the stock-recruitment (S-R) model of Beverton and Holt (1957) is fitted within the SAM. The parameters of the S-R model are estimated according to:

$$\alpha = \left(\frac{1-h}{4h}\right)\left(\frac{S_1}{\bar{R}}\right) \quad (8)$$

$$\beta = \left(\frac{5h-1}{4h\bar{R}}\right) \quad (9)$$

were R_0 is the unexploited recruitment, S_0 is the unexploited spawning stock biomass, and h is the steepness (=0.75), which is assumed to be known.

Detection of recruitment shift

In the current SAM of Payá and Canales (2012) the expected recruitment is considered stationary (Eq. 1 and 2). In order to detect if the recruitment change of 2000 was not spurious, a sensitivity analysis of the stock assessment considered different coefficients of variation (CV) for the different abundance indices available for the assessment, as well as for the recruitment deviations and the fit of the S-R model (Table 2). The E2 is the base case and represents the results communicated by Payá and Canales (2012).

Tabla 3: Sensitivity of the current stock assessment model according to changes in the coefficient of variations (CV) of the abundance indices and the recruitment deviations (CV_R) of Patagonian grenadier. The abundance indices are the catch per unit effort of the southern trawl fishery (CV_CPUEst) and the hydroacoustic biomass (CV_HB). The Escenario E2 is the base case representing the results obtained by Payá and Canales (2012). The asterisc represents the CV for two block of time periods of the CPUE, being equal to 0.4 for the period before 1990.

Escenario	Cv_CPUEst	Cv_S-R	Cv_B-H
E1	0.4-0.2	0.6	0.05
E2	0.4-0.3	0.6	0.05
E3	0.4-0.4	0.6	0.05
E4	0.4-0.5	0.6	0.05
E5	0.4-0.3	0.3	0.05
E6	0.4-0.3	0.4	0.05
E7	0.4-0.3	0.5	0.05
E8	0.4-0.3	0.8	0.05
E9	0.4-0.3	0.6	0.1
E10	0.4-0.3	0.6	0.15
E11	0.4-0.3	0.6	0.2
E12	0.4-0.3	0.6	0.3

E2:caso Base (SAM)

The statistical approach to detecting a regime shift in the recruitment time series used the sequential algorithm for detecting regime points of Rodionov (2004) and the Bayesian analysis for change point of Berry and Hartigan (1993). The method of Rodionov calculates the so-called regime shift index (RSI), which represents a cumulative sum of normalized anomalies relative to the critical level (diff):

$$\mathrm{RSI}_{i,j} = \sum_{i=j}^{j+m} \frac{x_i - (\bar{x}_{R1} + diff)}{l\sigma_i} \quad (m=0,1,..,l\text{ -}1). \tag{10}$$

Where $\bar{x}_{R1}$ is the average recruitment of the first regime (*R1*) on log scale, *diff* is the difference from the average recruitment (on log scale) of the second regimen (*R2*) that would statisically significant (Student's *t*-test) is given by $diff = t\sqrt{2\sigma_l^2/l}$, *t* is the value of the t-distribution with 2*l*-2 degrees of freedom at a probability level 0.05 and *l* set the cut-off (Radionov 2004). Erdman and Emerson (2007) implemented the Bayesian analysis for change points of Barry and Hartigan (1993) in the package "bcp" for the R software (R Core Team 2014). The detection of regime shift was on the basis of 5000 simulations, burning the first 50 samples from each chain and using priors of 0.2 for both the signal noise ratio and the probability of detecting a shift.

Simulation and Projections under decadal recruitment changes (SAMR)

The SAM of Payá and Canales (2012) was modified in order to simulate projections under recruitment regime shift scenarios (SAMR), with constant exploitation rates for 40 years (2011-2050). The simulation in the SAMR included the occurrence of a favorable period for the recruitment of P. grenadier during the long-term projections, according to three scenarios. The first one consisted in projections by simulating that the current low recruitment regime will remain during the projection period. The second one consisted of a change point for a high recruitment within a period of ten years (± five years) in the near future, from the current low productivity to higher productivity modulated by the S-R relationship. It is assumed that the change could occur in 2021 (10 years after 2010) because the decadal variability, but chosen randomly from a uniform distribution between 2015 and 2025. The third approach consisted of simulating interdecadal variability in recruitment according to cyclical changes modulated by constant amplitude and phase.

In the case of a regime shift in recruitment, the SAMR considered the stock-recruitment model of Beverton and Holt (1957) with two regimes, and expressed according to the re-parameterised Beverton-Holt model (see Mace and Doonan, 1988):

High-recruitment regime:

$$\alpha_1 = \left(\frac{1-h}{4h}\right)\left(\frac{S_1}{\bar{R}_1}\right) \quad (11)$$

$$\beta_1 = \left(\frac{5h-1}{4h\bar{R}_1}\right) \quad (12)$$

low-recruitment regime:

$$\alpha_1 = \left(\frac{1-h}{4h}\right)\left(\frac{S_1}{\bar{R}_1}\right) \quad (13)$$

$$\beta_2 = \left(\frac{5h-1}{4h\bar{R}_2}\right) \quad (14)$$

where h is the steepness (h = 0.75) of the stock-recruit curve, $\overline{R}_1$ is the average recruitment of the high recruitment regime (1980-1999), and $\overline{R}_2$ is the average recruitment in the low recruitment regime (200 2010). This approach considered a change in the productivity of the stock-recruitment relationship along the replacement line (see Figure 1).

.

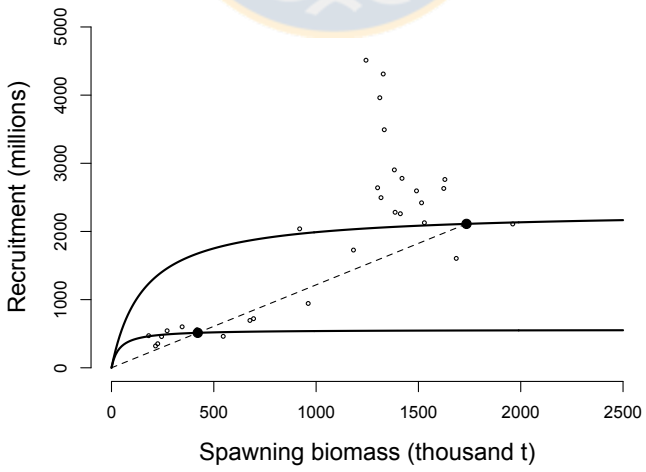

Figura 2. Model of two recruitment regimes in the stock-recruitment relationship of the P. grenadier, which was used to simulate projections according to either the low or the high recruitment. The points are the data for the period 1980-2010.

During the projection phase, the low recruitment regime was defined according to the parameters alpha2 y beta2. Instead, the high recruitment regime was defined by:

$$R_t = \begin{cases} \frac{S_{t-1}}{\alpha+\beta_1 S_{t-1}}, & t \leq yfav \\ \frac{S_{t-1}}{\alpha+\beta_2 S_{t-1}}, & t > yfav \end{cases} \quad (15)$$

where S_t represents the projected spawning biomass in year t, and y_{fav} is the year in which the change will occur, which was chosen randomly from a uniform distribution between 2015 and 2025.

For the case of cyclical recruitment, we fitted the following equation to the recruitments of the period 1980-2010, i.e.,

$$R_t = [\overline{R} + A * \cos(\pi * t * n - \phi)] \exp(\varepsilon_t) \quad (16)$$

where R is the average recruitment in the period 1980-2010, A is the amplitude (=7.15), n=0.06 and ϕ= 2.48 are the phase of a sine cosine curve. The model was fitted by least square, and used only to simulate future cyclical changes in the average recruitment of P. grenadier.

Probability of recovery

In order to evaluate probabilities of recovery for the spawning potential ratio under the three scenarios of recruitment changes, the long-term projections considered constant exploitation rates. One of them was the current target exploitation rate, associated with 40% of the spawning potential ratio (μ=0.18), which was compared with a moderate exploitation rate (μ=0.1) and unexploited conditions (μ=0.001). The performance measure function consisted of the ratio between the projected spawning biomass at a given year and the unexploited spawning biomass (S_t/S_0). The unexploited spawning stock biomass, S_0, was estimated by SAMR and it is a quantity approximately equal to the S_1 level of the high recruitment regime. The 40%S_0 is a proxy of the spawning stock biomass at maximum

sustainable yield (S_{msy}) and it is a desirable reference from the point of view of the fisheries management. In absence of a recovery plan, in this paper S_{msy} was the reference for recovery.

The status of stock was calculated as $Pr[S_t/S_0>0.4]$ for specific years (2011, 2015, 2020, 2025, 2030, 2040 and 2050), indicating a status of a healthy and recovered stock. In turn, the probability that the stock remained at the current situation was equivalent to the probability of depletion, which was calculated according to $Pr[S_t/S_0<0.2]$ for the same years. In addition, the relative recovery of the stock from the status in 2010 was carried out by calculating the probability $Pr[S_t>S_{2010}]$ for the same specific years previously mentioned. The decision confidence level can be thought of as a one-tailed α probability from standard statistical hypothesis testing. For each decision confidence level there is a corresponding $Pr[S_t>S_{2010}]$ that forms a probability profile, given the confidence level (Helser *et al.* 2001). The expected catch was also calculated for each scenario, as well as the coefficient of variation. All projections were carried out by 40 years using Monte-Carlo of Markov's Chain (MCMC) in ADMB (Fournier *et al.* 2012), by using 1000 MCMC samples, from 100,000 MCMC.

Results

Detection of a recruitment regime shift

The methods used to detect regime shifts yielded consistent results for determining the change of regime in the abundance of recruitment of Patagonian grenadier. The Bayesian change point showed 80% probability that in 1999 there was a change in the magnitude of recruitment for scenarios E1 to E8, with change posterior means of 6.3 to 0.89 after of 1999 (on log-scale). Similar results were obtained with the method's Rodionov, showing that for 2000 existed a major regime change ($p<0.05$) in the abundances of recruits for scenarios E1-E9 (Table 3). However, when the coefficient of variation for hydroacoustic biomass was set higher than 0.15 (Scenarios E19-E12), the probability of a regime shift was zero. The method's Rodionov did not detect significant regime change in recruitment for scenarios E10; E11, and E12 ($p>0.05$), for the years 1983, 2000 and 2008 (Table 3).

However, for scenarios E09-E12, the magnitude of the total biomass was re-escalated to unrealistic values, 2 or 3 orders of magnitude higher.

Tabla 4. Detection of regime shifts in the recruitment time series of P. grenadier according to different values for the coefficient of variation for the abundance indices (CPUE and Acoustic survey) and deviations of recruitment in the current stock assessment model (SAM).

	Bayesian change point		Change point Rodionov		Relative change (Rodionov)
Scenarios	Shift year	Posterior Prob.	Shift year	$P < 0.05$	(logRegime 2-Regime 1)
E1	1999	0.892	2000	<0.01	-1.39
E2	1999	0.940	2000	<0.01	-1.44
E3	1999	0.968	2009	0.040	5.30
E4	1999	0.874	2000	<0.01	-1.44
E5	1999	0.942	2000	<0.01	-1.33
E6	1999	0.928	2000	<0.01	-1.29
E7	1999	0.930	2000	<0.01	-1.42
E8	1999	0.872	2000	<0.01	-1.43
E9	-	0	2000	<0.01	-1.47
E10	-	0	2000	0.111	-0.31
E11	-	0	1983	0.157	0.47
E12	-	0	2008	0.227	0.41

Stock assessment model with a regime shift in recruitment

The stock assessment model with an explicit regime shift in recruitment (SAMR) was able to estimate the two regimes stock-recruitment model (Figure 1). The high recruitment was 2111 million fish for the period 1980-1999, producing a spawning stock biomass of 1856 thousand t without exploitation. Instead, the average recruitment for the low recruitment period (2000-2010) was 512 million fish, and the reference biomass without exploitation becomes 451 thousand t. In addition, the annual deviations of recruitment showed lower standard deviation (CV=0.30) than the SAM (CV=0.77), with variance more homogeneous and without significant trends (Figure 2). The objective function of the SAMR was 5812.53

with 2 additional parameters, which was slightly better than the objective function of the current SAM (=5822.91).

Tabla 5. Value for the parameters estimate of model without regime and model with two regime

Parameter	Symbols	Model SAM	Change point SAMR
Mean recruitment	R	1001	-
Mean recruitment (1980-1999)	$\bar{R}_1$	-	2111
Mean recruitment (2000-2010)	$\bar{R}_2$	-	512
Alpha (Parameter S-R)	α	0.0704	0.0731
Beta (Parameter S-R)	β	0.0009	-
Beta (Parameter S-R/ 1980-1999)	β_1	-	0.0004
Beta (Parameter S-R/ 2000-2010)	β_2	-	0.0017
Spawning biomass unexploited	S_0	1361	-
Spawning biomass unexploited (1980-1999)	S_1	-	1856
Spawning biomass unexploited (2000-2010)	S_2	-	451
Natural Mortality	M	0.35	0.35
Steepness	h	0.750	0.750

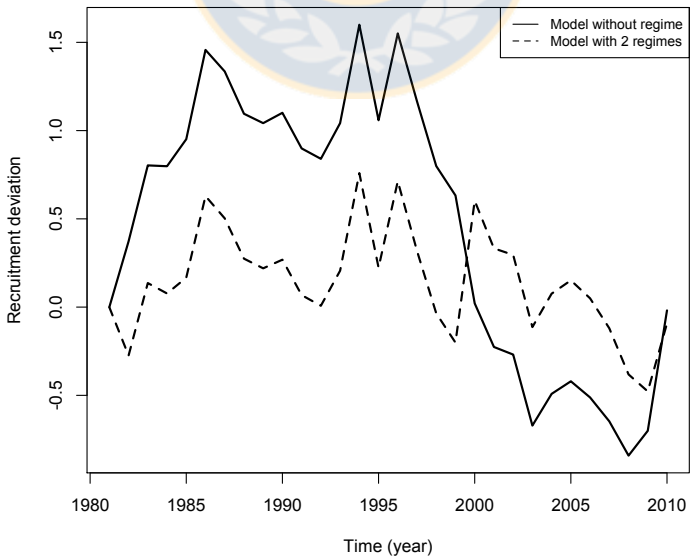

Figura 3. Recruitment deviations applying the original SAM (solid line, without explicit recruitment regimes) as compared with a SAMR that incorporates two regimes in the stock-recruitment relationship (discontinuous line).

Total catches of Patagonian grenadier showed three periods of change according to differential participation of fishing fleets. The first period was characterized by very low catches, from 1980 to 1985. Catch during the second period was higher and fluctuating and mainly due to the purse-seine fleet between 1987 and 1999. The last period exhibited lower catch between 2000 and 2010, which is consistent with the regulated period for total allowable catches (Tascheri et al., 2010). In the last period, the purse-seine fishery no longer operated, and the central-southern bottom trawl fishery began (Figure 3).

According to SAMR both the total biomass and the spawning stock biomass showed a declining trend from 1980 to 2010, with fluctuations between 1985 and 1998 and with a faster decline after 1999 (Figure. 3). The recruitment showed a time with higher and fluctuating recruitments from 1980 to 1999, and a dramatic decline from 2000 to 2010. The predicted recruitment by the S-R model shows the shift in 2000, and this lower recruitment period was determining the faster decline in the total biomass. The higher exploitation rate was due to the purse-seine fleet that operated from 1987 to 2002. However, from 2000 up to 2010 the exploitation rate exerted by the southern bottom trawl fleet started to grow from less than 10% up to 20% by 2010 (Figure 3).

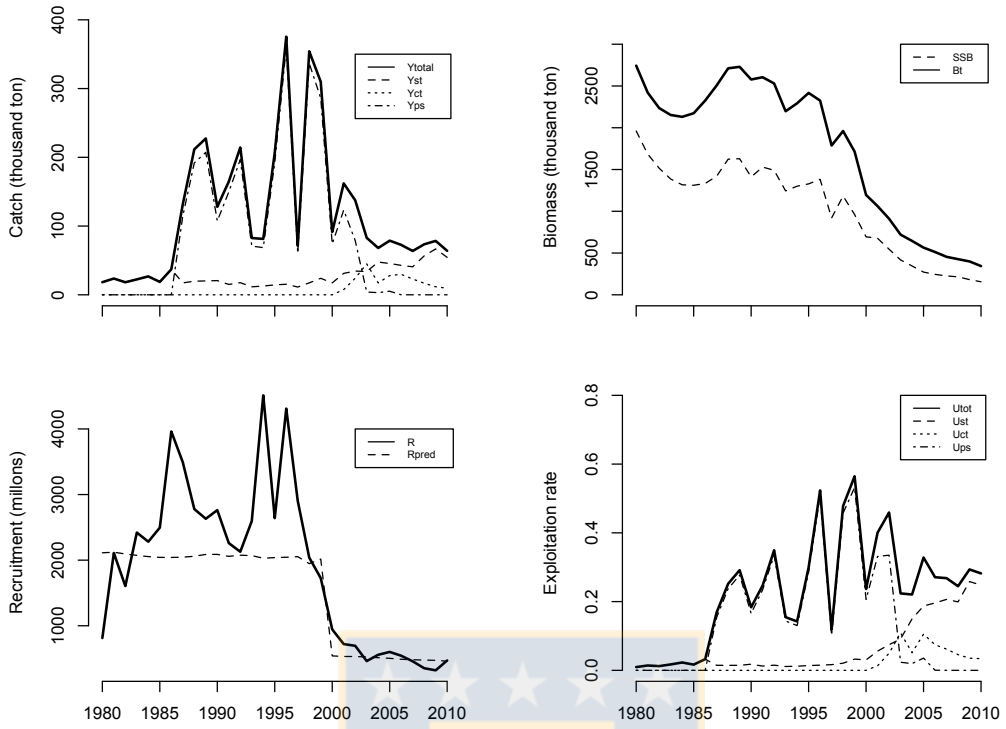

Figura 4. Total catch (Ytotal) and partial catch per fishing fleets (Yst: southern bottom trawl fishery, Yct: central bottom trawl fishery, Yps: purse-seine fishery). Total biomass (Bt) and spawning stock biomass (SSB). Recruitment and predicted recruitment obtained by the S-R model. Total exploitation rate (Utot), and partial exploitation rates per fishing fleets (Ust: southern bottom trawl fishery, Uct: central bottom trawl fishery, Ups: purse-seine fishery), for model with two regimes (SAMR).

Projections with recruitment regime shift scenarios

Under the low recruitment level scenario, the spawning stock biomass of Patagonian grenadier did not show a recovery during all of the projection period, either with μ=10% or μ=18% (Figure 4, upper panel). The depleted status tends to persist with a probability higher than 69% at μ=10%, and higher than 90% at μ=18%. In addition, the expected catches tend to be close to 50 thousand ton at μ=18% (Table 4). When the exploitation rate was negligible (μ=0.1%), the S_t/S_0 ratio showed a better status during the projection period, but with the probability of depletion was close to 20% (Table 4).

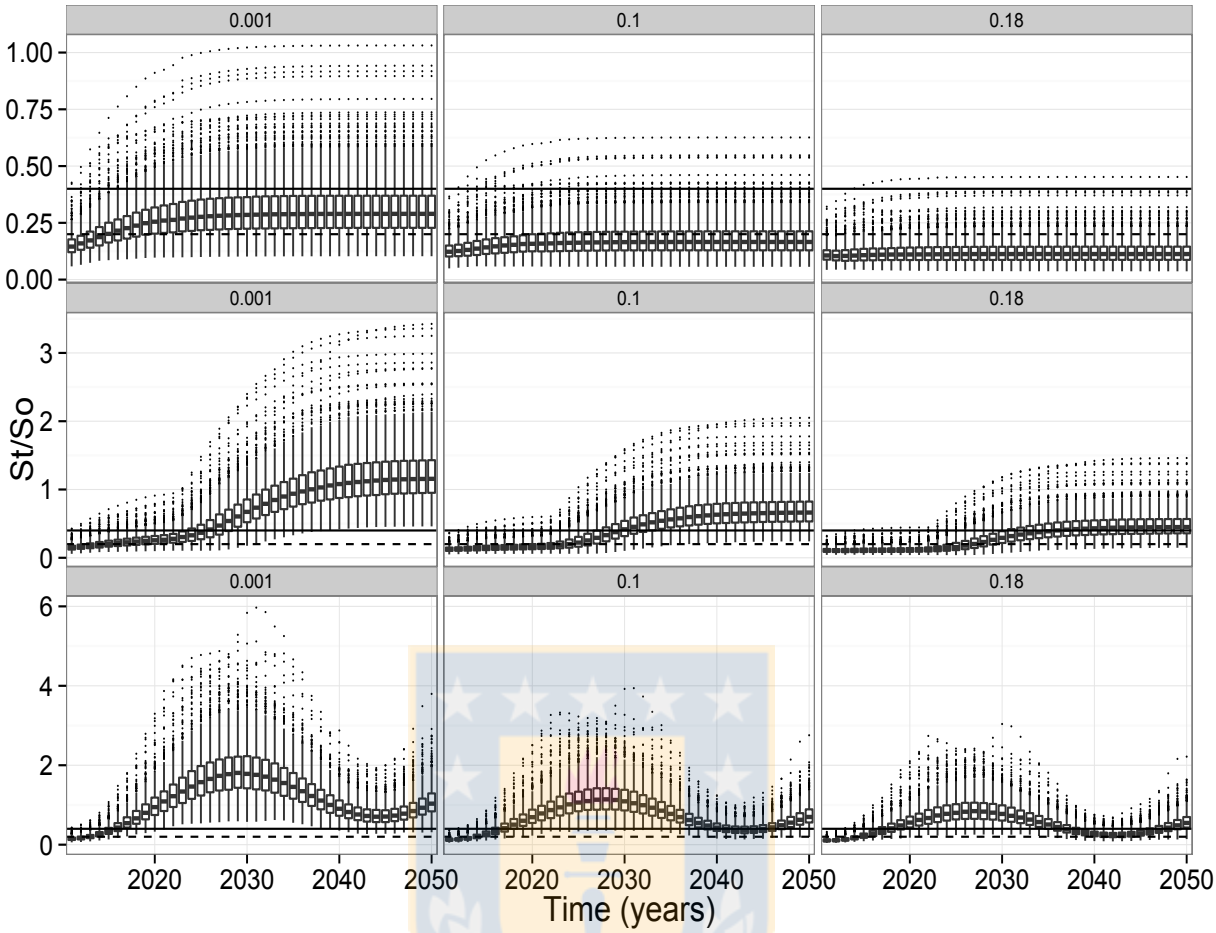

Figura 5. Performance of the ration between the projected spawning stock biomass and the unexploited spawning stock biomass (S_t/S_0) by considering three exploitation rates, and according to: a) upper: the persistence of the low recruitment regime, b) middle: high recruitment shift after 10 ±5 years, and c) lower: cyclical recruitment. The black line indicates the threshold for recovery $S_t/S_0>0.4$, and the dashed line defines depletion when $S_t/S_0<0.2$.

Simulations considering the scenario of a recruitment shift to high recruitments within 10±5 years showed a recovery of the stock between 2025 and 2030, depending on the exploitation rate used. The stock recovery consolidated after 2035, when the spawning stock biomass ratio surpasses the recovery threshold of 40%S_0 and with a probability of recovery higher than 50% at μ=18% (Figure 4, middle panel). At μ=10%, the probability of recovery was 11% in 2015 and 54% in 2030, but at μ=18% the probability was 23% in

2030 and 58% in 2040 (Table 4). The expected catch after the recovery was approximately 175 thousand t by applying μ=18%.

By considering cyclical recruitment for Patagonian grenadier, notable increases in the ratio S_t/S_0 were observed during the period from 2016 to 2027 (Figure 4, lower panel). Under this scenario the recovery was faster than the previous scenario, and consolidated after 2015. Indeed, the probability of recovery was 80% at μ=18% in 2020 (Table 4). During the 2040's, the ratio S_t/S_0 decreased again because the cyclical behavior. In 2040, the probability of depletion was 20% and the status was 12% higher than the threshold of $40\%S_0$ (Table 4). The expected catch after the recovery was over 300thousand t between 2020 and 2030, and declined to approximately 100 thousand t during the 2040's (Table 4).

Probability of recovery regarding the status in 2010

The decision confidence level at 80% showed that the stock did not show a significant recovery under the persistence of the current low recruitment level of Patagonian grenadier because the cumulative values for the spawning stock biomass tended to overlap (Figure 5). However, under the scenario of a high recruitment shift a clear tendency to recovery was observed after 2025 and at 80% of decision confidence level. The most optimistic scenario was the cyclical recruitment, illustrating a faster recovery after 2015 (Figure 5).

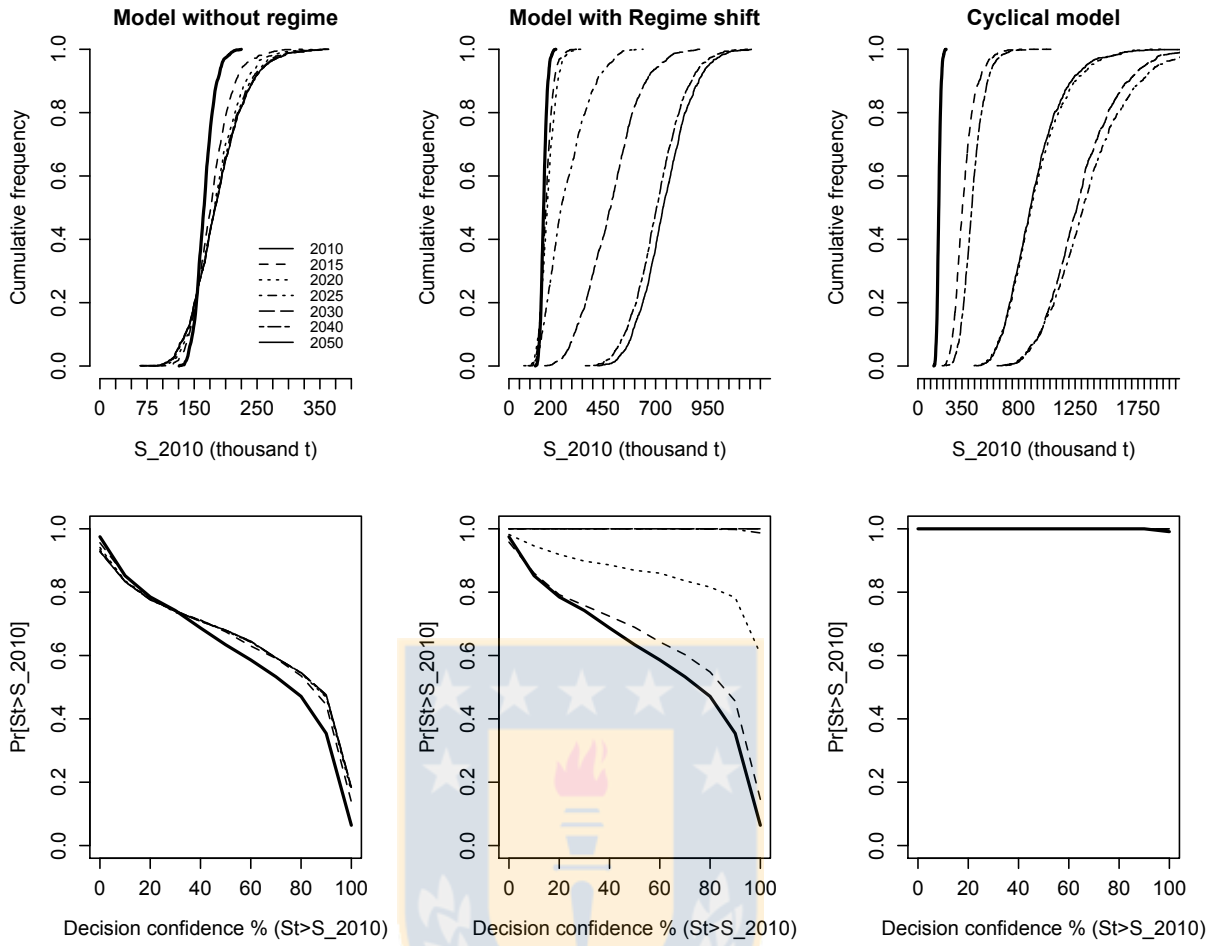

Figura 6. The stochastic decision-making framework for assessing the recovery of the Patagonian grenadier stock. The top plot shows the cumulative empirical probability of St in 2010, and for the years indicated by applying μ=18%. The bottom plot shows the probability profile specifying the $Pr[S_t>S_{2010}]$ for different levels of decision confidence.

Tabla 6. Status of Patagonian grenadier at some years of the projected period. The probability of depletion (Pr[S_t/S_0<0.2]) and the probability of recovery (Pr[S_t/S_0>0.4]) were calculated, as well as the expected catch for three exploitation rate levels (μ) that remained constant during the projected period.

		Model without regime			**Model with Regime shift**			**Cyclical model**		
Period		μ=0.001	μ=0.1	μ=0.18	μ=0.001	μ=0.1	μ=0.18	μ=0.001	μ=0.1	μ=0.18
	Depletion	0.85	0.94	0.97	0.85	0.94	0.97	0.86	0.94	0.98
	Recovery	0.00	0.00	0.00	0.02	0.00	0.00	0.00	0.00	0.00
	average catch	0.050	25.770	43.170	0.050	25.770	43.170	0.050	26	43.21
	desv	0.00	2.02	3.36	0.00	2.02	3.36	0.00	2.01	3.36
2010	Cv	7.91	7.82	7.78	6.00	7.82	7.78	7.75	7.79	7.77
	Depletion	0.48	0.84	0.96	0.48	0.84	0.96	0.04	0.21	0.41
	Recovery	0.03	0.01	0.00	0.03	0.01	0.00	0.29	0.11	0.05
	average catch	0.07	29.96	43.98	0.07	29.96	43.98	0.113	53.398	84.811
	desv	0.01	5.11	7.85	0.01	5.11	7.85	0.02	12.88	22.10
2015	Cv	14.29	17.06	17.85	14.29	17.06	17.85	21.24	24.12	26.06
	Depletion	0.23	0.75	0.94	0.23	0.75	0.94	0.00	0.00	0.00
	Recovery	0.09	0.01	0.00	0.09	0.01	0.00	0.99	0.94	**0.80**
	average catch	0.08	33.35	45.98	0.08	33.38	45.55	0.331	147.7	227.16
	desv	0.01	6.53	7.86	0.01	6.52	9.21	0.08	39.47	63.74
2020	Cv	12.50	19.58	17.09	12.50	19.53	20.22	24.17	26.72	28.06
	Depletion	0.18	0.71	0.93	0.08	0.41	0.70	0.00	0.00	0.00
	Recovery	0.15	0.01	0.00	0.42	0.11	0.04	1.00	0.99	**0.97**
	average catch	0.09	34.56	46.04	0.128	48.5	65.4944	0.547	227.16	333.8
	desv	0.02	7.56	10.20	0.04	17.95	25.10	0.12	55.10	85.83
2025	Cv	22.22	21.88	22.15	31.25	37.01	38.33	22.30	24.26	25.71
	Depletion	0.16	0.69	0.92	0.00	0.06	0.20	0.00	0.00	0.00
	Recovery	0.18	0.01	0.00	0.88	0.54	0.23	1.00	0.99	**0.97**
	average catch	0.09	35.01	46.23	0.23	88	118.15	0.616	233.06	324.25
	desv	0.02	7.94	10.55	0.06	23.59	33.03	0.12	49.73	74.92
2030	Cv	22.22	22.68	22.82	26.09	26.81	27.96	19.25	21.34	23.10
	Depletion	0.15	0.70	0.93	0.00	1.00	0.03	0.00	0.01	0.20
	Recovery	0.19	0.01	0.00	1.00	0.90	**0.58**	1.00	0.59	0.12
	average catch	0.1	35.21	46.32	0.369	132.13	174.94	0.301	89.044	107.53
	desv	0.02	8.13	10.71	0.05	20.63	29.64	0.05	16.87	23.60
2040	Cv	20.00	23.10	23.12	13.55	15.62	16.94	16.28	18.95	21.95
	Depletion	0.15	0.69	0.92	0.00	0.00	0.01	0.00	0.00	0.00
	Recovery	0.19	0.01	0.00	1.00	0.94	**0.64**	1.00	0.95	**0.82**
	average catch	0.1	35.24	46.33	0.396	139.23	183.41	0.358	149.03	223.89
	desv	0.02	8.15	10.73	0.06	20.76	29.25	0.08	38.03	61.80
2050	Cv	20.00	23.13	23.16	14.14	14.91	15.95	22.35	25.52	27.60

Discussion

Because the current low productivity level exhibited by recent stock assessment (e.g., Payá and Canales 2012), one of the goals of this paper was to evaluate the potential for recovery of Patagonian grenadier under different scenarios of regime changes in recruitment in the near future. Cubillos *et al.* (2014) detected a regime shift in the recruitment time-series provided by Payá and Canales (2012), without questioning whether that regime was spurious or not. Indeed, the stock assessment of Patagonian grenadier is a complex task and supported by different kind of data and assumptions. The sequential participation of different fishing fleets covering different time periods, as well as auxiliary indices, could lead to determine spurious changes in productivity. For example, total catch declined dramatically when the purse seine finished its participation by 2003. Nevertheless, our sensitivity analysis identified that a recruitment shift occurred regarding the changes in the coefficient of variation of the catch-per-unit effort and for the annual deviations of recruitment. Only when the coefficient of variation for the acoustic biomass data was higher than 0.15, the regime shift in recruitment was not detected. One must bear in mind that the current stock assessment set a CV between 0.05 and 0.1 for the acoustic biomass, which is indicating a very precise and accurate data for stock assessment. Indeed, for CVs greater than 0.15 the stock assessment was escalated to biomass levels two to three orders of magnitude greater. Of course, those biomass levels were absurd; hence, the CV for the acoustic was kept lower in the stock assessment model. Therefore, it is demonstrated that the index of acoustic biomass of Patagonian grenadier had impact on the detection of the regimen shift in recruitment. Indeed, the acoustic biomass index started to be monitored since 2000, and because it is the unique fishery-independent index of biomass the influence on the stock assessment was emphasized with coefficient of variation between 0.05 and 0.1 in the stock assessment (Payá and Canales 2012). Although the regime shift in recruitment of Patagonian grenadier could be spurious, from the point of view of the management the hypothesis of a change in the recruitment level of a resource must be taken into account because rejecting a null hypothesis when it is true could have important consequences, especially from the point of view of rebuilding a depleted stock. In this context, modeling an explicit change in the average recruitment into the stock assessment model (SAMR) had

slightly better performance than the original SAM of Payá and Canales (2012). The coefficient of variation for the interannual recruitment deviations was lower than the original model. In the original SAM of Payá and Canales (2012), the annual recruitment deviations were modeled around the historical average recruitment and thereafter they exhibited a higher standard deviation to explain very higher and very lower recruitments. When the regime change was explicitly incorporated into the SAMR, the standard deviation was lower and was consistent with a homogeneous variance. The statistical properties were better, but the explicit model with 2 regimes has also important consequences for the management and the recovery of the stock in the near future.

If the current low recruitment regime tends to persist in the near future, the stock will not recover ever to levels of unexploited spawning stock biomass estimated previous to 1980. The unique alternative could be to adjust the reference level to those that the stock is able to produce without exploitation, which was estimated near to 451 thousand ton by SAMR. Therefore, an effective recovery plan must be adjusted to consider that S_{msy}~180 thousand ton (i.e., 40%S_2). However, if the recruitment of Patagonian grenadier could be fluctuating according to interdecadal recruitment shifts or cyclical behavior, then there is a chance of recovery to 40%S_0 level (~742 thousand ton). The best scenario for recovery is under the assumption that the recruitment is cyclical, because the recovery tends to occur within 5 to 8 years after 2010. However, this scenario is assuming that the cycles have amplitude and phase constants, a situation rarely observed in fish populations (Spencer *et al.* 1997a). The case of a recruitment shift seems to be more real, but there is high uncertainty in terms of the time when the reversal conditions for a favorable change in recruitment will occur. It is recommendable to monitor the recruitment throughout a recruitment index, which should be incorporated into the stock assessment model.

In this paper the change in the recruitment level was not modeled as a function of environmental factors because changes in recruitment level must not be necessarily related to environmental conditions (Vert-Pre *et al.* 2013). Nevertheless, the current lower recruitment period of Patagonian grenadier seems to be associated with large-scale changes in sea surface temperature in southern Humboldt (Cubillos *et al.* 2014), and therefore the recovery of the stock seems to be uncertain. Payá (2013)[2] attempted to relate the annual

[2] Payá I (2013) A new body-size hypothesis for variability and level shift of Chilean hoki recruitment. In:

deviations of the recruitment of Patagonian grenadier to the Humboldt Current Index (HCI, http://www.bluewater.cl/HCI/hci.html) and found lower but significant coefficients of determination (r^2=0.39, $p<0.05$). According to Payá, changes in the average weight-at-age were better explained by environmental variability associated with El Niño-Southern Oscillation variability, and hence involved in the lower productivity of Patagonian grenadier after 2000. Nevertheless, although the average weight-at-age is involved in the spawning stock biomass estimation it is not involved directly in the recruitment abundance.

The growing exploitation rate of Patagonian grenadier during the period 2000-2010 was due to the southern trawl fishery, producing a significant reduction in the average age and the juvenescence of the population. The catch-at-age data of this fishery, as well as in the catch-at-age of the acoustic surveys, revealed the reduction in the average age and greater incidence of juveniles from 2008 to 2010, a situation that is occurring up to 2013 (C. Canales, IFOP, com.pers.).

In this way, the recovery of the spawning stock biomass of Patagonian grenadier could be complemented with a rebuilding plan, because our results are suggesting that the chances for the recovery of the spawning potential are slower under a recruitment shift to high recruitment levels of Patagonian grenadier within 10 years.

In this paper, only constant harvest rates were applied during the projections. This approach seems to be simple, but it has the advantage of tracking directly the changes in abundance. For cyclical fluctuations, Walters and Parma (1996) emphasize that a constant exploitation rate is better at adjusting to changing conditions as expected under climate change. Of course, some management strategies must be designed and evaluated to investigate the performance of a rebuilding plan, and future research should advance

in that direction. According to Punt *et al.* (2013), the management strategies attempting to account for changes in productivity over time can actually lead to greater risk when there are no such changes. Indeed, modifying management strategies to include environmental factors did not improve the performance of management (Basson, 1999, De Oliveira 2006, Brunel *et al.* 2010). Consequently, the harvest strategy must be adjusted in order to give a real chance for the rebuilding the stock of Patagonian grenadier. In this paper, a lower

---

ICES/NAFO Symposium Gadoid Fishries: The ecology and Management of Rebuilding. Saint Andreews, Canada (https://sites.google.com/site/fishassessment/curriculumvitae/scientific-presentations)

exploitation rate had better performance than the current exploitation rate. However, the rebuilding process must take into account the body-growth of the population and especially the path of productivity defined in the biological time scale to prevent overexploitation and the collapse in the medium term. Reducing the exploitation rate will lead to a decrease in the expected catch, and this would increase the probability of stock recovery. The recovery, however, would be feasible only if the recruitment is higher due to a favorable shift. Today the stock has been declared overfished and at risk of depletion, lower spawning stock (2000-2010), lower recruitment levels between 2000-2010 (unfavorable), and deterioration of the age structure (2008-2010). In addition, juveniles are dominating in the age and length composition, and the age at maturity of females showed a reduction of 2.4 years (Lillo *et al.* 2011). The current situation of Patagonian grenadier is very affected by exploitation, and therefore the probability of rebuilding the stock of Patagonian grenadier is uncertain.

It is suggested that incorporating explicitly a recruitment regime shift in the stock assessment model of Patagonian grenadier could help in identifying better trajectories of recovery. In addition, it is recommendable to apply lower exploitation rates that permit to reduce the current catch. Furthermore, it is necessary to establish further restrictions in terms of harvest rule, and to implement actions to reduce the impact on the reproductive fraction and on juveniles by intensifying the monitoring of indicators of the resource, especially recruitment levels and ultimately to maintain a constant exploitation strategy to set the allowable catch equal to a constant fraction of the population of Patagonian grenadier.

Acknowledgements

This study was supported by the CONICYT master scholarship to SCO, and the COPAS Sur-Austral program PFB-31/2014. In addition, we also thank to researcher of EPOMAR at the Department of Oceanography, University of Concepcion, Chile. Thank also goes to CSIRO by facilitating the Postgraduate Studenteship to SCO, and G Tuck for review of an early version of this paper.

References

Barry, D., and Hartigan, J.A. (1993). "Bayesian Analysis for Change Point Problems. *Journal of the American Statistical Association*, 35(3): 309-319.

Basson, M. (1999). The importance of environmental factors in the design of management procedures. *ICES Journal of Marine Science*, 56: 933–942.

Brunel, T., Piet, G. J., and Ro¨ckmann, C. (2010). Performance of harvest control rules in a variable environment. *ICES Journal of Marine Science*, 67: 1051–1062.

Cubillos L., & Arcos. 2002. Recruiment of common sardine (*Strangomera bentincki*) and anchovy (*Engraulis ringens*) off central-south Chile in the 1990s and the impact of the 1997-1998 El Niño. Aquat. Living Resour, 15:87-94.

Cubillos, L.A., Niklitschek, E.J., and Cahuin S. (2014). Relating a recruitment shift of Patagonian grenadier (*Macruronus magellanicus* Lönnberg) to large-scale environmental changes off Southern Chile. *New Zealand Journal of Marine and Freshwater Research* 48(2), 284-293.

Cook, R.M. (1998). A sustainability criterion for the exploitation of North Sea cod. *ICES Journal of Marine Science,* 55, 1061–1070.

De Oliveira, J. A. A. (2006). Long-term harvest strategies for small pelagic fisheries under regime shifts: the South African fishery for pilchard and anchovy. In Climate Change and the Economics of the World's Fisheries. *Examples of Small Pelagic Stocks*, pp. 151–204.

Espino M. 2013 El jurel Trachurus murphui y las variables ambientales de microescala, Revista Peruana de Biología 20: 09-20.

Helser, T.E., Sharov, A., and Kahn, D.M. (2001). A stochastic decision-based approach to assessing the status of the Delaware Bay blue crab (Callinectes sapidus) stock, Pages 9-24 In Uncertainty in Fisheries Models (J. Berkson and L. Kline, eds.). *American Fisheries Society Symposium* 24.

Helle K., Pennington M., Bogstad B. & G. Ottersen. 2002. Early environmental influences on growth of Arcto-Norwegian cod, *Gadus morhua*, from the 0-group to adults. Environmental Biology of Fishes 65, 341-348

Hurrell W. & H. Van Loon. 1997. Decadal variations in climate associated with the North Atlantic oscillation. Climatic Change 36, 301-326.

Hutchings, J.A., Minto, C., Ricard, D., Baum, J.K., and Jensen, O.P. (2010). Trends in the abundance of marine fishes. *Canadian Journal of Fisheries and Aquatic Sciences* 67, 1205-1210.

Erdman, C., and Emerson, J.W. (2007). Bcp: An r package for performing a bayesian analysis of change point problems. *Journal of Statistical Software* 23(3), 1-13.

Fiksen, O., and Slotte, A. (2002). Stock-environment recruitment models for Norwegian spring spawning herring (*Clupea harengus*). *Canadian Journal of Fisheries and Aquatic Sciences* 59, 211–217.

Fournier, D.A., Skaug, H.J., Ancheta, J., Ianelli, J., Magnusson, A., Maunder, M.N., Nielsen, A., and Sibert, J. (2012). AD Model Builder: using automatic differentiation for statistical inference of highly parameterized complex nonlinear models. *Optimization Methods Software* 27, 333-249.

Glantz, M.H., and Feingold, L.E. (1992). Climate variability, climate change, and fisheries: a summary. In: Glantz, M.H. (Ed.), Climate Variability, Climate Change, and Fisheries. *Cambridge University Press, UK* 17, 417–438.

ICES, 2006a. Report of the Working Group on the Assessment of Demersal Stocks in the North Sea and Skagerrak. *ICES CM 2006/ACFM* 09, 890.

Kell, L.T., Pilling, G.M., and O'Brien, C.M. (2005). Implications of climate change for the management of North Sea cod (*Gadus morhua*). *ICES Journal of Marine Science.* 62, 1483–1491.

Lillo, S., Molina, E., Ojeda, V., and Muñoz, L (2011). Evaluación de stock desovante de merluza del sur y merluza de cola en la zona sur austral, año 2011. Informe de Avance proyecto FIP 2011-04. *Instituto de Fomento Pesquero*. 66 p.

Mace, P.M. and Doonan, I.J. (1988). A generalised bioeconomic simulation model for fish population dynamics. New Zealand Fishery Assessment Research Document 88/4. Fisheries Research Centre, MAFFish, POB 297, Wellington, NZ.

Mantua N.J., Hare S.R., Zhang Y., Wallace J.M. & R.C. Francis. 1997. A Pacific decadal climate oscillation with impacts on salmon. B.A.M. Meteorol. Soc., 78:1069-1079.

Namias J. & D.R. Cayan. 1981. Large-scale air-sea interactions and short-period climate fluctuations. Science 214, 869–878

Nichols, J.H. (2001). Management of North Sea herring and prospects for the new millennium. Herring. Expectations for a New Millennium, pp. 645–665. Lowell Wakefield Fisheries Symposium Series no. 18, Alaska Sea Grant Coll. Program, Fairbanks, AK, USA.
Niquen, M., and Bouchon, M. (2004). Impact of El Niño events on pelagic fisheries in Peruvian waters. *Deep-Sea Research.* II 51, 563–574.

Payá, I., Montecinos, M., González, J., Céspedes, R., Adasme, L., Ojeda, V., and Lillo, S. (2005). Investigación CTP regionalizada de merluza de cola, 2005 Fase II. *Subsecretaria de Pesca – Instituto de Fomento Pesquero* 41.

Payá, I., and Canales, C. (2012). Estatus y posibilidad de Explotación Biológicamente Sustentable de los Principales Recursos Pesqueros Nacionales, año 2012. Merluza de cola. Informe Complementario. *Instituto de Fomento Pesquero* 345.

Perry, I., Cury, P., Brander, K., Jennings, S., Möllmann, C., and Planque, B. (2010). Sensitivity of marine systems to climate and fishing: Concepts, issues and management responses. *Journal of Marine Systems* 79, 427-435.

Pörtner H.O., Berdal B., Blust R., Brix O., Colosimo A., De Watcher B., Giuliani A., Johansen T., Fischer T., Knust R., Lanning G., Naevdal G., Nedenes A., Nyhammer G., Sartoris F.J., Serendero I., Sirabella P., Thorkildsen S. & M. Zakhartsev. 2001. Climate induced temperature effects on growth performance, fecundity and recruitment in the marine fish: developing a hypothesis for cause and effect relationships in Atlantic cod (*Gadus morhua*) and common eelpout (*Zoarces viviparus*). Continental Shelf Research 21, 1975-1997

Planque B., Fox C.J., Saunders A.S. & P. Rockett. 2003. On the prediction of short term changes in the recruitment of North Sea cod (*Gadus morhua*) using statistical temperature forecasts. Scientia Marina 67, 211-218

Punt, A.E., A'mar, T., Bond, N.A., Butterworth, D.S, de Moor, C.L., De Oliveira, J.A.A., Haltuch, M.A., Hollowed, A.B., and Szuwalski, C. (2013) Fisheries management under climate and environmental uncertainty: control rules and performance simulation. *ICES Journal of Marine Science* doi:10.1093/icesjms/fst057.

Rodionov, S. (2004). A sequencial algorithm for testing climate regime shifts, *Geophysical Research Letters* 31, L09204.

Sánchez G., Calienes R. & S. Zuta. 2000. The 1997-98 El Nino and its effects on the coastal marine ecosystem off Peru. CalCOFI Report. 41, 62-86.

Sánchez R., Sánchez F. & J. Gil. 2002. The Optimal Environmental Window that control the hake (*Merluccius merluccius*) recruitment in the Cantabrian Sea ICES Journal of Marine Science 57, 152-170.

Simmonds, E.J. (2007). Comparison of two periods of North Sea herring stock management: success, failure, and monetary value. *ICES Journal of Marine Science.* 64, 686–692.

Shelton, P.A., Sinclair, A.F., Chouinard, G.A., and Mohn, R. 2006. Fishing under low productivity conditions is further delaying recovery of Northwest Atlantic cod (*Gadus morhua*). *Canadian Journal of Fisheries and Aquatic Sciences.* 63, 235–238.

Spencer, P.D., and Collie, J.S. (1997a). Patterns of population variability in marine fish stocks. *Fisheries. Oceanography.* 6:188-204.

Stein M. & V.A. Borovkov. 2004. Greenland cod (*Gadus morhua*): modeling recruitment variation during the second half of the 20th century. Fisheries Oceanography 13, 111-120

Tascheri, R., Saavedra-Nievas, J.C., and Roa-Ureta, R. (2010). Statistical models to standardize catch rates in the multi-species trawl fishery for Patagonian grenadier (*Macruronus magellanicus*) off Southern Chile. *Fisheries Research* 105, 200-214.

Toresen, R., and Ostvedt, O.J. (2000). Variation in abundance of Norwegian spring spawning herring (*Clupea harengus*, Clupeidae) throughout the 20th century and the influence of climatic fluctuations. *Fish and Fisheries* 1, 231–256.

Vert-pre, K.A., Amoroso, R.O., Jensen, O.P., and Hilborn, R. (2013). Frequency and intensity of productivity regime shifts in marine fish stocks *Proceeding of the National Academy of Science* 110, 1779-1784.

Visbeck M., Chassignet E., Curry R., Delworth T., Dickson B. & G. Krahmann 2003. The oceans´s response to North Atlantic Oscilation Variability. En: J. Hurrell, Y. Kushnir, G. Ottersen, M. Visbeck (Eds.) The North Atlantic Oscilation: climatic significance and environmental impact 113-146 pp. American Geophysycal Union.

Walters, C., and Parma, A. M. (1996). Fixed exploitation rate strategies for coping with effects of climate change. *Canadian Journal of Fisheries and Aquatic Sciences*, 53: 148–158.

Watanabe, Y. (2007). Latitudinal variation in the recruitment dynamics of small pelagic fishes in the western North Pacific. *Journal of Sea Research* 58, 46–58.

Wayte, S.E. (2013). Management implications of including a climate-induced recruitment shift in the stock assessment for jackass morwong (*Nemadactylus macropterus*) in south-eastern Australia. *Fisheries Research* 147, 47-55.

Yáñez, E., Barbieri, M.A., Silva, C., Nieto, K., and Espíndola, F. (2001). Climate variability and pelagic fisheries in northern Chile. *Prog. Oceanogr* 49, 581–596.

CAPITULO II

The performance of an age-structured stock assessment model for the Patagonian grenadier (*Macruronus magellanicus*) in the face of decadal regime shifts of recruitment

S. Curin-Osorio[1,3], Luis A. Cubillos[2,3]

[1]Programa de Magíster en Ciencias con mención en Pesquerías, Universidad de Concepción, Chile, Programa COPAS Sur-Austral, Departamento de Oceanografía, Universidad de Concepción, Chile. [3]Laboratorio de Evaluación de Poblaciones Marinas (EPOMAR), Departamento de Oceanografía, Facultad de Ciencias Naturales y Oceanográficas, Universidad de Concepción, Casilla 160-C, Concepción, Chile.

Artículo por enviar: Fisheries Research (En preparación)

Abstract

Interdecadal step-like changes or cyclical fluctuations in recruitment could affect the performance of an age-structured stock assessment, particularly when uncertainty in recruitment is high and abundance indices are based on commercial catch rates mainly. The performance of the stock assessment model (SAM) of the Patagonian grenadier (*Macruronus magellanicus*) stock was evaluated under decadal changes in recruitment. An operative model (OM) considered two structural hypotheses of decadal fluctuations in recruitment allowed to simulating the current fishery-dependent and fishery-independent data under constant exploitation rates. Each simulation consisted of a projection of 40 years by sampling parameters from the posterior of the OM through the Markov Chain Monte Carlo (MCMC) technique. In each year of the 40-year projection, the SAM estimated the main population variables and provided estimates of catch per fleet that impacted in the OM. The performance of the current SAM was evaluated by considering a combination of two sources of error: a) structural and process error in the recruitment fluctuations and b) observation error in the abundance indices. The SAM had better performance when the recruitment was cyclical, estimating changes in biomass with MARE of 5.7 to 6.7%. However, the SAM showed a tendency to underestimating the recruitment during the transition from lower to higher recruitment levels, and to overestimating when the recruitment changed from higher to lower levels. The worst performance occurred when the exploitation rate was high and when the recruitment changed abruptly from low to higher recruitment levels (step-like shift). The mean bias was higher for recruitment than for total biomass or spawning biomass. Under step-like interdecadal shift in recruitment, it is highly recommendable to incorporate a recruitment index in the current SAM, particularly during the phase of low recruitments. In addition, because *M. magellanicus* is overexploited, the recruitment index could help in better performance during the current phase of low recruitments

Key-words: operating model, regimen, recruitment, performance.

Introduction

The Patagonian grenadier, *Macruronus magellanicus*, is an important demersal fish resource for Chile, being caught by two bottom trawl fleets operating on the continental shelf off central (34ºS-42ºS) and southern (42ºS-57ºS) Chile. Also, a purse-seine fleet operated on the Patagonian grenadier fishery off central Chile during the austral spring, achieved higher catches and sustained by juveniles mainly Cubillos et al. (2009). According to Payá and Canales (2012), the stock assessment considers a single and homogeneous stock unit from Valparaíso (33ºS) to the Tierra del Fuego (57ºS). The assessment is a complex task for Patagonian grenadier due to numerous assumptions and treatment of data. The stock assessment model (SAM) consists of an age-structured population dynamics, assuming that capture of each fleet is known without error and occurring instantaneously at different time periods within the year. Biological parameters, such as natural mortality, maturity, and steepness of the stock-recruitment are constants. The age composition data ranged between ages 1 and 14, and available for both the southern trawl fleet (1980-2010) and the central trawl fleet (2003-2009). The age composition data of the purse seine fleet covers only from 1997 to 2001. Abundance indices based on catch and effort data covers different years and spatial stratum. For example, the standardized catch per unit effort (CPUE) based on the purse-seine fleet only includes central Chile (34ºS-42ºS) and from 1997 to 2001. The CPUE of the southern bottom trawl fleet includes from 1988 to 2009, and treated with three periods in which the coefficient of catchability remains constant because changes in fishing regime (Tascheri et al., 2010). In addition, acoustic biomass and the survey age composition are the only independent fishery data. The acoustic biomass is evaluated during the peak of the spawning period by assuming that the stock is concentrated to spawn Lillo et al. (2009). Uncertainty in the assessment of Patagonian grenadier can arise from the several sources of errors, particularly at the moment of weighting the relative importance of the different piece of data. Although the structural statistical treatment of the different piece of data is important to conditioning the SAM, the performance could be affected in those stocks in which the abundance is driven by recruitment regime shifts (Punt and Kennedy, 1997; Breen et al., 2001; Bentley et al., 2001).

In 2010, the stock of Patagonian grenadier was overexploited and prognosticated with higher risk of depletion due to intense exploitation. However, Cubillos et al. (2014) suggested the possibility that a recruitment regime shift from a high to low level after 1999 could also be contributing to the depleted status of the stock in 2010. A reversal to the higher productive recruitment level could be uncertain in the future. Therefore, it is expected that the SAM must estimate any significant change in the recruitment level precisely and without bias. The use of an operative model is the main approach to evaluate the performance of a SAM by considering both observation error and process error. The process error propagates in time due to variability not considered in the stock-recruitment function, and the observation error affects mainly due to variability in the abundance indices (Hilborn and Walters, 1992). The approaches have considering the influence of different models for the observation error in the abundance indices (Ludwig and Walters, 1981; Schnute 1991; Hilborn and Walters, 1992), but the final evaluation of both the process error and the observation error can permit to known the precision and bias of the estimates obtained with a SAM (Freeman and Kirwood, 1995; Punt, 2003). The objective of this paper is to evaluate the performance of the SAM of Patagonian grenadier under uncertainty in future decadal recruitment fluctuations. The hypothesis considers that the SAM is able to track step-like recruitment shifts in recruitment of Patagonian grenadier.

Materials and methods

General approach

The present study was carried out using a simulation framework with an age-structured model as the operating model (OM) and the estimation model (SAM). The main difference between the OM and the SAM is that the OM included two cases of interdecadal variation in recruitment (see below). One of the advantages of evaluating the performance of assessment methods by using simulation is that the true parameter values and the true status of the population are known exactly (Butterworth and Punt, 1999; **Punt, 2003**). In this paper the approach was to carry out simulations by sampling the parameters from the posterior of the OM and whose samples were obtained through Markov Chain Monte Carlo (MCMC), as implemented in the AD Model Builder software Fournier et al. (2012).

The simulation framework consisted of the steps described in Figure 7. The first step was the conditioning of an operating model, which represented the 'true' population dynamics of Patagonian grenadier. The second step was generating data using the operating model to provide fishery data (partial catch and age composition) and abundance indices (catch per unit effort, acoustic biomass and the age-composition of the survey) for each year of a 40-year period of projection. In each year of the projection, the SAM provided total catch and the estimates of interest (recruitment, total biomass, and spawning stock biomass). The total catch impacted in the OM and therefore in the population dynamics during the 40-year period of projection. The third step was to repeat the previous steps for 100.000 times and saving each 100 by using MCMC.

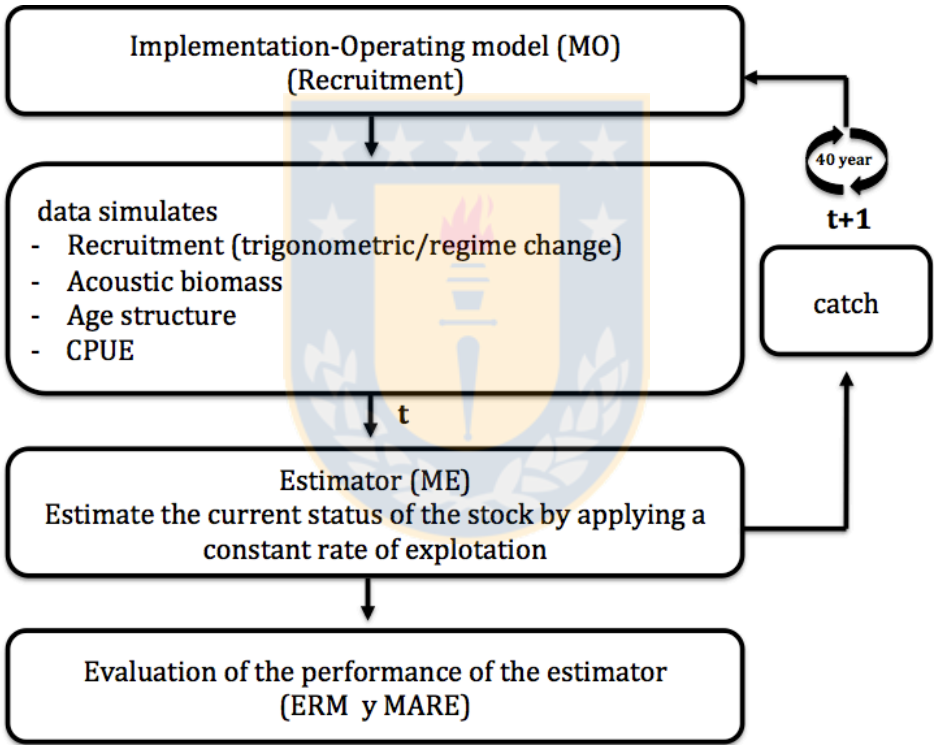

Figura 7: General approach used to evaluate the performance of the stock assessment model of Patagonian grenadier under interdecadal fluctuations in recruitment.

The performance of the SAM was evaluated in the future by considering constant exploitation rates (μ=0, μ=0.1, and μ=0.18). In each year, the SAM estimated the total catch associated to each exploitation rate. The total catch (Q_i) estimated from the SAM, was allocated among fishing fleets according to:

$$
\begin{aligned}
Y_i &= 0.95 \times Q_i \\
Y_i^{ps} &= 0.01 \times Y_i \\
Y_i^{ct} &= 0.59 \times Y_i \\
Y_i^{st} &= 0.4 \times Y_i
\end{aligned}
\qquad (17)
$$

where Y_i is the total catch attained in year i, and assumed to be 95% of the total catch estimated by SAM. The participation of the purse-seine fleet was assumed to be negligible in the future (Y_i^{ps}), and that the bottom trawl fleet operating off central Chile will contribute with 59% to total catch, while the southern trawl fleet only 40%. The allocation of total catch is in agreement with the current allocation of total allowable catches of Patagonian grenadier between central (60%) and southern Chile (40%), from 95% of the TAC. The 5% is reserved for bycatch or for research (Payá and Canales, 2011a)

2.1. Stock assessment model

The stock assessment model (SAM) used in this study was described by Payá and Canales (2012), and covered the period 1980-2010. The SAM assumes that Patagonian grenadier is a self-sustained and homogeneous stock distributed in the southeast Pacific and distributed from northern Valparaíso to Magellan's strait (Aviles *et al.,* 1979, Arana, 1970). The SAM is a discrete age-structured model in which catch is known without error. The partial catch come from three fishing fleets (Table 7). The bottom trawl fleet of the central zone covered the period from 2003 to 2010, and operated mainly on the continental shelf off central Chile (33ºS-41º40'S). The purse-seine fleet operated on surface waters off central Chile from 1980 to 2003, and the bottom trawl fleet operated along the continental shelf of Patagonian waters (42ºS-52ºS) from 1980-2010. Weight-at-age data by fishing fleets covered the same periods previously described, and the weight-at-age data from the southern bottom trawl fleet allowed to compute the weight-at-age at the beginning of each year for the stock. The indices of abundance were acoustic biomass and catch per unit effort (CPUE). The acoustic biomass and the age composition in the survey covered from 2000-2010. The CPUE data were obtained from the purse-seine fleet (1980-2003) and from the southern bottom trawl fleet (1980-2010). Payá and Canales (2012) documented details of the data as well as methodological aspects of the SAM. Natural mortality was set at 0.35 per year, and maturity was assumed to be constant across years.

Tabla 7. Data used in the age-structured stock assessment model of Patagonian grenadier, showing the period covered for each one.

Area	Fleet	Catch	Catch at age	Acoustic Biomass and age composition	CPUE
Central	Purse-seine	1987-2005	1997-2001	-	1988-2002
(33ºS-41º40'S)	Bottom trawl	2001-2010	2003-2009	-	-
Southern	Bottom trawl	1980-2010	1988-2009	2000-2010	1980-2009
(41º40'S-57ºS)					

2.2. Operating model

The operating model was conditioned on the basis of the SAM. The main modification of SAM consisted in the recruitment function in order to carry out future projections under uncertainty. The OM incorporated a step-like regime shift in the stock-recruitment model of Beverton and Holt, i.e.,

$$R_i = \begin{cases} \dfrac{S_{i-1}}{\alpha_1 + \beta_1 S_{i-1}} \exp(\varepsilon_i) & i \le 1999 \\ \dfrac{S_{i-1}}{\alpha_2 + \beta_2 S_{i-1}} \exp(\varepsilon_i) & i > 1999 \end{cases} \tag{18}$$

where R_i is the recruitment at the beginning of year i, S_i is the spawning stock biomass, α and β are parameters to be estimated, and ε_i are deviations of recruitment from the S-R model, which are assumed to be normally distributed with constant variance, i.e., $N(0,\sigma_R^2)$ with σ_R set equal to 0.6. The parameters α and β were estimated according to the re-parameterization of Mace and Doonan (1998), i.e,

$$\alpha_k = \frac{(1-h)}{4h}\frac{S_{0,k}}{\overline{R}_k}$$
$$\beta_k = \frac{(5h-1)}{4h\overline{R}_k} \tag{19}$$

where h is the steepness (h = 0.75) of the stock-recruit curve, $R_{k=1}$ is the average recruitment in the high recruitment regime (1980-1999), and $R_{k=2}$ is the average recruitment in the low recruitment regime (200-2010); $S_{0,k}$ is the expected spawning stock biomass

without exploitation as a function of the k average recruitment level. This approach considered a change in the productivity of the stock-recruitment relationship along the replacement line (Figure 8), without changes in maturity, weight-at-age and natural mortality.

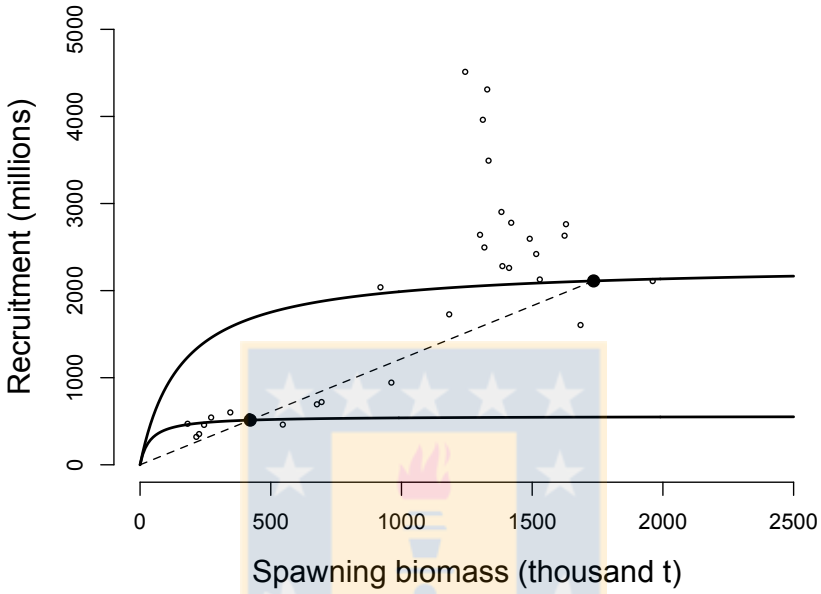

Figura 8. Model of two recruitment regimes in the stock-recruitment relationship of the Patagonian grenadier. The segmented line represents the replacement line of the S-R, and the points are the data of recruitment and spawning stock biomass for the period 1980-2010, according to results of the SAM of Payá and Canales (2012).

During the projection period, a recruitment shift from low to high recruitment was modeled to occur within 10±5 year in the OM to mimic interdecadal recruitment. The ±5 year was chosen because it is the half of 10 year period. The point of change was chosen at random from an uniform distribution between 2015 and 2025.

As an alternative, and because the performance of the SAM was evaluated by simulating future changes, further interdecadal recruitment simulations considered cyclical fluctuations according the following trigonometric model, i.e.,

$$R_i = [\overline{R} + A \times \cos(2\pi \times n \times i - \varphi]\exp(\varepsilon_i) \qquad (20)$$

where R is the average recruitment in the period 1980-2010, A is the amplitude (=7.15), n=0.06 and φ=2.48 are the phases of the cosine curve, and ε_i are deviations of recruitment from the S-R model assumed to be normally distributed with constant variance $N(0,\sigma_R^2)$. The model was fitted by least square to the recruitment of the period 1980-2010, and used in the OM to simulate future cyclical changes in the average recruitment of Patagonian grenadier.

2.3. Evaluation of the performance

The bias and precision of the SAM was evaluated according to the relative error and the mean of absolute relative error (Punt, 2003; Johnson et al., 2014; Kotaro-Ono et al., 2014) for a set of scenarios (Table 2). The relative error was calculated according to:

$$E_{i,j,k} = 100 \times \frac{Q^{SAM}_{i,j,k} - Q^{OM}_{i,j,k}}{Q^{OM}_{i,j,k}} \quad (21)$$

where $E_{i,j,k}$ is the relative error in year i, for the quantity j and simulation k, $Q^{SAM}{}_{i,j,k}$ is the quantity of interest estimated by the SAM, and $Q^{OM}{}_{i,j,k}$ is the quantity of interest assumed to be true and provided by the operating model. The quantities of interest were the recruitment, the spawning stock biomass, and the total biomass of Patagonian grenadier. The bias was evaluated by computing the confidence intervals at 75% and 90% of $E_{i,j,k}$, and the precision was computed according to the MARE for the 40 years of projections. The scenarios considered 8 combinations between step-like and cyclical fluctuations of recruitment, and between observation error and process error (Table 8).

Table 8: Scenarios to evaluate the performance of the stock assessment model of the Patagonian grenadier under interdecadal recruitment fluctuations (1: step-like recruitment shift, 2: cyclical recruitment), considering process error in recruitment (1: with process error, 2: without process error), and observation error (1: without observation error, 2: with observation error).

Escenarios	S-R	EP	EO
E1	1	1	2
E2	1	1	1
E3	1	2	1
E4	1	2	2
E5	2	2	2
E6	2	2	1
E7	2	1	1
E8	2	1	2

Results

On average, the MARE showed that the bias of the SAM varied among scenarios. The less bias was registered when cyclical recruitment was simulated with process error (scenarios S7 and S8 in Table 3). When the cyclical recruitment was simulated without process error, the bias of the recruitment estimates by the SAM fluctuated between 15.0% and 16% at μ=0.01 and μ=0.1, respectively (Table 9). The simulations under step-like recruitment shift without process error (S3 and S5), the bias of the SAM was also higher in the recruitment, being more biased for scenarios S1 and S2 at μ=0.18 (Table 9).

The relative error showed that the SAM tends to underestimate the recruitment (R), the spawning stock biomass (SSB) and the total biomass (B) when the recruitment was either step-like or cyclical and when the harvest rate was low (μ=0.01) or moderate (μ=0.1). However, the SAM overestimated the R, SSB and B when the exploitation rate was set at the target μ=0.18 (Table 9).

Table 9: Performance of the stock assessment model of Patagonian grenadier through the mean of the absolute relative error (MARE) under different exploitation rates (μ) for recruitment (R), spawning stock biomass (SSB) and total biomass (B_t).

	μ1=0.01			μ2=0.1			μ3=0.18		
	R	SSB	B	R	SSB	B	R	SSB	B
S1	4.5	1.3	1.4	1.2	0.3	1.3	13.9	14.2	15.9
S2	4.2	1.6	1.4	1.7	0.8	1.2	13.3	13.2	15.2
S3	15.2	1.7	1.0	12.0	0.9	1.7	0.9	9.8	13.8
S4	15.7	1.7	1.0	12.3	1.0	1.5	0.7	9.7	13.5
S5	15.8	3.2	3.3	15.0	3.3	2.3	8.4	4.9	7.0
S6	16.0	3.2	3.5	15.5	3.3	2.3	8.5	4.9	7.0
S7	7.0	3.0	3.8	7.6	3.2	3.2	1.4	5.3	5.8
S8	6.3	2.8	3.5	6.7	2.8	3.0	0.3	5.7	6.2

The SAM had better performance in the scenario S8 (i.e., cyclical recruitment with both the process error and the observation error) with lower MARE (Table 9). In this case the SAM tends to overestimate the recruitment when it is actually low, and tends to underestimate the recruitment when it is in the period with higher recruitment in the cycle (Fig. 9). Nevertheless, the SAM was able to follow the tendency in SSB and B with lower relative error (Fig. 9). Although the MARE was lower, the distribution of frequency showed the tendency to overestimate (Fig. 10), particularly under the target harvest rate and when the recruitment started to decline the SAM overestimated the recruitment and biomass during the period 2030-2040 (Fig. 11). The tendency to overestimate the R, SSB and B was greater when the exploitation rate was 0.18, and expressed with greater variability (Fig. 11).

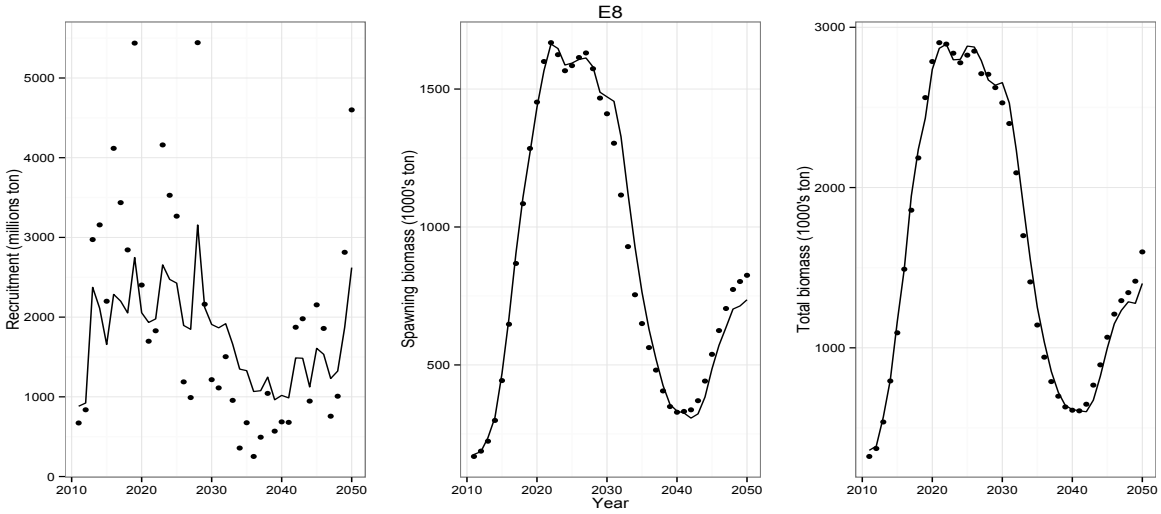

Figura 9: Example of a realization during a 40-year projection of recruitment, spawning stock biomass, and total biomass of Patagonian grenadier. The dots represent quantities coming from the operating model and the lines represent estimates obtained with the stock assessment model. Case E8 (cyclical recruitment, with both process and observation errors).

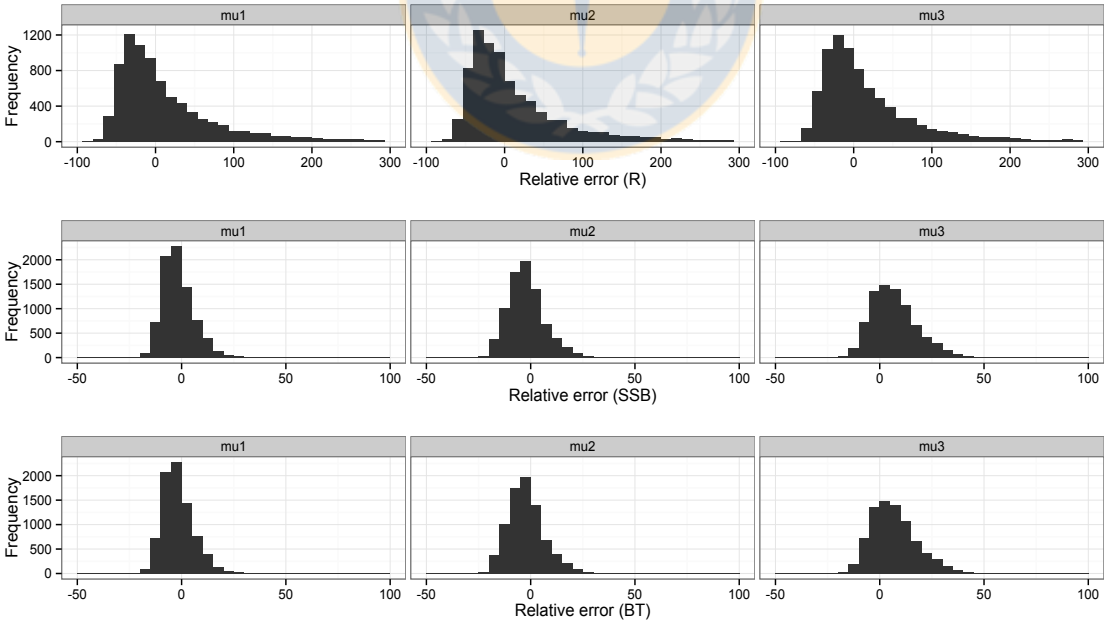

Figura 10. Frequency distribution of the relative error for recruitment (R), spawning stock biomass (SSB) and total biomass (BT) for scenario E8 (cyclical recruitment, with both process and observation errors).

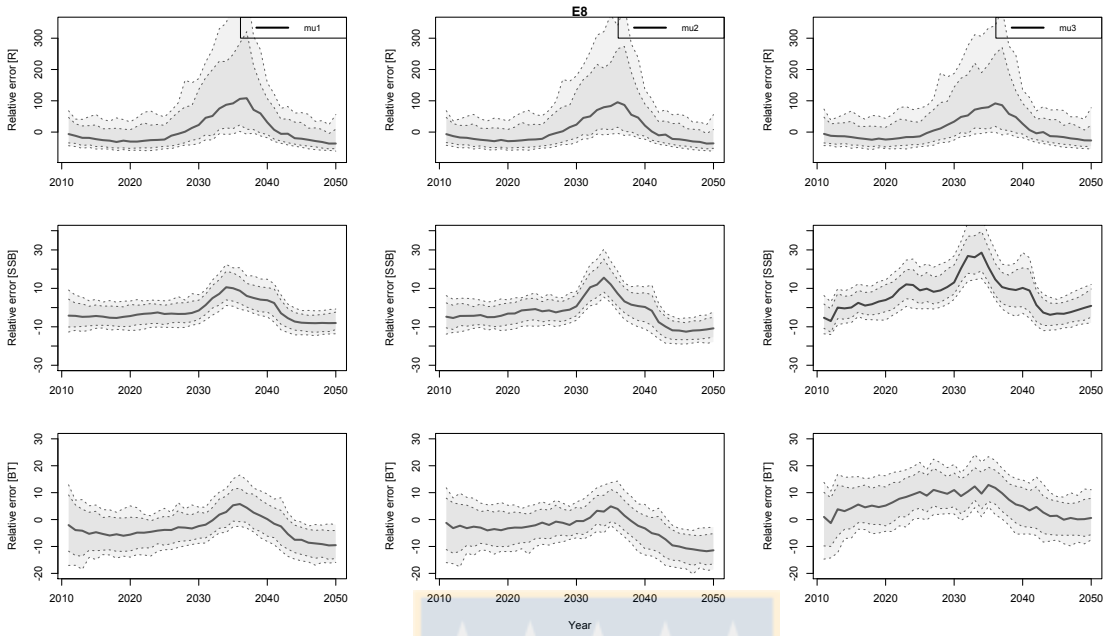

Figura 11. Time series for the relative error of recruitment (R), spawning stock biomass (SSB) and total biomass (BT), escenario E8. The dark region represents confidence intervals of 75% and the lighter region confidence intervals of 90%, the black line represents the average relative error.

The worst performance of the SAM occurred under scenario S1 (i.e., step-like recruitment, with both the process error and the observation error) under the target harvest rate (μ=0.18) (Table 9). The overestimation of the recruitment occurred between 2011 and 2025 when the recruitment was still in the low recruitment level and underestimated during the high recruitment level (Fig. 12). The recruitment was overestimated by 13.9%, the SSB by 14.2% and the B by 15.9%. Nevertheless, the distribution of frequency of the relative error showed less range and less bias under the lower harvest rates (Fig. 13). The relative error showed that during the period 2030-2040, the SSB was overestimated and particularly when the harvest rate was the highest (Fig. 14).

The SAM was able to estimate the step-like recruitment shift, but the recruitment estimates were higher than the OM during 2011-2025 and lower during the period 2030-2050. The relative error indicated that SSB and B were estimated with less relative error on average, but 90% confidence level showed that the relative error of SAM was wider and less precise at μ=0.18 and more narrow and precise for μ=0.1 and μ=0.01 (Fig. 14).

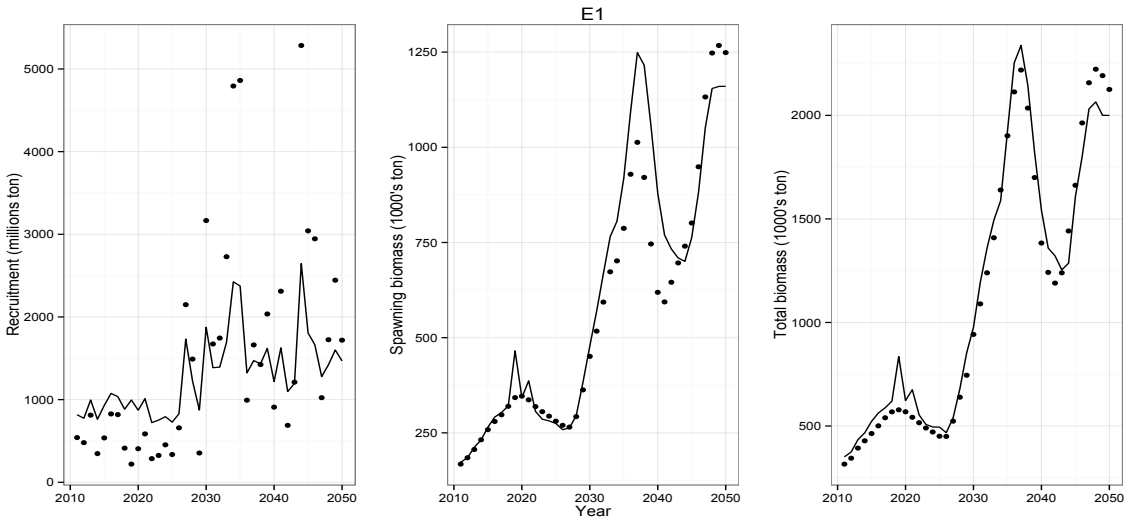

Figura 12. Example of a realization during a 40-year projection of recruitment, spawning stock biomass, and total biomass of Patagonian grenadier. The dots represent quantities coming from the operating model and the lines represent estimates obtained with the stock assessment model. Case E1 (step-like recruitment, with both process and observation errors).

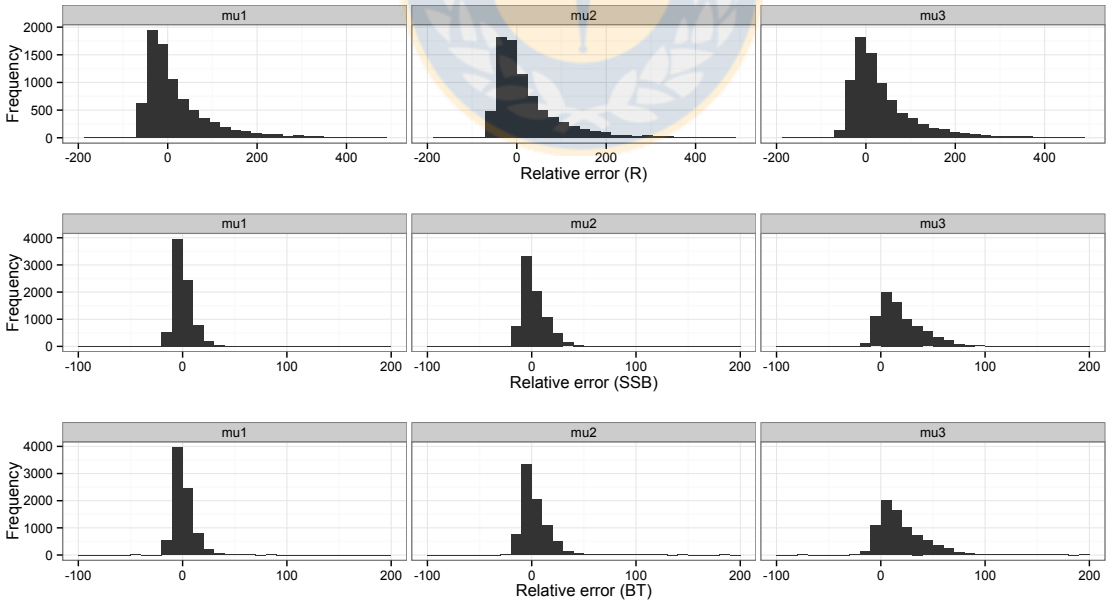

Figura 13. Frequency distribution of the relative error for recruitment (R), spawning stock biomass (SSB) and total biomass (BT) for scenario E1 (with both process and observation errors).

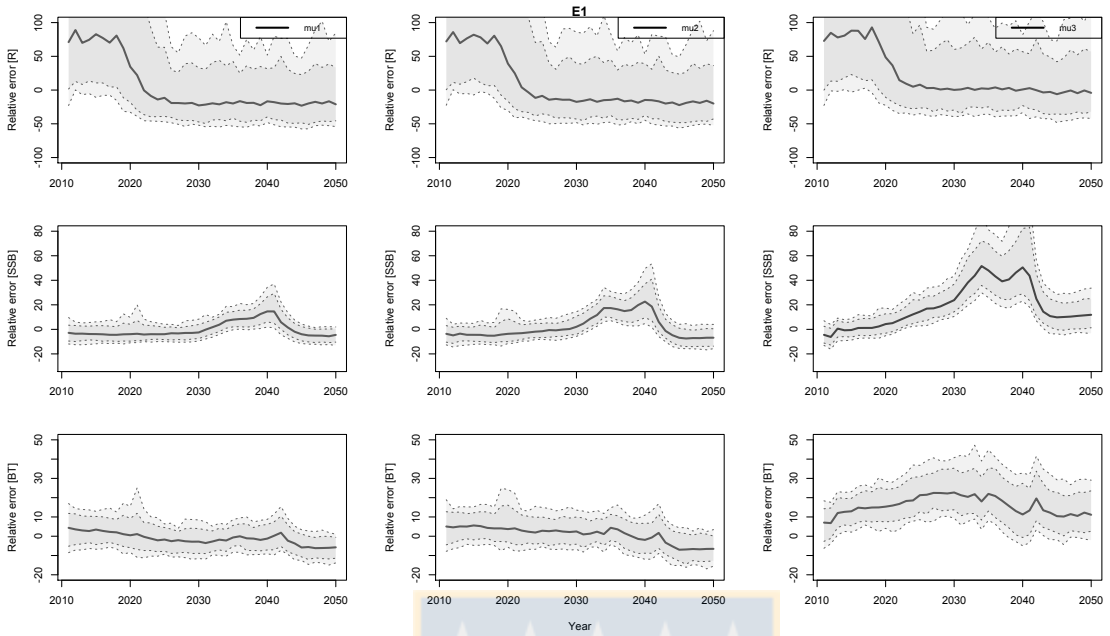

Figura 14. Time series for the relative error of recruitment (R), spawning stock biomass (SSB) and total biomass (BT), escenario E1. The dark region represents confidence intervals of 75% and the lighter region confidence intervals of 90%, the black line represents the average relative error.

Discussion

Despite the effects of intense exploitation on fish populations, long-term fluctuations in abundance of fish populations can be driven by interdecadal variability in recruitment (Clark et al., 1999; Chavez et al., 2003). For the Patagonian grenadier stock, Cubillos et al. (2014) suggested a recruitment shift after 1999. The change from high to low recruitment was coincident with large- scale changes in sea surface temperature anomalies in the nursery areas of Patagonian grenadier. It is not at all clear what mechanisms are at work and the reversal to previous high recruitment level is in fact uncertain. In this way, the assumption that the stock assessment model of Patagonian grenadier must be able to estimate the recruitment precise and accurately was here evaluated.

If the population dynamics of Patagonian grenadier is being driven by step-like recruitment changes, the SAM (with/without process and observation errors) could to overestimate the recruitment during the low recruitment regime and underestimate the recruitment during the high recruitment regime. Similarly, the SAM tended to overestimate the recruitment during the transition from higher to lower under cyclical fluctuations in recruitment, with process and observation errors. Although the interannual deviations of recruitment are estimated by setting σ=0.6, the underestimation and overestimation of recruitment could be due to the fit of the stock-recruitment model of Beverton and Holt in the SAM. The stock-recruitment could be important for the most recent year in the SAM by forcing the estimated recruitment to lying close to the expected recruitment of the Beverton and Holt model.

On average, the MARE values of the SAM were acceptable, but in some years or periods the relative error (bias) could be very higher. The bias of the SAM increased the variance and the mean of the relative error between 2030 and 2040 under cyclical recruitment, and between 2011-2025 under a step-like recruitment shift. The SAM was not able to estimate accurately the recruitment during the transition from low to higher levels when the true recruitment was cyclical, arising the variability and overestimating the recruitment. This effect was channelized to the total biomass and spawning stock biomass. From the point of view of the MARE, the worst performance of the SAM was applying the target harvest rate under a recruitment regime shift from low to high levels, i.e., scenario E1 with process and observation errors. The MARE was better for the same scenario when the harvest rate was moderate (i.e., 10%) or very lower (i.e., 1%). Although the precision was better according to the MARE, the bias was higher and variable during the projection. The worst performance under scenario E1 was due to the target harvest rate (μ=18%), the high interannual variability of recruitment (i.e., σ=0.6), and the shift in the stock-recruitment relationship from low to high levels. These factors seems to be adding variability in recruitment and the SAM was not able to estimate accurately that variability, which was propagated to the total biomass and the spawning stock biomass between 2030 and 2040. Although the variability observed in the relative error was high during periods of transition, the MARE could be even more sensitive to outliers of recruitment (Punt, 2003; Ono et al., 2014). For the case of cyclical recruitment, the variability registered in the relative error occurred during transition periods from high to low recruitments. From the point of view of

the MARE, the SAM had better performance following a population with cyclical recruitment for each exploitation rate applied. The recruitment was estimated with MARE of 6.29%, 6.71% and 0.25% for exploitation rate of 1%, 10% and 18%, respectively. Nevertheless, important biases occurred during 2030-2040, even for the best scenario (E8). The SAM was not able to detect exactly the year in which a regime shift occurred. This result is in agreement with those of Szuwalski and Punt (2012) for the snow crab fishery in the Bering Sea.

According to Szuwalski and Punt (2012), when a population is functioning with decadal regime shifts in recruitment and if the management or the stock assessment ignores that characteristic. In this way, incorporating changes in inferred productivity in SAM and management strategies of Patagonian grenadier could reduce bias in calculating the target biomasses in regime-based systems. Probably, a model with regime shifts in the stock-recruitment model will require to observing pre-recruit abundance or a recruitment index of abundance. The SAM would be improving by observing recruits some years before they entering to the fishery, but probably the challenge would be for the management because a stock may be falsely declared overexploited under current not regime-based target biomass (Szuwalsky and Punt, 2012). Similar results found A'mar et al. (2009) for Theragra cholcogramma, demonstrating that incorporating regime shifts into the SAM would increase the probability of overfishing. In addition, the authors found similar performance between a regime-based model and one standard model that not took into account changes in productivity associated to the recruitment. Nevertheless, Polovina (2005), McFarlane (2006), Szuwalski and Punt (2012) and Vert-pre et al. (2013), demonstrated that stock assessment models regime-based of pelagic and demersal species explained more than 60% the changes in productivity associated to the recruitment, or 40% for the case of models incorporating explicitly decadal changes of the environment impacting the recruitment. The better performance of models incorporating explicitly regime shifts in recruitment would be better for the management, in terms of adjusting the target biomass.

Although the SAM of the Patagonian grenadier had acceptable performance, the SAM was not able to estimate accurately the recruitment for the most recent year. Precision and bias are important components, and therefore it is advisable to evaluate the performance of the SAM by incorporating explicitly regime changes with observations based on a recruitment

index of abundance. The challenge on regime-based stock assessment and management lye on detecting exactly and precisely the year in which a shift occurred because within-regime interannual variability, and to adjust opportune the reference for management.

Acknowledgements

This study was supported by the CONICYT master scholarship to SCO, and the COPAS Sur-Austral program PFB-31/2014. In addition, we also thank to researcher of EPOMAR at the Department of Oceanography, University of Concepcion, Chile. Thank also goes to CSIRO by facilitating the Postgraduate Studenteship to SCO, and G Tuck for review of an early version of this paper.

Reference

Arana, P. 1970. Nota sobre la presencia de ejemplares de merluza de cola (*Macruronus magellanicus* Lonnberg) frente a las costas de Valparaíso. Invest. Mar., Valparaíso, 1(3): 55-68.

Aviles, S., M. Aguayo & J. Cañón. 1979. Merluza de cola *(Macruronus megallanicus* Lonnberg). In: Estado Actual de las Principales Pesquerías Nacionales. Bases para un desarrollo Pesquero. Peces. CORFO/IFOP, AP79-18: 1-25.

Bentley, N., Breen, P.A., Starr, P.J., Kendrick, T., 2001. Assessment of the CRA3 and NSS substocks of red rock lobster (Jasus edwardsii) for 2000. New Zealand Fisheries Assessment Report 2001/69, 84 pp.

Breen, P.A., Starr, P.J., Bentley, N., 2001. Rock lobster stock assessment for the NSN substock and the combined CRA 4 and CRA 5 areas. New Zealand Fisheries Assessment Report 2001/7, 73 pp

Butterworth, D.S. and A.E. Punt. 1999. An initial examination of possible inferences concerning MSYR for Southern Hemisphere minke whales from recruitment trends estimated in catch-at-age analyses. *J. Cetacean Res. Manage*. 1(1): 33-39.

Chavez, F., J. Ryan, S. Lluch-Cota, and Ñiquen C. M. (2003), From anchovies to sardines and back: Multidecadal change in the Pacific Ocean, Science, 299(5604), 217–221.

Cubillos, L.A., Riquelme, K., Ernst, B., 2009. Cambios latitudinales en la pesquería pelágica de merluza de cola (*Macruronus magellanicus*) de la zona centro-sur (1986-2003). Latin American Journal of Aquatic Research 37, 121-129.

Cubillos L.A, Niklitschek E.J, Cahuin S. 2014. Relating a recruitment shift of Patagonian grenadier (*Macruronus magellanicus* Lönnberg) to large-scale environmental changes off Southern Chile. New Zealand Journal of Marine and Freshwater Research, 48(2): 284-293

Ernt, B., Armstrong, D.A., Burgos, J., and Orensanz, J.M. (2012). Life history schedule and periodic recruitment of female snow crab (chionoecetes opilio) in the eastern Bering Sea. Can. J. Fish. Aquat. Sci. 69(3): 532-550.

Freeman, S.N. and Kirkwood, G.P. (1995). On a structural time series method for estimating stock biomass and recruitment from catch and effort data. Fish. Res., 22: 77–98

Fournier, D.A., Skaug, H.J., Ancheta, J., Ianelli, J., Magnusson, A., Maunder, M.N., Nielsen, A., and Sibert, J. (2012). AD Model Builder: using automatic differentiation for statistical inference of highly parameterized complex nonlinear models. *Optimization Methods Software* 27, 333-249.

Hilborn, R. and Walters, C. (1992). Quantitative Fisheries Stock Assessment. Choice, Dynamics and Uncertainty. Chapman-Hall, New York, 570 pp.

Johnson, K. F.,Monnahan, C. C., McGilliard, C. R., Vert-pre, K. A., Anderson, S. C., Cunningham, C. J., Hurtado-Ferro, F., Licandeo, R. R., Muradian, M. L., Ono, K., Szuwalski, C. S., Valero, J. L., Whitten, A. R., and Punt, A. E. 2014. Time-varying naturalmortality in fisheries stock assessment models: identifying a default approach. – ICES Journal of Marine Science, doi: 10.1093/icesjms/fsu055.

Kotaro Ono, Roberto Licandeo, Melissa L. Muradian, Curry J. Cunningham, Sean C. Anderson, Felipe Hurtado-Ferro, Kelli F. Johnson, Carey R. McGilliard, Cole C Monnhan, Cody S. Szuwalski, Juan L. Valero, Katyana A. Vert-Pre, Athol R. Whitten, and André E. Punt (2014). The importance of length and age composition data in statistical age-structured models for marine species. ICES Journal of Marine Science,doi:10.1093/icesjms/fsu007.

Lillo, S., E. Molina, J. Saavedra, J. Olivares, E. Díaz, S. Núñez, E. Navarro, S. Vásquez, R. Alarcón, A. Sepúlveda, M. Braun & A. Saavedra. 2009. Evaluación hidroacústica de merluza común, año 2008. Informe Final FIP-IT/2008-14: 209 pp.

Ludwig, D. and Walters, C. (1981). Measurement errors and uncertainty in parameter estimates for stock and recruitment. Can. J. Fish. Aquat. Sci., 38: 711–720.

Mace, P.M. and Doonan, I.J. (1988). A generalised bioeconomic simulation model for fish population dynamics. New Zealand Fishery Assessment Research Document 88/4. Fisheries Research Centre, MAFFish, POB 297, Wellington, NZ.

Payá, I. y C. Canales. 2011 a. Estatus y Posibilidades de Explotación Biológicamente Sustentables de los Principales Recursos Pesqueros Nacionales, año 2012. Merluza de cola. Segundo Informe. Octubre 2011. IFOP. 103 p.

Payá, I., and Canales, C. (2012). Estatus y posibilidad de Explotación Biológicamente Sustentable de los Principales Recursos Pesqueros Nacionales, año 2012. Merluza de cola. Informe Complementario. *Instituto de Fomento Pesquero* 345.

Punt, A.E., Kennedy, R.B., 1997. Population modelling of Tasmanian rock lobster, Jasus edwardsii, resources. Mar. Freshwater Res. 48, 967–980.

Punt, A. 2003. The performance of a size-structured stock assessment method in the face of spatial heterogeneity in growth. Fisheries Research 65:391-409.

Punt, AE. 2003. Extending production models to include process error in the population dynamics. Can. J. Fish. Aquat. Sci. 60:1217-1228.

Schnute, J. (1991). The importance of noise in fish population models. Fish. Res., 11: 197–223.

Tascheri, R., Saavedra-Nievas, J.C., and Roa-Ureta, R. (2010). Statistical models to standardize catch rates in the multi-species trawl fishery for Patagonian grenadier (*Macruronus magellanicus*) off Southern Chile. *Fisheries Research* 105, 200-214.

DISCUSION GENERAL

La aplicación del modelo operativo con cambio de régimen en el reclutamiento de la pesquería de merluza de cola permitió evaluar el desempeño del modelo incorporando cambios en la productividad del reclutamiento de forma escalonada u cíclico, y a su vez estimar la probabilidad de recuperación de merluza de cola. Sin embargo este cambio decadal en la productividad del reclutamiento observado por Paya y Canales 2012; Cubillos et al., 2014, fueron espurios cuando el coeficiente de variación de la biomasa hidroacustica fue mayor a 0.05. Sin embargo los valores de biomasa con coeficiente de variación mayor a 0.05 eran absurdos, por lo que el CV de la biomasa hidroacústica se mantuvo bajo en el modelo de evaluación (SAMR), como consecuencia, se detecto la presencia de un cambio de régimen en el 2000.

el modelo que incorporó explícitamente el cambio de régimen (SAMR) tuvo un mejor desempeño que el modelo original (SAMs), obteniendo coeficiente de variación para las deviaciones anuales del reclutamiento menores y menos variable que el modelo original (SAMs), esto implicó que el modelo SAMs ignoró el cambio de régimen utilizando el reclutamiento promedio histórico independiente de los cambio de productividad decadal que presentó el stock, incrementando la varibilidad de las desviaciones del reclutamiento, por el contrario al incorporar dos reclutamientos promedios uno que represente el períodos de alta productividad y otro de baja productividad se tradujó en una suavización de la serie de tiempo, disminuyendo la varianza de las desviaciones anuales del reclutamiento y como consecuencia mejor ajuste.

En el contexto de un futuro plan de manejo para Patagonian grenadier considerando los cambios de productividad en el modelo de evaluación de stock (SAMR), los resultados mostraron que la presencia de un cambio en el reclutamiento a bajas o altas abundancia tiene importantes consecuencias para el manejo y recuperación de la población. Además, la baja productividad actual de la merluza de cola pareciera estar unido a anomalías de gran escala de la temperatura superficial del mar (Cubillos et al., 2014) lo que concuerda con Payá (2013) quien encontró un relación significativa entre las desviaciones del índice de corriente de Humbolt (HCI) y las desviaciones del reclutamiento a través de dos modelo S-R (Ricker y Beverton-Holt) pero con bajo coeficiente de relación para ambos modelos

(0.32 y 0.39 respectivamente), por lo que Paya (2013) concluyó que el peso a la edad es la variable responsable de este cambio de régimen y que el modelo que incorpora esta variación presenta mejor ajuste en la relación S-R tanto para el modelo Beverton-Holt como Ricker y con desviaciones más bajas y menos variable que el modelo que incorpora el cambio de régimen . Sin embargo el peso promedio a la edad no tiene una incidencia directa en la estimación del reclutamiento como lo es el valor de coeficiente de variación que se le asigne al índice de biomasa hidroacústica o como la creciente tasa de explotación aplicado por la pesquería de arrastre de fondo sur la que podría haber determinado una reducción significativa en la edad media y una mayor incidencia de juveniles en la población, tales como se revela en la encuesta de datos de captura por edad y el Catch-comercial datos por edad (Payá y Canales 2012).

El modelo SAMs el cual no incorpora cambio de régimen, al plicar una tasa de explotación objetiva (U40%PHPR=0.18), los resultados mostraron que hay cero probabilidad de recuperación entre el 2011-2050 y sobre un 92% de probabilidad que el stock este bajo el umbral limite (Pr[St/S0<0.2), mientras que el modelo SAMR el cual incorpora tácitamente el cambio de régimen, este al aplicar el punto biológico biológico objetivo mostró que la proporción de la biomasa reproductora (St/S0) disminuyó significativamente en el tiempo de proyección reduciendo el stock reproductor a niveles críticos con tan solo 23% de probabilidad de recuperación para y con un 20% de probabilidad de depleción en el año 2030, en el caso del modelo con reclutamiento cíclico, este se recupera en el año 2020 con un. Por otra parte, esta misma evaluación estimó que las tasa de explotación habría llegado a remover mas del 60% del stock en 1999, lo que es completamente insustentable para una especie de mediana productividad con las características de *M. magellanicus*. En consecuencia, la estrategia de explotación pesquera en tiempo real debería fundamentarse en el proceso de crecimiento diferencial de la población y muy especialmente en la trayectoria de productividad definida en la escala de tiempo biológico para evitar la sobreexplotación y los colapsos a mediano y largo plazo, si bien la reducción de la tasa de explotación dará lugar a una disminución de la captura estimada esta incrementara la probabilidad de recuperación del stock, solo si el reclutamiento se encuentra en un período de altos reclutamientos (favorable), niveles de alta abundancia en la biomasa reproductora y condiciones ambientales optimas, este seria el escenario mas favorable al que pueda estar

expuesto la merluza de cola y por lo tanto recuperarse significativamente después del 2050, sin embargo, en la actualidad el stock fue declarado sobreexplotado y con riesgo de agotamiento o colapso debido a la pesca excesiva ejercida en años anteriores, adicionalmente se evidenció bajos niveles de reclutamiento entre 2000-2010 (desfavorable), condiciones ambientales adversas (ENSO: 2000-2010), bajos niveles del stock reproductor (2000-2010), además se evidenció un progresivo deterioro en la estructura de longitudes y edades del stock desovante, una ostensible reducción en la abundancia del recurso, y una reducción de 2.4 años en la edad de primera madurez al 50% de las hembras (Lillo et al., 2011) por lo que la probabilidad de recuperación del stock *M magellanicus* es incierta. En este contexto se recha la hipótesis que la estrategia de manejo actual es robustos a escenarios de fluctuaciones interdecadales para merluza de cola, ya que la probabilidad de recuperación en el stock incorporando cambios en la productividad y aplicando una tasa de explotación 40%PHPR ocurre solo después del 2045 y con una probabilidad de depleción mayor al 70% durante 2011-2025.

Si bien la dinámica poblacional de merluza de cola está siendo impulsado por los cambios en el reclutamiento, los resultados obtenidos sugieren que el desempeño del modelo de evaluación SAM que incorpora cambio de productividad de forma cíclica/escalona, con/sin error de observación o con/sin error de proceso, resultaron en una sobreestimación a bajo niveles de reclutamientos y subestimación a altos niveles de reclutamientos. El modelo SAM en general tuvo un buen desempeño con sesgos dentro de los niveles aceptables, sin embargo el sesgos se incrementó cuando hubo cambio de productividad en el reclutamiento.

El escenario con peor desempeño al aplicar una tasa de explotación objetiva, fue el modelo E1 (con cambio de régimen, con error de proceso y con error de observación) sobrestimando el reclutamiento en 13.9%, biomasa desovante en 14.24% y biomasa total en 15.96%, sin embargo al disminuir la tasa de explotación a media o baja el E1 tiende a subestimar las cantidades de interés pero con una mejor precisión que al aplicar una tasa de explotación objetivo. Si bien el E1 fue más preciso a baja explotación el sesgo de la estimación del reclutamiento fue alta y variable en el tiempo (2011-2050) . Al parecer y dado los resultados en el E1, el mal desempeño se generó por la alta tasa de explotación, la incorporiación del error de proceso en la relación stock-recluta, la alta incertidumbre del

reclutamiento (Cv=0.6) y la incorporación de un cambio de régimen en la relación stock-recluta, quienes sumaron variabilidad en los errores relativos medios de las estimaciones de las desviaciones del reclutamiento la que se tradujo en una propagación en el tiempo y que la cual se intensifico cuando las desviaciones del reclutamiento pasaron de bajos a altos niveles de reclutamiento incrementado significativamente la varianza de la mediana del error relativo (MARE) entre el modelo operativo y el modelo de estimación en el año 2040. Si bien esta variabilidad del sesgo es alta en períodos de transición del reclutamiento aplicando una tasa de explotación alta, esta puede ser aun mayor si se utiliza como medida central el promedio de los errores relativos absoluto siendo más sensibles a los puntos outlier del reclutamiento entre amobos modelos (Punt 2003, Ono et al., 2014). En el caso del reclutamiento cíclico el incremento en la variabilidad del sesgo parece estar asociado a las desviaciones del reclutamiento, la alta penalidad del reclutamiento y al error designado en el modelo trigonométrico y no específicamente a la tasa de explotación ni al error de proceso u observacion ya que el modelo que tuvo mejor desempeño fue el escenario E8 (reclutamiento cíclico, con error de proceso y con error de observación) subestimando el reclutamiento en tan solo 6.29%, 6.71% y 0.25% a una tasa de explotación baja, media y alta respectivamente, siendo bastante precisas en las estimaciones de interes. Sin embargo y al igual que el escenario con cambios régime el escenario E8 presentó estimaciones sesgadas en las desviaciones del reclutamiento incrementando la varibilidad de los errores relativos medios cuando las desviaciones del reclutamiento pasaron de bajos a altos niveles de reclutamiento. Otras posibles causas en las estimaciones sesgadas del reclutamiento podría estar dada por la poca precisión de los métodos para detectar exactamente en el año que se produjó el cambio de regimen, debido a la alta variabilidad que contiene la serie de las desviaciones del reclutamiento dado los dos niveles en las desviaciones del reclutamiento (alto y bajo) y por ende incrementa la variabilidad de los errores relativos medio generando estimaciones inverosímiles para la biomasa desovante y total. Estos resultados concuerdan con los resultados de Szuwalski and Punt (2012) para la pesquería snow crab en el este del Mar de Bering quienes detectan la misma variabilidad del MARE en las estimaciones del reclutamiento al incorporar un cambio de regimen.

Sin embargo esta impresición de los errores relativos medios se pierde al utilizar modelos que no son basados en regímenes teniendo estimaciones de biomasa más precisas, pero no

necesariamente representativa de la dinámica del stock de m cola. Si bien la observación de reclutas antes de entrar a la pesquería era una oportunidad potencial para identificar los cambios de regímenes A'mar et al., 2009 demostró que incorporar cambios de régimen en el modelo de evaluación de stock de *Theragra cholcogramma* incrementa la sobrepesca obeteniendo un desempeño muy similares al modelo que no incorpora cambios en la productividad del reclutamiento concluyendo que el modelo de evaluación de stock con y sin cambio de régimen en el reclutamiento no diferen en su desempeño. Sin embargo Polovina 2005, McFarlane 2006, Szuwalski and Punt 2012 y Vert-pre et al 2013, difieren con A'mar et al 2009 quienes demostraron que aquellas evaluaciones de stock (demersales o pelágicas) basadas en modelos con cambio de régimen en el reclutamiento explican más 60% los cambios en la productividad del reclutamiento o 40% aquellos incorporan los cambios decadales del ambiente y del reclutamiento, obeteniendo un mejor desempeño que los modelos que no incorporan cambio de régimen, siendo relevante para el manejo de los recursos y concordando con los resultados obtenidos en esta estudio donde los cambios de productividad y la alta tasa de explotación son importante al momento de evaluar el desempeño del modelo de evaluación que el error de proceso y error de observación. Lo que difiere con Ernst et al., 2012 quien cuestiona el impacto de la pesca sobre la dinamíca del reclutamiento de snow crab.

Si bien el modelo SAM tiene un buen desempeño en términos de la precisión promedio, éste no fue capaz de estimar el reclutamiento de una forma exacta ya que se observaron sesgos importantes en la estimación del reclutamiento durante cambios de regimen (E3, E4, E5 y E6). En este contexo se rechaza la hipótesis de robustez del modelo de evaluación de stock bajos escenarios con fluctuaciones interdecadales futuras del reclutamiento de merluza de cola (*Macruronus magellanicus*) en la zona sur austral de Chile.

Para futuras investigaciones se sugiere, incluir los cambios de productividad del reclutamiento en la evaluación de stock, utilizar un índice de reclutamiento para Patagonia grenadier que pueda reproducir los cambios de productividad del reclutamiento con el fin de obtener estimaciones más fiables de las cantidades de interés lo que podría reflejarse en un mejor desempeño del modelo con cambio de régimen, establecer restricciones adicionales a la forma de una regla de decisión y mantener la estrategia de explotación constante, si bien una tasa de explotación constante (cantidad) no es ecológicamente

sostenible, establecer la captura permisible igual a una fracción constante del tamaño de la población es sostenible, en un stock en condiciones deterioradas como es el caso de *M magellanicus*.

BIBLIOGRAFÍA

A'Mar Z.T., Punt A.E & Dorn N.M. 2009. The impact of regime shifts on the performance of management strategies for the Gulf of Alaska walleye pollock (Theragra chalcogramma) fishery. Canadian Journal Fisheries Aquatic Sciences, 66, 2222-2242.

Aguayo M., Young Z., Bustos R., Peñailillo T., Ojeda V., Vera C., Hidalgo H & I. Céspedes. 1987. Diagnóstico de las principales pesquería nacionales demersales (peces) zona sur-austral. 1986. Estado de situación del recurso. Instituto de Fomento Pesquero AP 87/3, 209 p.

Aguayo M., Paya I., Bustos R., Ojeda V., Gili R., Vera C., Céspedes I & L. Cid. 1990. Diagnóstico de las principales pesquería nacionales demersales (peces) zona sur-austral. 1988. Estado de situación del recurso. Instituto de Fomento Pesquero AP 89/17a, 161 p.

Angelescu V., Gneri F & A. Nani. 1958. La merluza del mar argentino (Biología y Taxonomía). Publicaciones. Servicio Hidrográfico Naval, Secretaria de Marina, Buenos Aires H 1004: 1-224.

Arana P. 1970. Nota sobre la presencia de ejemplares de merluza de *cola (Macruronus magellanicus* Lönnberg) frente a la costa de Valparaíso. Investigaciones Marinas 1 (3): 50-60.

Bailey K.M., Ciannelli L & V. Agostini. 2003. Complexity and constraints combined in simple models of recruitment. En: Browman, H. and Skiftesvik, A. (Eds.) Proceedings of the 26th Annual Larval Fish Conference. 293-301. Institute of Marine Research Bergen, Norway.

Bakun A. 1996. Patterns in the Ocean, Ocean Processes and Marine Populations Dynamics. California Sea Grant College System, NOAA, 323 pp.

Canales C, P. Galvez, V. Escobar, R. Tascheri, R. Céspedes, J. Quiroz, R. Roa, 2008. Investigación CTP Regionalizada de merluza de cola, 2007. SUBPESCA. Informe Final, IFOP, 51 p

Canales C., P. Galvez, R. Tascheri, D. Bucarey, R. Cespedes. 2009. Investigación CTP Regionalizada de merluza de cola, 2009. SUBPESCA. Informe Final, IFOP, 75 p (más anexos).

Canales C., R. Tascheri, J.C. Saavedra y R. Céspedes. 2010. Investigación del estatus y evaluación de estrategias de explotación en merluza de cola, 2010. SUBPESCA. Informe Final, IFOP, 71 p (más 1 anexo).

Chesheva Z.A. 1992. Data on the biology of the Magellan hake, *Macruronus magellanicus*, from the Southwestern Atlantic. Journal of Ichthyology 32(7): 137-141.

Chong J.V. 2000. Ciclo de maduración ovárica, fecundidad y talla de madurez en *Macruronus magellanicus* (Lönnberg, 1907) de la zona sur de Chile. Biología Pesquera 28:3-13

Chong J.V. 2002. Revisión de la reproducción en merluza de cola y merluza de tres aletas. En: Evaluación de merluza de cola y merluza de tres aletas, Informe Final Proyecto FIP 2000-15, Tomo II.

Cohen D., Inada T., Iwamoto T & N. Scialabba. 1990. Gadiform fishes of the world (Order Gadiformes). FAO Species Catalogue. FAO Fisheries Synopsis 125 (10): 1-442.

Cubillos L., & Arcos. 2002. Recruiment of common sardine (*Strangomera bentincki*) and anchovy (*Engraulis ringens*) off central-south Chile in the 1990s and the impact of the 1997-1998 El Niño. Aquat. Living Resour, 15:87-94.

Cubillos L.A, Niklitschek E.J, Cahuin S. 2014. Relating a recruitment shift of Patagonian

grenadier (*Macruronus magellanicus* Lönnberg) to large-scale environmental changes off Southern Chile. New Zealand Journal of Marine and Freshwater Research, 48(2): 284-293

Cushing D.H. 1995. Population production and regulation in the sea. Cambridge University Press, Cambridge, UK.

Cushing D.H. 1996. Towards a Science of recruitment in fishpopulations. En O. Kinne (Ed.), Excellence in ecology 7. Ecology Institute, Nordbünte 23, D-21385 Oldendorf/Luhe, Germany.

Czaja A. 2003. On the time variability of the net ocean-to-atmosphere heat flux in midlatitudes, with application to the North Atlantic basin. Quarterly Journal of the Royal Meteorological Society 129, 2867-2878.

D'Amato M.E & Carvalho G.R. 2005. Population genetic structure and history of the long-tailed hake, Macruronus magellanicus, in the SW Atlantic as revealed by mtDNA RFLP analysis. ICES Journal of Marine Science 62: 247-255.

Ernst B., Aedo G., Roa R., Cubillos L., Rubilar P., Zuleta A., Castro L & M. Landaeta. 2005. Evaluación del reclutamiento de merluza de cola entre la V y X Region: revisión metodologica. Informe Final FIP 2004-12.

Fogarty M.J., Sissenwine M.P & E.B. Cohen. 1991. Recruitment variability and the dynamics of exploited marine populations. Trends Ecology and Evolution 6, 241–246

Fogarty M. 1993. Recruitment in randomly varying environments. ICES Journal of Marine Science 50, 247-260.

Fournier D.A., Skaug H.J., Ancheta J., Ianelli J., Magnusson A., Maunder M.N., Nielsen A & J. Sibert. 2012. AD Model Builder: using automatic differentiation for statistical inference of highly parameterized complex nonlinear models. Optim. Methods Softw. 27:233-249.

Francis M. P. 1993. Does water temperature determine year class strength in New Zealand snapper (*Pagrus auratus*, Sparidae)? Fish. Oceanogr. 2:65−72.

Giussi A.R., Hansen J.E. & O. Wöhler. 2002. Estimated total abundance and numers at-age of longtail hake (*Macruronus magellanicus*) in the Southwest Atlantic durin the years 1987-2000. Scientia Marina, 66: 283-291.

Hollowed, A. B., Hare, S. R., and Wooster, W. S. 2001. Pacific Basin climate variability and patterns of Northeastern pacific marine fish production. Progress in Oceanography, 49: 257–282.

Helle K., Pennington M., Bogstad B. & G. Ottersen. 2002. Early environmental influences on growth of Arcto-Norwegian cod, *Gadus morhua*, from the 0-group to adults. Environmental Biology of Fishes 65, 341-348

Hurrell W. & H. Van Loon. 1997. Decadal variations in climate associated with the North Atlantic oscillation. Climatic Change 36, 301-326.

King, J.R., and McFarlane, G.A. 2006. A framework for incorporating climate regime shifts into the management of marine resources. Fish. Manag. Ecol. 13(2): 93–102.

Kim J and Cheon S. 2009 A Bayesian regime-switching time-series model. Journal of Time Series Analysis 31 365–378

Köster F., Hinrichensen H-H., St.John M., Schnack D., MacKenzie B.R. & M. Plikshs. 2001. Developing Baltic cod recruitment models. II. Incorporation of environmental variability and species interaction. Canadian Journal of Fisheries and Aquatic Sciences 58, 1534-1556

Kuo C. & S. Tanaka. 1984. Distribution and migration of the hoki *Macruronus novaezelandidae* (Hector) in water around New Zealand. Bulletin of the Japanese Society of Scientific Fisheries. 50 (3):391-396.

Lett P.F. & A.C. Kohler. 1976. Recruitment: a problem of multispecies interaction and environmental perturbations, with special references to Gulf of St. Lawrence Atlantic herring (*Clupea harengus harengus*). Journal of Fisheries. Research Board of Canada. 33, 1353-1371.

Lillo S., Espejo M., Céspedes R., Adasme L., Blanco J., Letelier J., Braun M. & V. Valenzuela. 1997. Evaluación directa del stock de merluza de cola en la X y XI Regiones. Final FIP 95-18. 70 p.

Mantua N.J., Hare S.R., Zhang Y., Wallace J.M. & R.C. Francis. 1997. A Pacific decadal climate oscillation with impacts on salmon. B.A.M. Meteorol. Soc., 78:1069-1079.

Mantua, N. J., and Hare, S. R. 2002. The Pacific decadal oscillation. Journal of Oceanography, 58: 35–44.

Miller J.M., Burke J.S. & G.R. Fitzhugh. 1991. Early life history patterns of Atlantic North American flatfish: likely (and unlikely) factors controlling recruitment. Netherland Journal of Sea Research 27, 261–275

Mohn R. 1991. Stability and sustainability of harvestingstrategies in a modelled fishery. En: Management Under Uncertainties Related to Biology and Assessments, with Case Studies on some North Atlantic Fisheries. Northwest Atlantic Fisheries Organ 16, 133 - 135. Dartmouth (NS), Canada

Myers R.A. 1998 When do environment-recruit correlations work? Reviews in Fish Biology and Fisheries 8, 285-305

Namias J. & D.R. Cayan. 1981. Large-scale air-sea interactions and short-period climate fluctuations. Science 214, 869–878

Parada C., Yannicelli B., Hormazábal S., Vásquez S., Porobic J., Ernts Billy, Arteaga M., Montecinos A., Nuñez S. & A. Gretchina. 2013. Variabilidad ambiental y recursos pesqueros en el Pacífico suroriental: estado de la investigación y desafíos para el manejo pesquero. Latin American. Journal of Aquatic Research 41, 1-28.

Payá I., N. Ehrhardt, P. Rubilar, C. Montenegro y V. Espejo. 2000. Investigación CTP regionalizada de merluza de cola 2000. Informe Técnico. Instituto de Fomento Pesquero.
Payá I., P. Rubilar, H. Pool, R. Céspedes, H. Reyes, N. Ehrhardt, L. Adasme, H. Hidalgo. 2002. Evaluación de merluza de cola y merluza de tres aletas. FIP 2000-15. Instituto de Fomento Pesquero. 156 páginas (tomo I) y anexos (tomo II).

Payá I., L. Caballero, H. Hidalgo y M. Montecinos 2003. Investigación Captura Total Permisible regionalizada merluza de cola 2003. 25 páginas, 47 figuras, 4 tablas y anexos. Instituto de Fomento Pesquero.

Payá, I., M. Montecinos, J. González, R. Céspedes, L. Adasme, V. Ojeda y S. Lillo. 2005. Investigación CTP regionalizada de merluza de cola, 2005 Fase II. Subsecretaria de Pesca – Instituto de Fomento Pesquero. 41 p.

Payá I. 2006. Investigación evaluación de stock y CTP merluza común, 2006. Informe Prefinal BIP Nº 30043787-0, Instituto de Fomento Pesquero (IFOP), Valparaiso, 39 pp.

Payá, I., and Canales, C. 2012. Estatus y posibilidad de Explotación Biológicamente Sustentable de los Principales Recursos Pesqueros Nacionales, año 2012. Merluza de cola. Informe Complementario. *Instituto de Fomento Pesquero* 345.

Planque B., Fox C.J., Saunders A.S. & P. Rockett. 2003. On the prediction of short term changes in the recruitment of North Sea cod (*Gadus morhua*) using statistical temperature

forecasts. Scientia Marina 67, 211-218.

Polovina, J.J. 2005. Climate variation, regime shifts, and implications for sustainable fisheries. Bull. Mar. Sci. 76: 233–244.

Pörtner H.O., Berdal B., Blust R., Brix O., Colosimo A., De Watcher B., Giuliani A., Johansen T., Fischer T., Knust R., Lanning G., Naevdal G., Nedenes A., Nyhammer G., Sartoris F.J., Serendero I., Sirabella P., Thorkildsen S. & M. Zakhartsev. 2001. Climate induced temperature effects on growth performance, fecundity and recruitment in the marine fish: developing a hypothesis for cause and effect relationships in Atlantic cod (*Gadus morhua*) and common eelpout (*Zoarces viviparus*). Continental Shelf Research 21, 1975-1997

Rodionov, S., and Overland, J. E. 2005. Application of a sequential regime shift detection method to the Bering Sea ecosystem. ICES Journal of Marine Science, 6: 328–332.

Rothschield B. 1986. Dynamics of Marine Fish Populations. Harvard University Press, Cambridge, Massachusetts.

Sabatini M.E. 2004. Caracteristicas ambientales, reproduccion y alimentacion de la merluza *(Merluccius hubbsi*) y la Anchoita (*Engraulis anchoita*) en su hábitat reproductivo patagonico. Sínteis y perspectivas. Invest. Desarr.Pesq 16, 5-25.

Sánchez G., Calienes R. & S. Zuta. 2000. The 1997-98 El Nino and its effects on the coastal marine ecosystem off Peru. CalCOFI Report. 41, 62-86.

Sánchez R., Sánchez F. & J. Gil. 2002. The Optimal Environmental Window that control the hake (*Merluccius merluccius*) recruitment in the Cantabrian Sea ICES Journal of Marine Science 57, 152-170.

Schuchert P.C., Arkhipkin A.I. & Koening A.E. 2010. Traveling around Cape Horn: otolith chemistry reveals a mixed stock of Patagonian hoki with separate Atlantic and Pacific spawning grounds. Fisheries Research 102:80-86.

Stein M. & V.A. Borovkov. 2004. Greenland cod (*Gadus morhua*): modeling recruitment variation during the second half of the 20th century. Fisheries Oceanography 13, 111-120

Szuwalski,C and Punt A.E. 2012. Fisheries management for regime-based ecosystems: a management strategy Evaluation for the snow crab fishery in the Eastern Bering Sea. ICES Journal of Marine Science. Doi: 10.1093/icesjms/frss182.

Tascheri R., Saavedra J.C. & R. Roa. 2010. Statistical models to standardize catch rates in the multi-species trawl fishery for Patagonian grenadier (*Macruronus magellanicus*) off Southern Chile. Fisheries Research, 105, 200-214.

Vert-pre, K.A., Amoroso, R.O., Jensen, O.P., and Hilborn, R. (2013). Frequency and intensity of productivity regime shifts in marine fish stocks *Proceeding of the National Academy of Science* 110, 1779-1784.

Visbeck M., Chassignet E., Curry R., Delworth T., Dickson B. & G. Krahmann 2003. The oceans´s response to North Atlantic Oscilation Variability. En: J. Hurrell, Y. Kushnir, G. Ottersen, M. Visbeck (Eds.) The North Atlantic Oscilation: climatic significance and environmental impact 113-146 pp. American Geophysycal Union.

Wayte S.E. 2013 Management implications of including a climate-induced recruitment shift in the stock assessment for jackass morwong (*Nemadactylus macropterus*) in south-eastern Australia. Fisheries Research, 142, 47-55.

ANEXO 1

Análisis de sensibilidad al cambio de régimen para el stock de merluza de cola (*Macrorunus magallanicus*)

Método secuencial para detectar cambio de régimen en el promedio y varianza

Tabla 10: Análisis de sensibilidad para la CPUE de la pesquería sur austral (CPUEst), Biomasa acústica (HB) y relación stock recluta (S-R), donde E_n son los escenarios plausible.

	E1*	**E2**	**E3**	**E4**	**E5**	**E6**	**E7**	**E8**	**E9**	**E10**	**E11**	**E12**
CPUEst	**0.4-03**	0.4-02	0.4-04	0.4-05	0.4-03	0.4-03	0.4-03	0.4-03	0.4-03	0.4-03	0.4-03	0.4-03
S-R	**0.6**	0.6	0.6	0.6	0.3	0.4	0.5	0.8	0.6	0.6	0.6	0.6
HB	**0.05**	0.05	0.05	0.05	0.05	0.05	0.05	0.05	0.1	**0.15**	**0.2**	**0.3**

* Modelo Base IFOP

Tabla 11: Detección de cambio de régimen en la abundancia de los reclutas a distintos escenarios (E_n)

	Bayesian change point		Change point Rodionov		Relative change
Response variable	Shift year	Posterior prob.	Shift year	*P* value	(Régimen 2-Regimen 1)
E1	1999	0.892	2000	3.2793E-10	-1.39
E2	1999	0.940	2000	6.0815E-11	-1.44
E3	1999	0.940	2009	0.040	5.30
E4	1999	0.968	2000	6.0815E-11	-1.44
E5	1999	0.874	2000	3.6489E-12	-1.33
E6	1999	0.942	2000	3.6489E-12	-1.29
E7	1999	0.928	2000	2.0929E-11	-1.42
E8	1999	0.930	2000	2.3391E-10	-1.43
E9	1999	0.872	2000	1.0858E-09	-1.47
E10	-	0	2000	0.111*	-0.31
E11	-	0	1983	0.157*	0.47
E12	-	0	2008	0.227*	-0.41

*No significativo (cuando el Cv de HB es 0.15; 0.2 y 0.3), lo que concuerda con el método Bayesian.

- MODELO BASE (ESCENARIO 1)

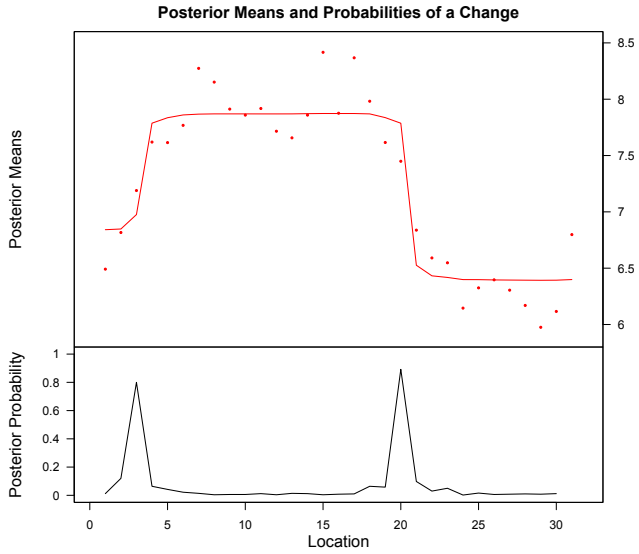

Figura 15: Probabilidad de encontrar un cambio régimen en el escenario (E1), en escala logarítmica. La grafica inferior representa la probabilidad posteriori de cambio de Barry and Hartigan's.

- ESCENARIO 2 (E2)

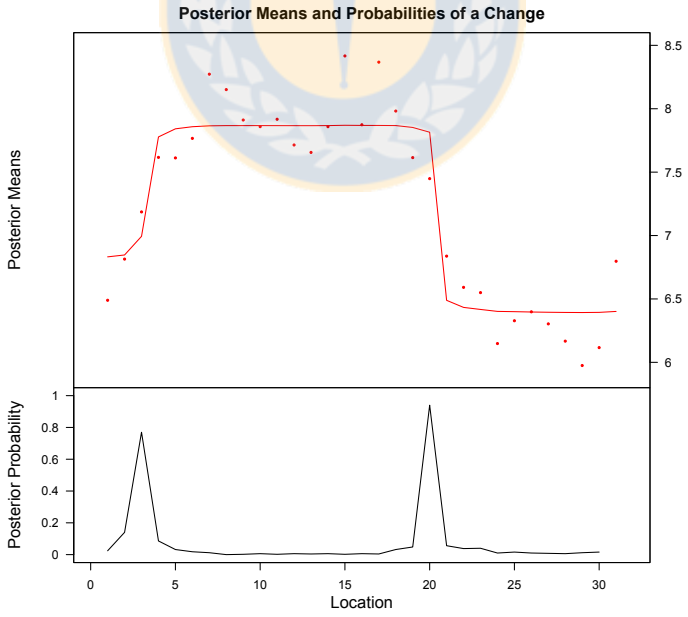

Figura 16: Probabilidad de encontrar un cambio régimen en el escenario (E2), en escala logarítmica. La grafica inferior representa la probabilidad posteriori de cambio de Barry and Hartigan's.

- ESCENARIO 3

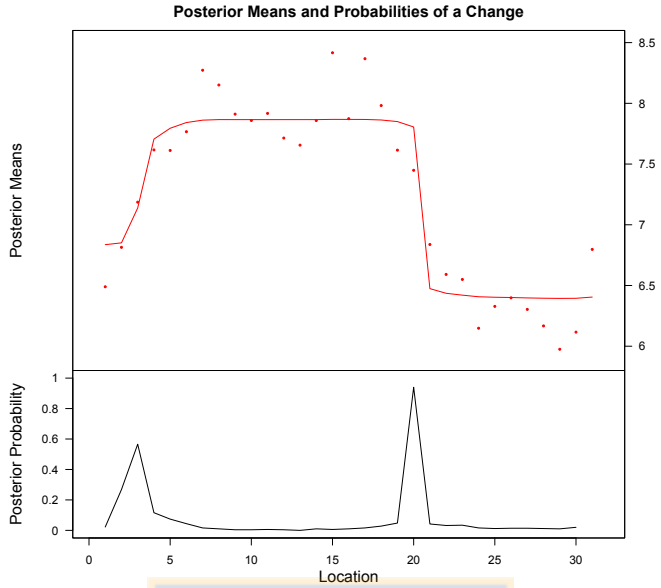

Figura 17: Probabilidad de encontrar un cambio régimen en el escenario (E3), en escala logarítmica. La grafica inferior representa la probabilidad posteriori de cambio de Barry and Hartigan's.

- ESCENARIO 4

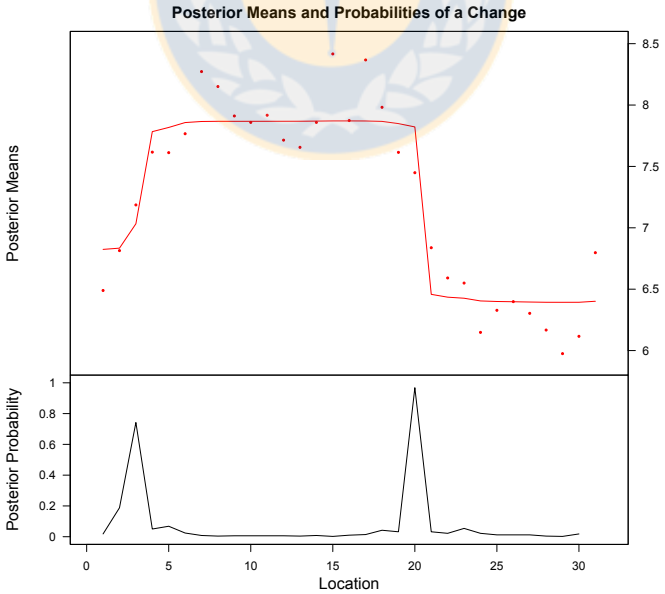

Figura 18: Probabilidad de encontrar un cambio régimen en el escenario (E4), en escala logarítmica. La grafica inferior representa la probabilidad posteriori de cambio de Barry and Hartigan's.

- ESCENARIO 5

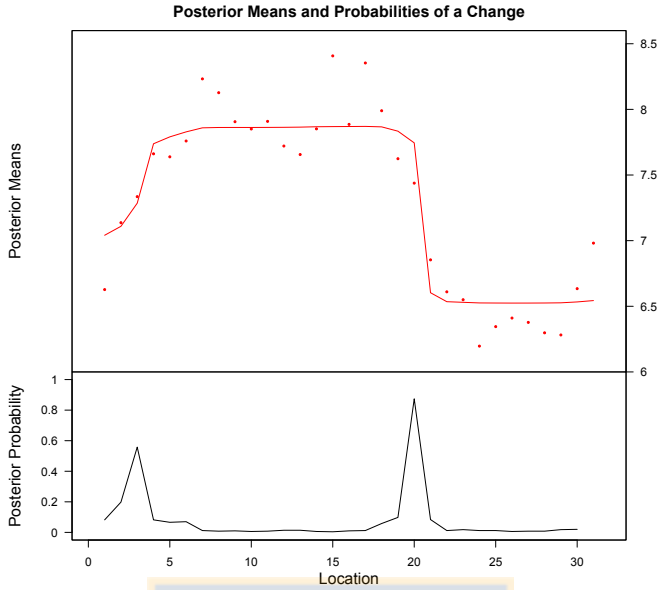

Figura 19: Probabilidad de encontrar un cambio régimen en el escenario (E5), en escala logarítmica. La grafica inferior representa la probabilidad posteriori de cambio de Barry and Hartigan's.

- ESCENARIO 6

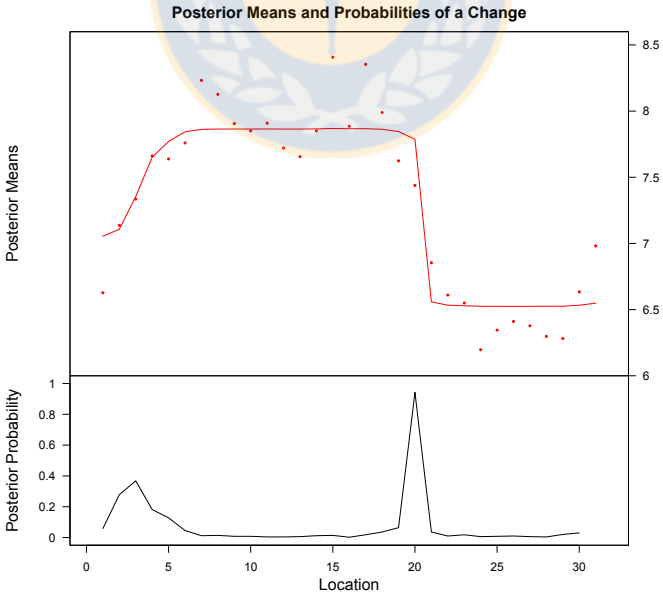

Figura 20: Probabilidad de encontrar un cambio régimen en el escenario (E6), en escala logarítmica. La grafica inferior representa la probabilidad posteriori de cambio de Barry and Hartigan's.

- ESCENARIO 7

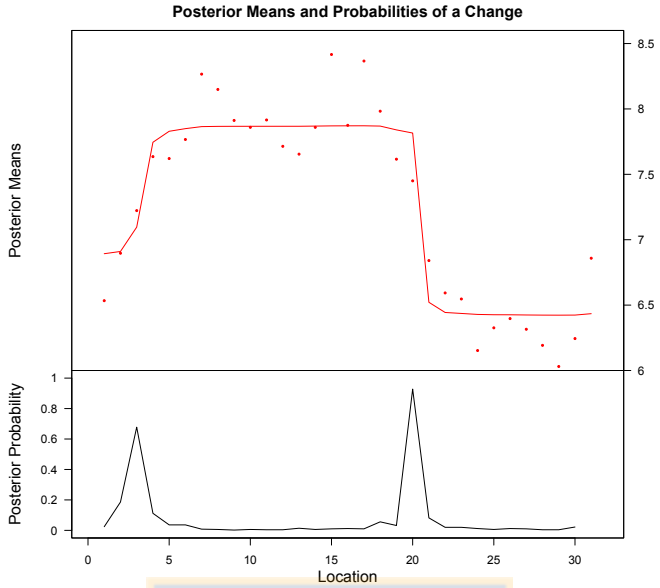

Figura 21: Probabilidad de encontrar un cambio régimen en el escenario (E7), en escala logarítmica. La grafica inferior representa la probabilidad posteriori de cambio de Barry and Hartigan's.

- ESCENARIO 8

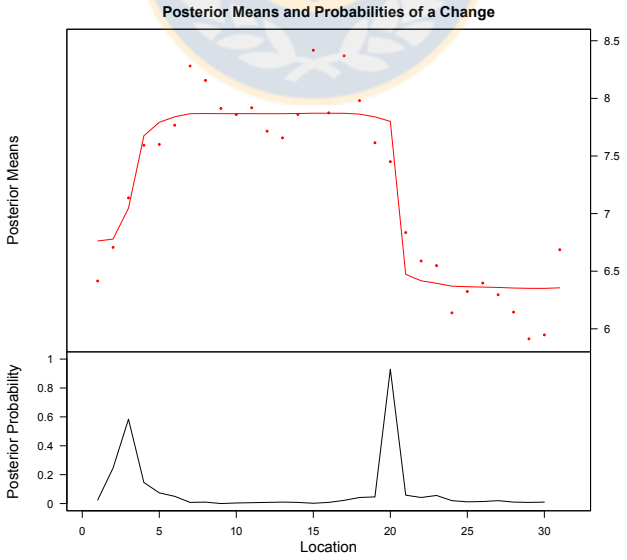

Figura 22: Probabilidad de encontrar un cambio régimen en el escenario (E8), en escala logarítmica. La grafica inferior representa la probabilidad posteriori de cambio de Barry and Hartigan's.

- ESCENARIO 9

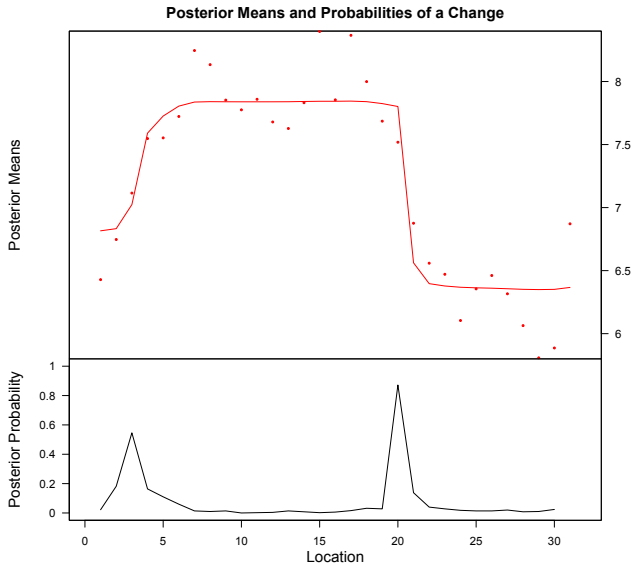

Figura 23: Probabilidad de encontrar un cambio régimen en el escenario (E9), en escala logarítmica. La grafica inferior representa la probabilidad posteriori de cambio de Barry and Hartigan's.

- ESCENARIO 10

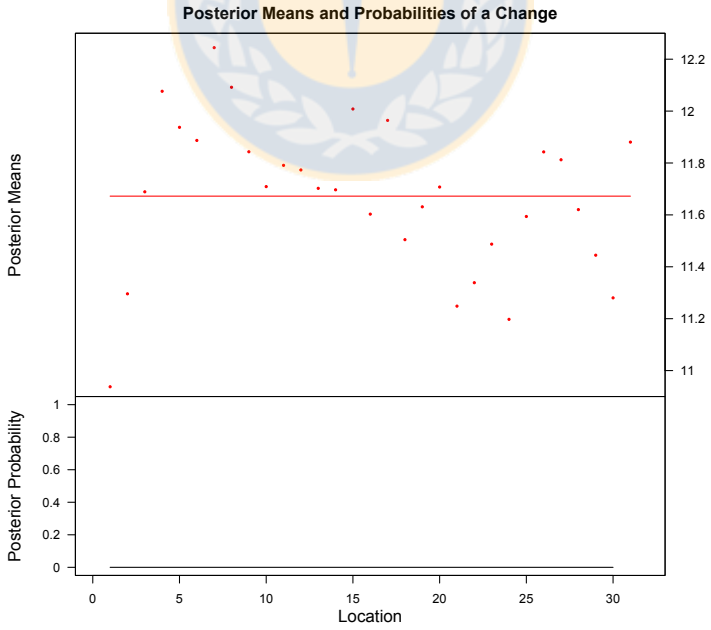

Figura 24: Probabilidad de encontrar un cambio régimen en el escenario (10), en escala logarítmica. La grafica inferior representa la probabilidad posteriori de cambio de Barry and Hartigan's.

- ESCENARIO 11

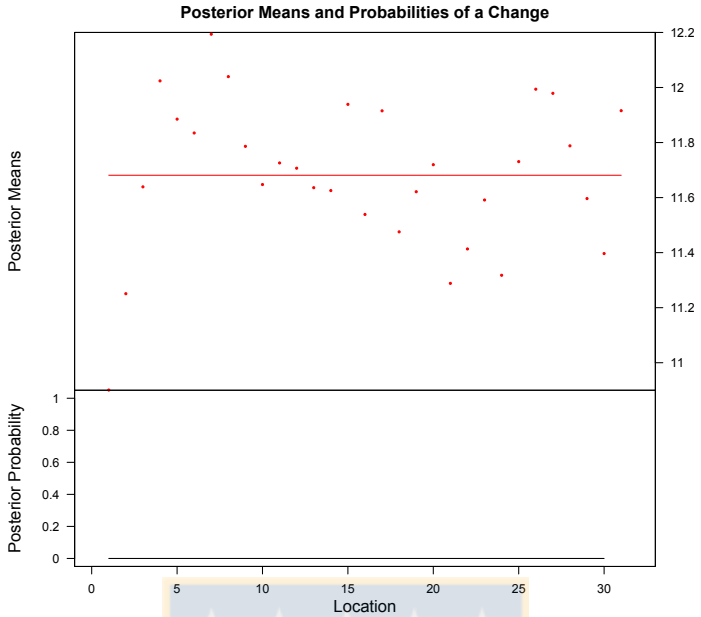

Figura 25: Probabilidad de encontrar un cambio régimen en el escenario (11), en escala logarítmica. La grafica inferior representa la probabilidad posteriori de cambio de Barry and Hartigan's.

- ESCENARIO 12

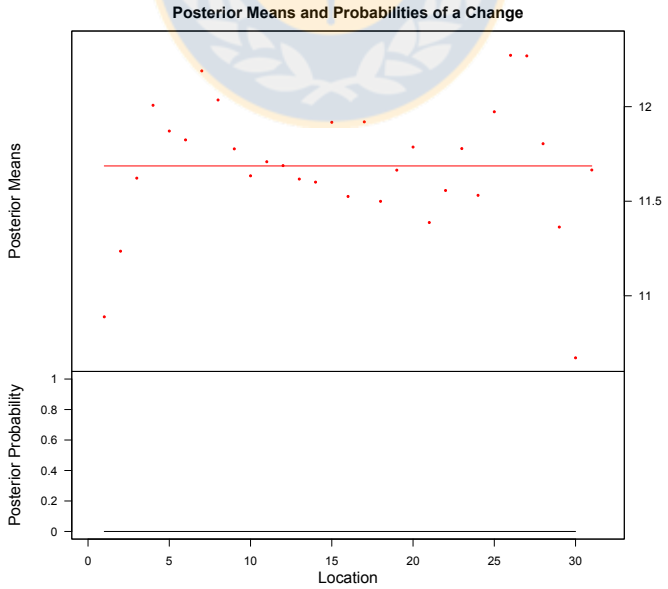

Figura 26: Probabilidad de encontrar un cambio régimen en el escenario (12), en escala logarítmica. La grafica inferior representa la probabilidad posteriori de cambio de Barry and Hartigan's.

ANEXO 2

Análisis de sensibilidad para indicadores en el modelo de evaluación de stock de merluza de cola (*Macrorunus magallanicus*)

Tabla 12: Escenario plausible de la Biomasa Hidroacustica de merluza de cola. Donde CPUEst es captura por unidad de esfuerzo de la pesquería arrastre sur austral, CPUEps pesquería de cerco centro-sur, HB Biomasa acústica y Yct captura zona centro sur (arrastre).

Escenario	HB_cv	CPUEst_cv	CPUEps_cv	Yps_cv	Yst_cv	Yct_cv
E1	0.05	0.4-0.3	0.1	0.05	0.05	0.05
E2	0.1	0.4-0.3	0.1	0.05	0.05	0.05
E3	0.15	0.4-0.3	0.1	0.05	0.05	0.05
E4	0.2	0.4-0.3	0.1	0.05	0.05	0.05
E5	0.3	0.4-0.3	0.1	0.05	0.05	0.05

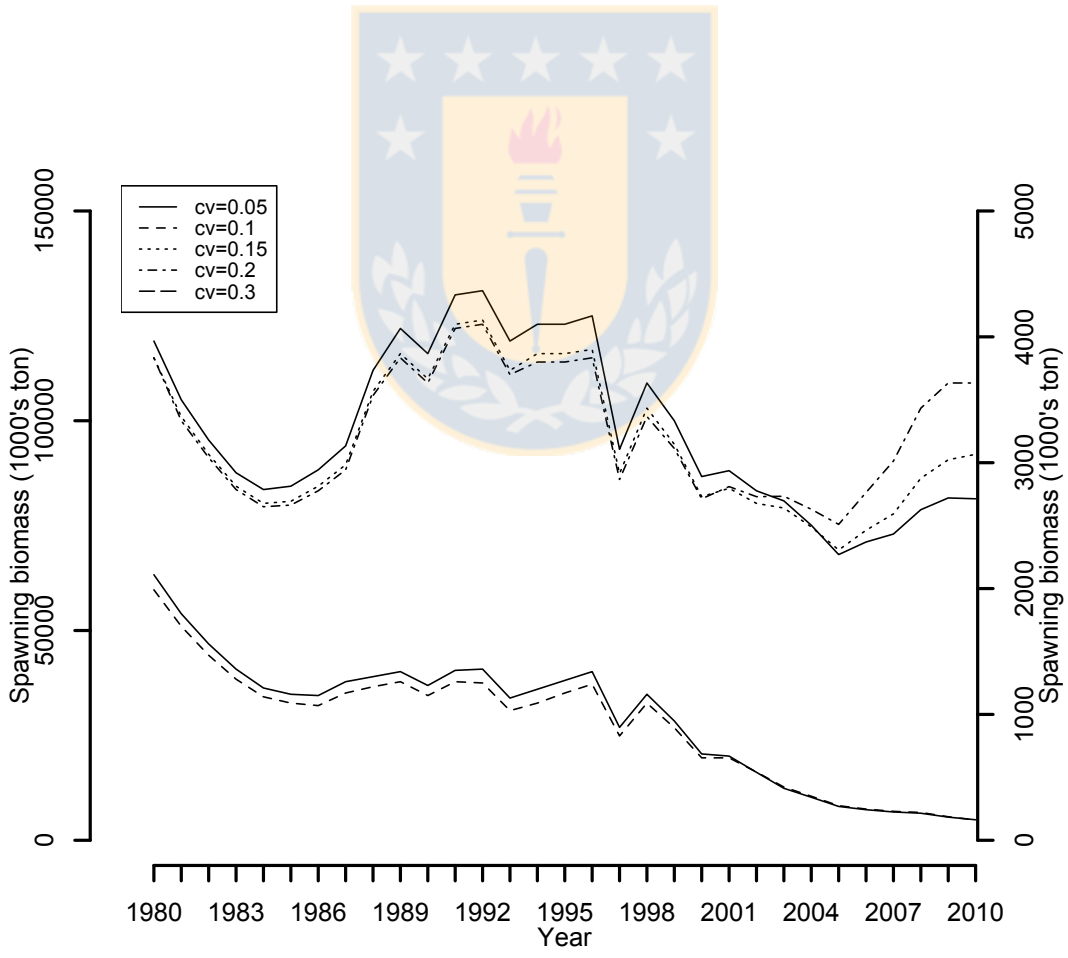

Figura 27: Variabilidad de la biomasa desovante (1000's de ton) de merluza de cola aplicando diferentes valores de coeficiente de variación en la biomasa hidroacústica

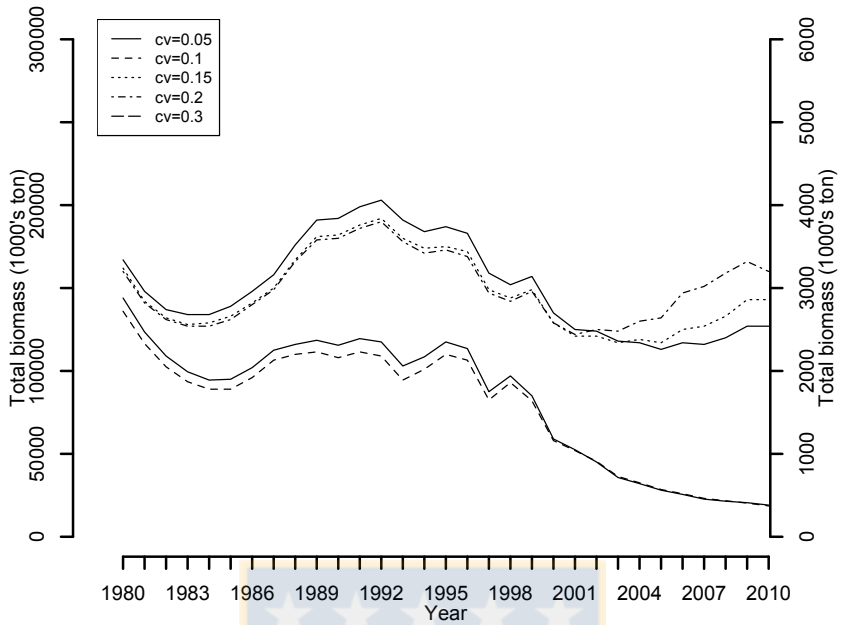

Figura 28: Variabilidad de la biomasa total (1000's ton) de merluza de cola aplicando diferentes valores de coeficiente de variación en la biomasa hidroacústica

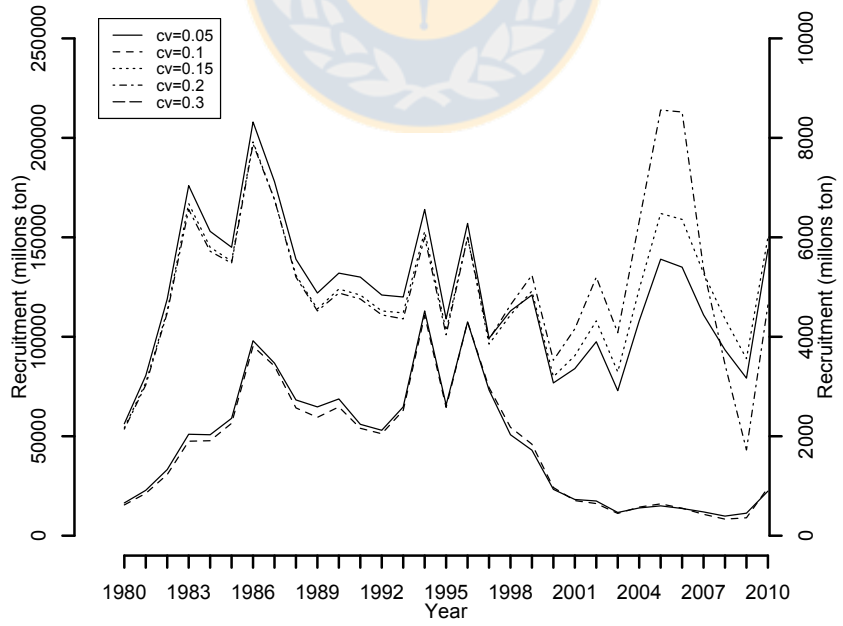

Figura 29: Variabilidad del reclutamientos (millones de ton) de merluza de cola aplicando diferentes valores de coeficiente de variación en la biomasa hidroacústica.

ANEXO 3

Modelo de Evaluación de merluza de cola (*Macrorunus magallanicus*)

Modelo de sobrevivencia

La pesquerías de merluza cola opera con tres flotas, la de cerco que pesca en la zona centro-sur (PS), la de arrastre que pesca en la zona centro sur (CT) y la de arrastre que pesca en la zona sur-austral (ST). Se supuso que las capturas ocurren instantáneamente y en forma secuencial a lo largo de un año. La primera captura en realizarse es la realizada por la flota CT en abril (t_1), y luego por la flota ST en septiembre (t_2) y finalmente por la flota PS en Noviembre (t_3). Por lo tanto el numero de sobrevivientes *N* se modeló como:

$$N_{a,t_1y} = N_{a,t_o,y}e^{-\frac{3}{12}M} \quad (22)$$

$$N_{a,t_2y} = N_{a,t_1,y}(1-\mu_{a,y}^{CT})e^{-\frac{5}{12}M} \quad (23)$$

$$N_{a,t_3y} = N_{a,t_2,y}(1-\mu_{a,y}^{ST})e^{-\frac{3}{12}M} \quad (24)$$

$$N_{a,t_4y} = N_{a,t_3,y}(1-\mu_{a,y}^{PS})e^{-\frac{1}{12}M} \quad (25)$$

La abundancia del grupo plus fue:

$$N_{z,t_4,y} = N_{z-1,t_3,y-1}\left(1-\mu_{z-1,y}^{PS}\right)e^{-\frac{1}{12}M} + N_{z,t_4,y-1} \quad (26)$$

donde N es la abundancia y μ es la tasa de explotación. La biomasa desovante fue expresada como:

$$S_t = \sum_a p_a w_a N_{a,t_3y} \quad (27)$$

donde p es la función de madurez y *w* es el peso promedio.

Selectividad

La selectividad de la pesquerias de arrastre en la zona sur austral fue modelada considerando dos modelos para dos periodos. Un modelo dome-shape que describe el patrón de explotación antes 1990, y un modelo logistico que describe los procesos entre 1991-2010. El modelo logistico fue expresada como:

$$S_{a,j(t),g} = \left(1 + exp\left[-\ln(19)\frac{a - A_{50,j(t),g}}{D_{1,j(t),g}}\right]\right)^{-1} \quad (28)$$

El modelo dome-shape considera la siguiente expression:

$$S_{a,j(t),g} = \begin{cases} exp\left[-0.5\left(\frac{a - A_{50,j(t),g}}{D_{1,j(t),g}}\right)^2\right], & a \leq A_{50,j(t),g} \\ exp\left[-0.5\left(\frac{a - A_{50,j(t),g}}{D_{2,j(t),g}}\right)^2\right], & a > A_{50,j(t),g} \end{cases} \quad (29)$$

donde A_{50} es la selectividad al 50% de madurez, D_1 es la pendiente de la parte ascendente de la curva de selectividad y D_2 es la parte descendiente.

Capturas

Las capturas *C*, fueron calculadas para cada flota (*f*) considerando el siguiente modelo:

$$C^f_{a,y} = \mu^f_{a,y} N_{a,t,y} \quad (30)$$

$$\mu^f_{a,y} = \mu^f_{a,y} S^f_a \quad (31)$$

$$\mu^f_y = \frac{Y^f_y}{BV^f_{t,y}} = \frac{Y^f_y}{\sum_a N_{a,t,y} S^f_a \bar{w}^f_{a,y/1e^{-6}}} \quad (32)$$

donde Y_y es la captura (tons) en años y, *S* es la selectividad, y $\bar{w}$ es el peso promedio en la captura ($\bar{w}^{ST}$ para las flotas de arrastre y w^{PS} para la flota de cerco).

Indice de abundancia basado en CPUE comercial

El índice en las tasas de capturas comerciales de las flotas de arrastre, I^T, fue estimado como:

$$I_y^T = q^T \sum_a N_{a,y}^{julio} S_{a,y}^T \overline{w}_{a,y}^{ST} \tag{33}$$

donde

S^T : La selectividad de las flotas de arrastre combinadas

N^{Julio} : La abundancia en julio fue calculada como:

$$N_{a,y}^{Julio} = \left[N_{a,t_o,y} e^{-\frac{3}{12}M}(1 - \mu_{a,y}^{CT})\right] e^{-\frac{3}{12}M} \tag{34}$$

q^T: Coeficiente de capturabilidad del arrastre estimado por máxima verosimilitud:

$$q^T = exp\left[\frac{1}{n^T}\sum_y ln\left(\frac{I_y^T}{\sum_a N_{a,y}^{julio} S_{a,y}^T \overline{w}_{a,y}^{ST}}\right)\right] \tag{35}$$

n^T : Numero de datos de I^T.

El índice de abundancia basado en las tasas de capturas de cerco, I^{PS} se estimaron como:

$$I_y^{PS} = q^{PS} \sum_a N_{a,t_3,y_{a,y}} S_a^{PS} \overline{w}_{a,y}^{PS} \tag{36}$$

$$q^{PS} = exp\left[\frac{1}{n^{PS}}\sum_y ln\left(\frac{I_y^{PS}}{\sum_a N_{a,t_3,y_{a,y}} S_{a,y}^{PS} \overline{w}_{a,y}^{PS}}\right)\right] \tag{37}$$

donde

$N_{a,t_3,y}$: Número al inicio de noviembre

S^{PS} : Selectividad de cerco

n^{PS} : Número de datos de I^{PS}

Indice de abundancia basado en la biomasa hidroacústica

El índice de biomasa basado en la biomasa estimada por hidroacústica realizadas en la zona principal de desove, I^{HB}, fue estimado como:

$$I_y^{HB} = q^{HB} \sum_a N_a^{Sept} S_a^{HB} \overline{w}_{a,y}^{ST} \tag{38}$$

$$q^{HB} = exp\left[\frac{1}{n^{HB}}\sum_y ln\left(\frac{I_y^{HB}}{\sum_a N_a^{sept} S_a^{HB} \overline{w}_{a,y}^{ST}}\right)\right] \tag{39}$$

donde

n^{HB} : Número de datos I^{HB}

S : Selectividad de hidroacústica fue modelada como una función logística

$$S_a^{HB} = \left[1 + e^{-\ln(19)\frac{a - a_{50\%}^{HB}}{\Delta f}}\right]^{-1} \quad (40)$$

$a_{50\%}^{HB}$: Parámetro de posición

Δf : Parámetro de dispersión

Ln de la verosimilitudes de las proporciones de tallas (o edades) en las capturas y abundancias.

Las proporciones de tallas (en capturas de cerco y en abundancia del área barrida en 1972) o la edad (en las capturas comerciales y en la abundancia acústica) contribuye al logaritmo natural de la verosimilitud como:

$$lnL = -0.5 \sum_{y=1}^{ny} \sum_{l=1}^{nl} ln\left[2\pi(\xi_{y,1} + \frac{0.1}{nl}\tau_y^2\right] + \sum_{y=1}^{ny} \sum_{l=1}^{nl} ln\left[exp\left\{\frac{-(\tilde{Q}3_{y,l} - Q3_{y,l})^2}{2(\xi_{y,l} + \frac{0.1}{nl})\tau_y^2}\right\}\right] \quad (41)$$

donde

$Q3_{y,l}$: Proporción de talla (o edad) observada *l* en el año *y*

$\widetilde{Q3}_{y,l}$: Proporción de talla (o edad) predicha *l* en el año *y*.

ny : Número de años.

nl : Número de datos de intervalos de tallas (o edades).

$\xi_{y,l}$: $(1 - \tilde{Q}3_{y,l})\tilde{Q}3_{y,l}$

τ_y^2 : 1/min(S_y, 1000)

S_y: tamaño de muestra del año *y*

ln de la verosimilitud de los indices de abundancia

Se parte del supuesto que los indices observados, Oy, son independientes, como una distribución log-normal con media ln(qEy) y coeficiente de variación conocido cy.

Aplicando la metodología de Bull et al (2002), el logaritmo de la verosimilitud es:

$$lnL = -0.5nln(2\pi) - \sum_{y=1}^{n} \ln(\sigma_y) - 0.5 \sum_{y=1}^{n} \left(\frac{\ln(O_y) - \ln(qE_y}{\sigma_y} + 0.5\sigma_y\right)^2 \quad (42)$$

donde $\sigma_y = \sqrt{\ln(1 + c_y^2}$ (43)

Penalizaciones

Las penalizaciones se usaron para asegurar que las selectividades de las flotas comerciales sobre la edad 1 fueran cercanas a cero. La ecuación ln de la verosimilitud esta dada por:

$$lnL = -0.5nkln(2\pi) - nkln(0.01) - 0.5\sum_{k=1}^{nk}\left(\frac{\ln(1)-\ln(1+S_{a=1}^{f})}{0.01}\right)^2 \quad (44)$$

donde *nk* fue el numero de parámetros penalizados.

Distribuciones a Priori

Las distribuciones a priori del parámetro *P* pudo presentar una distribución uniforme (*ln L=0*) o una distribución normal con media m_p y desviación estándar σ_p:

$$lnL = -0.5npln(2\pi) - \sum_{p=1}^{np}\ln(\sigma_p) - 0.5\sum_{p=1}^{np}\left(\frac{P_p-m_p}{\sigma_p}\right)^2 \quad (45)$$

donde np es el número de parámetros con distribuciones a priori.

La función total a maximizar

La función total a maximizar, LOSS fue la suma del logaritmo natural de todos los componentes de la verosimilitud:

$$LOSS = lnL_{Ca^{PS}} + lnL_{Ca^{ST}} + lnL_{Cl^{PS}} + lnL_{Ca^{CT}} + lnL_{HBa} + lnL_{I^{PS}} + lnL_{I^{T}} + lnL_{I^{HB}} + lnL_{I^{T}} + lnL_{SAl} + lnL_{I^{SA}} + lnL_{prior} + lnL_{penalties} \quad (46)$$

donde:

$lnL_{Ca^{PS}}$: ln L de la proporción de edades en las capturas de cerco

$lnL_{Ca^{ST}}$: ln L de la proporción de edades en las capturas de arrastre de la PDA

$lnL_{Cl^{PS}}$: ln L de la proporción de tallas en las capturas de cerco

$lnL_{Ca^{CT}}$: ln L de la proporción de edades en las capturas de arrastre de la PCS

lnL_{HBa} : ln L de la proporción de edades en la abundancia estimada por hidroacústica

$lnL_{I^{PS}}$: ln L del índice de abundancia basado en la CPUE de cerco

$lnL_{I^{T}}$: ln L del índice de abundancia basado en la CPUE de arrastre

$lnL_{I^{HA}}$: ln L de la biomasa acústica

lnL_{SAl} : ln L de la proporción de tallas en el área barrida de 1972

$lnL_{I^{SA}}$: ln L de la biomasa del área barrida de 1972

lnL_{prior} : ln L de las distribuciones a priori

$lnL_{penalties}$: ln L de las penalizaciones

ANEXO 4

Modelo Operativo (SAMR) de merluza de cola (*Macrorunus magallanicus*)

```
TOP_OF_MAIN_SECTION
arrmblsize=300000; //
gradient_structure::set_GRADSTACK_BUFFER_SIZE(30000000);
gradient_structure::set_CMPDIF_BUFFER_SIZE(50000000);
gradient_structure::set_MAX_NVAR_OFFSET(1000);
DATA_SECTION
int iseed
!!long int lseed=iseed;
!!CLASS random_number_generator rng(iseed);
init_int nyear
init_int nages
init_int nlength
init_matrix year_matrix(1,nyear,1,13)
init_vector ages(1,nages)
init_vector length2(1,nlength)
init_matrix Cps(1,nyear,1,nages)
init_matrix Cpsl(1,nyear,1,nlength)
init_matrix Cst(1,nyear,1,nages)
init_matrix Cct(1,nyear,1,nages)
init_matrix Chb(1,nyear,1,nages)
init_matrix Wmed(1,nyear,1,nages)
init_matrix Win(1,nyear,1,nages)
init_matrix Wps(1,nyear,1,nages)
!! ad_comm::change_datafile_name("MOM_op.ctl");
init_vector matur(1,nages);
init_number Bsa;
init_vector Csal(1,nlength);
init_vector nmus(1,6);
init_vector dt(1,3);
init_vector growth(1,2);
init_vector indSt(1,2);
init_vector indCt(1,2);
init_vector indSrv(1,2);
init_vector indq(1,2);
init_number Nyeq_ini; //  numbers of initial years on equilibrium condition
init_int    phase1;
init_int    phase2;
init_int    phase3;
init_int    phase4;
init_int    phase5;
init_int    phase6;
init_int    phase7;
init_int    phase8;
init_int    phase9;
init_int    phase10;
init_int    phase11;
init_int    phase12;
init_vector Mandh_pars(1,2);
init_vector cv_penal(1,6);
```

```
init_int SrType;
init_int SrErrProc;
init_int ErrObsType;
init_int nsimtmp;
//init_int numFst;
!! ad_comm::change_datafile_name("proyectaFs.ctl");
//init_int yr_sim
init_int nFt
init_vector mf(1,nFt)
number pi;
int opm; //activa el modelo operativo

INITIALIZATION_SECTION
//Some initial values
//log_Bo 8.45
log_Bo 8.45
log_qacus 0
log_A50ps 1.4
log_A50st 1.6
log_Dst 0
log_A50ct 1.6
log_Dct 0
Lo       29.8 //
cv       0.09
log_A50sa 0
log_Ssa 0
log_qsa -0.3567 // by default q=0.7
log_M -1.0498
log_h -0.2877

PARAMETER_SECTION

//Selectivity: acoustic and swept-area
init_bounded_vector log_A50hb(1,3,0,2.5,phase1)// acoustic logistic
init_bounded_vector log_Dhb(1,3,-2.3,1.3,phase1)
init_bounded_number log_A50sa(-2.3,0,phase1) // Swept-area  dome-shape
init_bounded_vector log_Ssa(1,2,-2.3,0.705,phase1)//

//Selectivity: purse-seine
init_bounded_number log_A50ps(0,1.38,phase1)  // dome-shape
init_bounded_vector log_Sps(1,2,-4.5,1.7,phase1)//

//Selectivity: trawl
init_bounded_vector log_A50st(1,3,1,2.5,phase1)//
init_bounded_vector log_Dst(1,4,-2.3,10.3,phase1)//
init_bounded_vector log_A50ct(1,3,1,2.5,phase1)//
init_bounded_vector log_Dct(1,3,-2.3,1.3,phase1)//

//Recruits
```

```
init_bounded_number log_Bo(4,12,phase2)
init_bounded_vector log_dev_Rt(1,nyear-1,-20,20,phase3)
init_bounded_vector log_dev_No(1,nages,-10,10,phase4)
init_bounded_number log_avgR1(2,20,phase2)  //reclutamiento promedio del primer periodo (1981-1998)
init_bounded_number log_PR2(-4,0,phase2)   //reclutamiento promedio del primer periodo (1999-2010)


//catchabilities
init_vector log_qst(1,3,phase6) // trawl
init_number log_qps(phase6) // purse-seine
init_number log_qacus(phase7) // acoustic
init_number log_qsa(phase8) // swept-area
vector qst(1,3)
number qps
number qacus
number qsa

//growth parameters
init_bounded_number Lo(1,100,phase9) // Mean length for first age-group
init_bounded_number cv(0.01,0.5,phase10) // cv

//M and h estimation
init_number log_M(phase11) //
init_number log_h(phase12) //

//mu40 en fase 3
//init_bounded_number mu40(0.01,0.5,3)
//number phi
//number spr40
//number sprpen
//matrix npr(1,2,1,nages)
//-------------------------------------------------
//Array definition
vector years(1,nyear)
vector Acous(1,nyear)
vector CPUEst(1,nyear)
vector CPUEps(1,nyear)
vector Yps(1,nyear)
vector Yst(1,nyear)
vector Yct(1,nyear)
vector Yps_pred(1,nyear)
vector Yst_pred(1,nyear)
vector Yct_pred(1,nyear)
vector min_N1(1,nyear)
vector min_N2(1,nyear)
vector min_N3(1,nyear)
vector sigma_age(1,nages)
vector mu_age(1,nages)
vector N1(1,nages)
```

vector N2(1,nages)
vector N3(1,nages)
vector N4(1,nages)
vector Neq(1,nages)
vector Ones_age(1,nages)
vector Ones_length(1,nlength)
vector Ones_yr(1,nyear)
vector ppred_sa(1,nlength)
vector pobs_sa(1,nlength)
sdreport_vector SSB(1,nyear)
sdreport_vector Biomass(1,nyear)
vector Bio_hb(1,nyear)
vector Bio_st(1,nyear)
vector Bio_ps(1,nyear)
vector Bio_ct(1,nyear)
sdreport_vector Recruits(1,nyear)
vector Rpred(1,nyear)
vector pred_Acous(1,nyear)
vector pred_CPUEps(1,nyear)
vector pred_CPUEst(1,nyear)
vector likeval(1,15);
vector penalty(1,10)
vector S_sa(1,nages)
vector N_sa(1,nages)
vector Bio_trw(1,nyear)
number So
number suma1
number suma2
number suma3
number suma4
number suma5
number alfa
number beta1
number beta2
number Bio_sa
sdreport_number log_Ro
number M;
number h;
number BPRo
number nn
number log_Rmed1
number log_Rmed2
number Prec
matrix S_ps(1,nyear,1,nages)
matrix S_st(1,nyear,1,nages)
matrix S_ct(1,nyear,1,nages)
matrix S_hb(1,nyear,1,nages)
matrix N(1,nyear,1,nages)
matrix N_st(1,nyear,1,nages)

```
matrix N_hb(1,nyear,1,nages)
matrix N_ps(1,nyear,1,nages)
matrix N_ssb(1,nyear,1,nages)
matrix mu_ct(1,nyear,1,nages)
matrix mu_st(1,nyear,1,nages)
matrix mu_ps(1,nyear,1,nages)
matrix Nj(1,nyear,1,nages)
matrix S_tot(1,nyear,1,nages)
matrix Cps_pred(1,nyear,1,nages)
matrix Cpsl_pred(1,nyear,1,nlength)
matrix Cst_pred(1,nyear,1,nages)
matrix Cct_pred(1,nyear,1,nages)
matrix pobs_ps(1,nyear,1,nages)
matrix pobs_st(1,nyear,1,nages)
matrix pobs_ct(1,nyear,1,nages)
matrix ppred_ps(1,nyear,1,nages)
matrix ppred_st(1,nyear,1,nages)
matrix ppred_ct(1,nyear,1,nages)
matrix pobs_hb(1,nyear,1,nages)
matrix ppred_hb(1,nyear,1,nages)
matrix pobs_psl(1,nyear,1,nlength)
matrix ppred_psl(1,nyear,1,nlength)
matrix P1(1,nages,1,nlength)
matrix P2(1,nages,1,nlength)
matrix P3(1,nages,1,nlength)
matrix p_age2length(1,nages,1,nlength)
vector cv1(1,nyear); //
vector cv2(1,nyear); //
vector cv3(1,nyear); //
vector cv4(1,nyear); //
vector cv5(1,nyear); //
vector cv6(1,nyear); //
vector sigma1(1,nyear);
vector sigma2(1,nyear);
vector sigma3(1,nyear);

//####### ACA SE ESPECIFICA LAS MATRICES, VECTORES Y NUMEROS DEL MOP en la fase de
proyeccion
vector Yps_fut(nyear+1,nyear+nsimtmp);
vector Yst_fut(nyear+1,nyear+nsimtmp);
vector Yct_fut(nyear+1,nyear+nsimtmp);
vector N2_fut(1,nages);
vector N3_fut(1,nages);
vector N4_fut(1,nages);
vector Biomass_fut(nyear+1,nyear+nsimtmp);
matrix N_fut(nyear+1,nyear+nsimtmp,1,nages);
vector SSB_fut(nyear+1,nyear+nsimtmp);
vector Bio_hb_fut(nyear+1,nyear+nsimtmp);
vector Bio_st_fut(nyear+1,nyear+nsimtmp);
```

```
vector Bio_ps_fut(nyear+1,nyear+nsimtmp);
vector Bio_ct_fut(nyear+1,nyear+nsimtmp);
vector Bio_trw_fut(nyear+1,nyear+nsimtmp);
vector acustica_epsilon(nyear+1,nyear+nsimtmp);
vector cpuest_epsilon(nyear+1,nyear+nsimtmp);
vector cpueps_epsilon(nyear+1,nyear+nsimtmp);
vector rec_epsilon(nyear+1,nyear+nsimtmp);
vector sim_Acous(nyear+1,nyear+nsimtmp);
vector sim_CPUEst(nyear+1,nyear+nsimtmp);
vector sim_CPUEps(nyear+1,nyear+nsimtmp);
vector yrs(nyear+1,nyear+nsimtmp);
matrix S_ps_fut(nyear+1,nyear+nsimtmp,1,nages);
matrix S_st_fut(nyear+1,nyear+nsimtmp,1,nages);
matrix S_ct_fut(nyear+1,nyear+nsimtmp,1,nages);
matrix S_hb_fut(nyear+1,nyear+nsimtmp,1,nages);
matrix N_hb_fut(nyear+1,nyear+nsimtmp,1,nages);
matrix mu_ct_fut(nyear+1,nyear+nsimtmp,1,nages);
matrix mu_st_fut(nyear+1,nyear+nsimtmp,1,nages);
matrix mu_ps_fut(nyear+1,nyear+nsimtmp,1,nages);
matrix Cps_pred_fut(nyear+1,nyear+nsimtmp,1,nages);
matrix Cst_pred_fut(nyear+1,nyear+nsimtmp,1,nages);
matrix Cct_pred_fut(nyear+1,nyear+nsimtmp,1,nages);
matrix Cpsl_pred_fut(nyear+1,nyear+nsimtmp,1,nlength);
matrix Win_fut(nyear+1,nyear+nsimtmp,1,nages);
matrix Wmed_fut(nyear+1,nyear+nsimtmp,1,nages);
matrix Wps_fut(nyear+1,nyear+nsimtmp,1,nages);
matrix Nj_fut(nyear+1,nyear+nsimtmp,1,nages);
matrix S_tot_fut(nyear+1,nyear+nsimtmp,1,nages);
matrix catch_fut(1,nFt,nyear+1,nyear+nsimtmp);

//Para la funcion de desempeño
matrix fut_Btot(1,nFt,nyear+1,nyear+nsimtmp);
matrix fut_SSBt(1,nFt,nyear+1,nyear+nsimtmp);
matrix fut_Rt(1,nFt,nyear+1,nyear+nsimtmp);
matrix fut_mups(1,nFt,nyear+1,nyear+nsimtmp);
matrix fut_muct(1,nFt,nyear+1,nyear+nsimtmp);
matrix fut_must(1,nFt,nyear+1,nyear+nsimtmp);
matrix fut_mutot(1,nFt,nyear+1,nyear+nsimtmp);
//Para guardar las estimaciones futuras del estimador
matrix keep_Btot(1,nFt,nyear+1,nyear+nsimtmp);
matrix keep_SSBt(1,nFt,nyear+1,nyear+nsimtmp);
matrix keep_Rt(1,nFt,nyear+1,nyear+nsimtmp);
matrix fut_Yps(1,nFt,nyear+1,nyear+nsimtmp);
matrix fut_Yct(1,nFt,nyear+1,nyear+nsimtmp);
matrix fut_Yst(1,nFt,nyear+1,nyear+nsimtmp);
matrix fut_Ytot(1,nFt,nyear+1,nyear+nsimtmp);
matrix keep_mups(1,nFt,nyear+1,nyear+nsimtmp);
matrix keep_muct(1,nFt,nyear+1,nyear+nsimtmp);
matrix keep_must(1,nFt,nyear+1,nyear+nsimtmp);
```

```
matrix keep_mutot(1,nFt,nyear+1,nyear+nsimtmp);

//proyeccion de un yr calculo de CTP
number Nplus; //Abundancia 1 yr despues
number mean_BDvp;
vector Nvp(1,nages)  //N sin explotacion
vector NDvp(1,nages); //Numero desovante en ausencia de pesca
matrix BDvp(1,nFt,nyear+1,nyear+nsimtmp);
matrix RPDdin(1,nFt,nyear+1,nyear+nsimtmp);
matrix RPDeqp(1,nFt,nyear+1,nyear+nsimtmp);
//matrix RPDeqm(nyear+1,nyear+yr_sim,1,nFt);
objective_function_value f

PRELIMINARY_CALCS_SECTION

years=column(year_matrix,1);// years
Acous=column(year_matrix,2);// acoustic
CPUEst=column(year_matrix,4); // CPUE trawl
CPUEps=column(year_matrix,6); // CPUE purse-seine
Yps=column(year_matrix,8); // Landings purse-seine
Yst=column(year_matrix,10);// Landings trawl
Yct=column(year_matrix,12);// Landings trawl, central zone

cv1=column(year_matrix,3);
cv2=column(year_matrix,5);
cv3=column(year_matrix,7);
cv4=column(year_matrix,9);
cv5=column(year_matrix,11);
cv6=column(year_matrix,13);
Ones_age=1;// ones vector (age size)
Ones_yr=1;// ones vector (year size)
Ones_length=1;// ones vector (length size)
M=Mandh_pars(1);
h=Mandh_pars(2);
pi = 3.141592653590;

PROCEDURE_SECTION

f=0;
Eval_selectivity();
Eval_mortality();
Eval_abundance();
Eval_age2length();
Eval_C_predicted();
Eval_stock_recruit();
Eval_indexes();
Eval_likelihood();

//LLAMA AL MODELO OPERATIVO
```

```
//if(last_phase()){Oper_model();}
if(mceval_phase())
{
Oper_model();
}

FUNCTION Oper_model

//Vectores de error de proceso y observacion para los indices:
dvector ran_rec(nyear+1,nyear+nsimtmp); //random para reclutamiento
dvector ran_acustica(nyear+1,nyear+nsimtmp); //random para cruceros acusticos
dvector ran_cpuest(nyear+1,nyear+nsimtmp);
dvector ran_cpueps(nyear+1,nyear+nsimtmp);
int yrfav; //year con un nuevo regimen favorable (elegido entre 2018 y 2022)
int upk; //actualiza los años
int l;
int k;
int numyear;
dvariable mupen=0.01;
simname = "esmeco.dat"; //nombre de los datos del estimador de ifop
dvector CatchNow(1,3); //para recibir las capturas del estimador
dvector eval_now(1,7); //son 7 los indicadores del estimador
//dvector p(1,nages); //vector proporcion de edades
//dvector freq(1,nages); //muestra de comp x edad
ofstream SaveOM("OPM_Out.csv",ios::app);


//Lectura del algoritmo
ran_rec.fill_randn(rng);
ran_acustica.fill_randn(rng);
ran_cpuest.fill_randn(rng);
ran_cpueps.fill_randn(rng);
yrfav=(int)round((46-38)*randu(rng)+38); //busca un salto aleatorio para un regimen favorable entre el yr
2025 y 2015 (5 years)
//Sigmas
dvariable sigma_acustica=cv1(nyear);
dvariable sigma_cpuest=cv2(nyear);
dvariable sigma_cpueps=cv3(nyear);
dvariable sigma_rec=cv_penal(2);

//corre el modelo esmeco para estimar las ctps iniciales q se leeran aqui como capturas
for(l=1;l<=nFt;l++) //por cada CTP
{
int rv=system("cp esmeco_real.dat esmeco.dat");
rv=system("./esmeco -nox -nohess");
//comienza el ciclo por cada una de las nFt CTPS
for(int i=nyear+1;i<=nyear+nsimtmp;i++)
{
//Error de observacionn de los indices
```

```
rec_epsilon(i)=(mfexp(ran_rec(i)*sigma_rec)); //desv. anual reclutamiento
acustica_epsilon(i)=(mfexp(ran_acustica(i)*sigma_acustica));
cpuest_epsilon(i)=(mfexp(ran_cpuest(i)*sigma_cpuest));
cpueps_epsilon(i)=(mfexp(ran_cpueps(i)*sigma_cpueps));

//Lee las Ctps
ifstream CTP_tmp("ctpmcol.dat");
CTP_tmp >> CatchNow;
CTP_tmp.close();
//Se usa 95% ya que se deja el 5% para investigación
catch_fut(l,i) = 0.95*CatchNow(l);
//Reparte la cuota entre pesquerias (70% V-X Región, y 30% X-XII)
Yps_fut(i)=0.01*catch_fut(l,i);
Yct_fut(i)=0.59*catch_fut(l,i);
Yst_fut(i)=0.4*catch_fut(l,i);
//Guarda las capturas por flota
fut_Yps(l,i)=Yps_fut(i);
fut_Yct(l,i)=Yct_fut(i);
fut_Yst(l,i)=Yst_fut(i);
fut_Ytot(l,i)=Yps_fut(i)+Yct_fut(i)+Yst_fut(i);

//cout << "catch_fut " << catch_fut(l,i)<<endl;exit(1);
//DINAMICA EN NUMERO DEL FUTURO (yrfut 1)
if(i==nyear+1)
{
//copia el peso inicial del último año en el peso inicial del futuro
//declarar la matriz Win_fut y Wmed_fut
Win_fut(i)=Win(nyear);
//cout<< "Win_fut "<< Win_fut <<endl;exit(1);


Wmed_fut(i)=Wmed(nyear);
Wps_fut(i)=Wps(nyear);
//cout<< "Wps_fut "<< Wps_fut <<endl;exit(1);

//copia selectividades del uñtimo año al futuro
S_ct_fut(i)=S_ct(nyear);
S_st_fut(i)=S_st(nyear);
S_ps_fut(i)=S_ps(nyear);
S_hb_fut(i)=S_hb(nyear);
S_tot_fut(i)=S_tot(nyear);
//cout<< "S_tot_fut "<< S_tot_fut <<endl;exit(1);

//Aqui considerar la sobrevivencia de 2010 al 2011
N_fut(i)(2,nages)=++N4(1,nages-1); //N4 desde la edad 1 hasta la n-1
//En ausencia de pesca
Nvp = N(nyear); //Copia la abundancia del ultimo anio
Nplus = Nvp(nages)*exp(-1.0*M);
Nvp(2,nages) = ++Nvp(1,nages-1)*exp(-1.0*M);
```

```
Nvp(nages) = Nvp(nages) + Nplus;// Grupo plus en ausencia de pesca
if(SrType==1)
{
//Relacion S-R regimen 1er con error de proceso (rec_epsilon)
if(SrErrProc==1)
{
N_fut(i,1)=SSB(nyear)/(alfa+beta2*SSB(nyear))*rec_epsilon(i);
Nvp(1)=N_fut(i,1);
}
else
{
N_fut(i,1)=SSB(nyear)/(alfa+beta2*SSB(nyear));
Nvp(1)=N_fut(i,1);
}
//Regimen bajo para el 1er year
}
else
{
//Trigonometrico
if(SrErrProc==1)
{
N_fut(i,1)=(mean(Recruits)+exp(7.150)*cos(pi*0.0662*double(i)-2.4838))*rec_epsilon(i);
Nvp(1)=N_fut(i,1);
}
else
{
N_fut(i,1)=mean(Recruits)+exp(7.150)*cos(pi*0.0662*double(i)-2.4838);
Nvp(1)=N_fut(i,1);
}
}

//Dinamica de la abundancia
Biomass_fut(i)=sum(elem_prod(N_fut(i),Win_fut(i)));
//Biomasa desovante sin pesca
NDvp=elem_prod(Nvp*exp(-0.67*M),matur);
BDvp(l,i)=sum(elem_prod(NDvp,Wmed_fut(i)));

//cout<< "N_fut "<< N_fut(i) <<endl;
//cout<< "B_fut "<< Biomass_fut(i) <<endl;exit(1);

N2_fut=N_fut(i)*exp(-dt(1)*M);
Bio_ct_fut(i)=sum(elem_prod(N2_fut,S_ct_fut(i)));
mu_ct_fut(i)=Yct_fut(i)/Bio_ct(i)*S_ct_fut(i);
Cct_pred_fut(i)=elem_prod(N2_fut,mu_ct_fut(i));
N3_fut=posfun(elem_prod(N2_fut,1-mu_ct_fut(i)),0.5,mupen);

Nj_fut(i)=N3_fut*exp(-0.25*M); //abundancia al 1 de julio
N2_fut=N3_fut*exp(-dt(2)*M); //sur
Bio_st_fut(i)=sum(elem_prod(elem_prod(N2_fut,S_st_fut(i)),Wmed_fut(i))+1E-10);
```

```
mu_st_fut(i)=Yst_fut(i)/Bio_st_fut(i)*S_st_fut(i);
Cst_pred_fut(i)=elem_prod(N2_fut,mu_st_fut(i));
N3_fut=posfun(elem_prod(N2_fut,1-mu_st_fut(i)),0.5,mupen);
N_hb_fut(i)=elem_prod(N3_fut,S_hb_fut(i));
Bio_hb_fut(i)=sum(elem_prod(N_hb_fut(i),Wmed_fut(i))+1E-10);
SSB_fut(i)=sum(elem_prod(elem_prod(N3_fut,matur),Wmed_fut(i))+1E-10);

N2_fut=N3_fut*exp(-dt(3)*M);
Bio_ps_fut(i)=sum(elem_prod(elem_prod(N2_fut,S_ps_fut(i)),Wps_fut(i))+1E-10);
mu_ps_fut(i)=Yps_fut(i)/Bio_ps_fut(i)*S_ps_fut(i);
Cps_pred_fut(i)=elem_prod(N2_fut,mu_ps_fut(i));
N3_fut=posfun(elem_prod(N2_fut,1-mu_ps_fut(i)),0.5,mupen);

N4_fut=N3_fut*exp(-(1.-sum(dt))*M);
N4_fut(nages)=N4_fut(nages)/(1-exp(-1.*M));

Bio_trw_fut(i)=sum(elem_prod(elem_prod(Nj_fut(i),Wmed_fut(i)),S_tot_fut(i)));

//Catch-at-length
Cpsl_pred_fut(i)=Cps_pred_fut(i)*p_age2length;
//cout<< "Cpsl_pred_fut "<< Bio_trw_fut(i) <<endl;exit(1);

//Simula los indices
if(ErrObsType==1)
{
//sin error de observacion
sim_Acous(i)=qacus*Bio_hb_fut(i);
if(Yps_fut(i)>0)
{
sim_CPUEps(i)=qps*Bio_ps_fut(i);
}
else
{
sim_CPUEps(i)=0;
}
sim_CPUEst(i)=qst(3)*Bio_trw_fut(i);
}
else
{
//Con error de observacion
sim_Acous(i)=qacus*Bio_hb_fut(i)*acustica_epsilon(i);
if(Yps_fut(i)>0)
{
sim_CPUEps(i)=qps*Bio_ps_fut(i)*cpueps_epsilon(i);
}
else
{
sim_CPUEps(i)=0;
}
```

```
sim_CPUEst(i)=qst(3)*Bio_trw_fut(i)*cpuest_epsilon(i);
}
//cout<<"SIM cpuest"<< sim_CPUEst(i)<<endl;exit(1);
yrs(i)=years(1)+double(i)-1;
upk=i;
numyear = i;
//AHORA ESCRIBE EN EL ARCHIVO *.dat DEL ESTIMADOR
ofstream simdata(simname);
simdata << "#num_yr" << endl;
simdata << numyear << endl;
simdata << "#num_edades"<<endl;
simdata << nages <<endl;
simdata << "#num_tallas"<<endl;
simdata << nlength << endl;
simdata << "#Data historica"<<endl;
simdata <<"#Yr  HB cv CPUEst cv CPUEps cv Yps cv Yst cv Yct cv "<<endl;
simdata << year_matrix <<endl;
simdata <<"#Data simulada futura"<<endl;
simdata <<"#Yr  HB cv CPUEst cv CPUEps cv Yps cv Yst cv Yct cv "<<endl;
for(k=nyear+1;k<=upk;k++)
{
simdata << yrs(k) << " " << sim_Acous(k) << " " << sigma_acustica << " " << sim_CPUEst(k) << " " <<
sigma_cpuest << " " << sim_CPUEps(k) << " " << sigma_cpueps << " " << Yps_fut(k) << " " << 0.05 << " "
<< Yst_fut(k) << " " << 0.05 << " " << Yct_fut(k) << " " << 0.05 << endl;
}
simdata <<"#edades"<<endl;
simdata << ages << endl;
simdata << "#tallas" << endl;
simdata << length2 << endl;
simdata << "#Captura a la edad Cerco"<<endl;
simdata << Cps << endl;
simdata << "#Captura a la edad cerco Simulado"<<endl;
for(k=nyear+1;k<=upk;k++)
{
simdata << Cps_pred_fut(k)<<endl;
}
simdata << "#Captura a la talla cerco "<<endl;
simdata << Cpsl <<endl;
simdata << "#Captura a la talla simulado"<<endl;
for(k=nyear+1;k<=upk;k++)
{
simdata << Cpsl_pred_fut(k) << endl;
}
simdata << "#Captura a la edad arrastre sur"<<endl;
simdata << Cst << endl;
simdata << "#Captura a la edad arrastre sur Simulado"<<endl;
for(k=nyear+1;k<=upk;k++)
{
simdata << Cst_pred_fut(k)<<endl;
```

```
}
simdata << "#Captura a la edad arrastre centro"<<endl;
simdata << Cct << endl;
simdata << "#Captura a la edad arrastre centro Simulado"<<endl;
for(k=nyear+1;k<=upk;k++)
{
simdata << Cct_pred_fut(k)<<endl;
}
simdata << "#Captura a la edad crucero"<<endl;
simdata << Chb << endl;
simdata << "#Captura a la edad crucero Simulado"<<endl;
for(k=nyear+1;k<=upk;k++)
{
simdata << qacus*N_hb_fut(k)<<endl;
}
simdata << "#Peso medio a la edad"<<endl;
simdata << Wmed << endl;
simdata << "#Peso medio sim"<<endl;
for(k=nyear+1;k<=upk;k++)
{
simdata << Wmed_fut(k) << endl;
}
simdata << "#Peso inicial a la edad"<<endl;
simdata << Win << endl;
simdata << "#Peso inicial sim"<<endl;
for(k=nyear+1;k<=upk;k++)
{
simdata << Win_fut(k) << endl;
}
simdata << "#Peso cerco a la edad"<<endl;
simdata << Wps << endl;
simdata << "#Peso cerco sim"<<endl;
for(k=nyear+1;k<=upk;k++)
{
simdata << Wps_fut(k) << endl;
}
//cout<<"N:"<<N(nyear)<<endl;
rv=system("./esmeco -nox -nohess");
//lee los indices de evaluacion actuales y los guarda para
//evaluar el desempeño
ifstream eval_indices("indices.dat");
eval_indices >> eval_now;
eval_indices.close();
//Guarda los indices del estimador
keep_Btot(l,i)=eval_now(1);
keep_SSBt(l,i)=eval_now(2);
keep_Rt(l,i)=eval_now(3);
keep_mups(l,i)=eval_now(4);
keep_muct(l,i)=eval_now(5);
```

```
keep_must(l,i)=eval_now(6);
keep_mutot(l,i)=eval_now(7);
//Guarda los indices del Mop
fut_Btot(l,i)=Biomass_fut(i);
fut_SSBt(l,i)=SSB_fut(i);
fut_Rt(l,i)=N_fut(i,1);
fut_mups(l,i)=max(mu_ps_fut(i));
fut_muct(l,i)=max(mu_ct_fut(i));
fut_must(l,i)=max(mu_st_fut(i));
fut_mutot(l,i)=fut_mups(l,i)+fut_muct(l,i)+fut_must(l,i);
}
else
{
//copia el peso inicial del último año en el peso inicial del futuro
//declarar la matriz Win_fut y Wmed_fut
Win_fut(i)=Win(nyear);
Wmed_fut(i)=Wmed(nyear);
Wps_fut(i)=Wps(nyear);
//copia selectividades del uñtimo año al futuro
S_ct_fut(i)=S_ct(nyear);
S_st_fut(i)=S_st(nyear);
S_ps_fut(i)=S_ps(nyear);
S_hb_fut(i)=S_hb(nyear);
S_tot_fut(i)=S_tot(nyear);

//Aqui considerar la sobrevivencia de 2010 al 2011
N_fut(i)(2,nages)=++N4_fut(1,nages-1); //N4 desde la edad 1 hasta la n-1
//En ausencia de pesca
Nvp = N_fut(i-1); //Copia la abundancia del ultimo anio proyectado
Nplus = Nvp(nages)*exp(-1.0*M);
Nvp(2,nages) = ++Nvp(1,nages-1)*exp(-1.0*M);
Nvp(nages) = Nvp(nages) + Nplus;// Grupo plus en ausencia de pesca
if(SrType==1)
{
//Relacion S-R regimen 1er con error de proceso (rec_epsilon)
if(SrErrProc==1)
{
if(i<=yrfav)
{
N_fut(i,1)=SSB_fut(i-1)/(alfa+beta2*SSB_fut(i-1))*rec_epsilon(i);      //desfavorable
Nvp(1)=N_fut(i,1);
}
else
{
N_fut(i,1)=SSB_fut(i-1)/(alfa+beta1*SSB_fut(i-1))*rec_epsilon(i);  //favorable
Nvp(1)=N_fut(i,1);
}
}
else
```

```
{
if(i<=yrfav)
{
N_fut(i,1)=SSB_fut(i-1)/(alfa+beta2*SSB_fut(i-1)); //desfavorable
Nvp(1)=N_fut(i,1);
}
else
{
N_fut(i,1)=SSB_fut(i-1)/(alfa+beta1*SSB_fut(i-1)); //favorable
Nvp(1)=N_fut(i,1);
}
}
//Regimen bajo para el 1er year
}
else
{
//Trigonometrico
if(SrErrProc==1)
{
N_fut(i,1)=(mean(Recruits)+exp(7.150)*cos(pi*0.0662*double(i)-2.4838))*rec_epsilon(i);
Nvp(1)=N_fut(i,1);
}
else
{
N_fut(i,1)=mean(Recruits)+exp(7.150)*cos(pi*0.0662*double(i)-2.4838);
Nvp(1)=N_fut(i,1);

}
}

//Dinamica de la abundancia
Biomass_fut(i)=sum(elem_prod(N_fut(i),Win_fut(i)));
//Biomasa desovante sin pesca
NDvp=elem_prod(Nvp*exp(-0.67*M),matur);
BDvp(l,i)=sum(elem_prod(NDvp,Wmed_fut(i)));


N2_fut=N_fut(i)*exp(-dt(1)*M);
Bio_ct_fut(i)=sum(elem_prod(N2_fut,S_ct_fut(i)));
mu_ct_fut(i)=Yct_fut(i)/Bio_ct(i)*S_ct_fut(i);
Cct_pred_fut(i)=elem_prod(N2_fut,mu_ct_fut(i));
N3_fut=posfun(elem_prod(N2_fut,1-mu_ct_fut(i)),0.5,mupen);

Nj_fut(i)=N3_fut*exp(-0.25*M);
N2_fut=N3_fut*exp(-dt(2)*M); //sur
Bio_st_fut(i)=sum(elem_prod(elem_prod(N2_fut,S_st_fut(i)),Wmed_fut(i))+1E-10);
mu_st_fut(i)=Yst_fut(i)/Bio_st_fut(i)*S_st_fut(i);
Cst_pred_fut(i)=elem_prod(N2_fut,mu_st_fut(i));
N3_fut=posfun(elem_prod(N2_fut,1-mu_st_fut(i)),0.5,mupen);
```

```
N_hb_fut(i)=elem_prod(N3_fut,S_hb_fut(i));
Bio_hb_fut(i)=sum(elem_prod(N_hb_fut(i),Wmed_fut(i))+1E-10);
SSB_fut(i)=sum(elem_prod(elem_prod(N3_fut,matur),Wmed_fut(i))+1E-10);

N2_fut=N3_fut*exp(-dt(3)*M);
Bio_ps_fut(i)=sum(elem_prod(elem_prod(N2_fut,S_ps_fut(i)),Wps_fut(i))+1E-10);
mu_ps_fut(i)=Yps_fut(i)/Bio_ps_fut(i)*S_ps_fut(i);
Cps_pred_fut(i)=elem_prod(N2_fut,mu_ps_fut(i));
N3_fut=posfun(elem_prod(N2_fut,1-mu_ps_fut(i)),0.5,mupen);

N4_fut=N3_fut*exp(-(1.-sum(dt))*M);
N4_fut(nages)=N4_fut(nages)/(1-exp(-1.*M));

Bio_trw_fut(i)=sum(elem_prod(elem_prod(Nj_fut(i),Wmed_fut(i)),S_tot_fut(i)));
//Catch-at-length
Cpsl_pred_fut(i)=Cps_pred_fut(i)*p_age2length;
//Simula los indices
if(ErrObsType==1)
{
//sin error de observacion
sim_Acous(i)=qacus*Bio_hb_fut(i);
if(Yps_fut(i)>0)
{
sim_CPUEps(i)=qps*Bio_ps_fut(i);
}
else
{
sim_CPUEps(i)=0;
}
sim_CPUEst(i)=qst(3)*Bio_trw_fut(i);
}
else
{
//Con error de observacion
sim_Acous(i)=qacus*Bio_hb_fut(i)*acustica_epsilon(i);
if(Yps_fut(i)>0)
{
sim_CPUEps(i)=qps*Bio_ps_fut(i)*cpueps_epsilon(i);
}
else
{
sim_CPUEps(i)=0;
}
sim_CPUEst(i)=qst(3)*Bio_trw_fut(i)*cpuest_epsilon(i);
}
yrs(i)=years(1)+i-1;
upk=i;
numyear = i;
//ESCRIBE EN EL ARCHIVO *.dat DEL ESTIMADOR
```

```
ofstream simdata(simname);
simdata << "#num_yr" << endl;
simdata << numyear << endl;
simdata << "#num_edades"<<endl;
simdata << nages <<endl;
simdata << "#num_tallas"<<endl;
simdata << nlength << endl;
simdata << "#Data historica"<<endl;
simdata <<"#Yr  HB cv CPUEst cv CPUEps cv Yps cv Yst cv Yct cv "<<endl;
simdata << year_matrix <<endl;
simdata <<"#Data simulada futura"<<endl;
simdata <<"#Yr  HB cv CPUEst cv CPUEps cv Yps cv Yst cv Yct cv "<<endl;
for(k=nyear+1;k<=upk;k++)
{
simdata << yrs(k) << " " << sim_Acous(k) << " " << sigma_acustica << " " << sim_CPUEst(k) << " " <<
sigma_cpuest << " " << sim_CPUEps(k) << " " << sigma_cpueps << " " << Yps_fut(k) << " " << 0.05 << " "
<< Yst_fut(k) << " " << 0.05 << " " << Yct_fut(k) << " " << 0.05 << endl;
}
simdata <<"#edades"<<endl;
simdata << ages << endl;
simdata << "#tallas" << endl;
simdata << length2 << endl;
simdata << "#Captura a la edad Cerco"<<endl;
simdata << Cps << endl;
simdata << "#Captura a la edad cerco Simulado"<<endl;
for(k=nyear+1;k<=upk;k++)
{
simdata << Cps_pred_fut(k)<<endl;
}
simdata << "#Captura a la talla cerco "<<endl;
simdata << Cpsl <<endl;
simdata << "#Captura a la talla simulado"<<endl;
for(k=nyear+1;k<=upk;k++)
{
simdata << Cpsl_pred_fut(k) << endl;
}
simdata << "#Captura a la edad arrastre sur"<<endl;
simdata << Cst << endl;
simdata << "#Captura a la edad arrastre sur Simulado"<<endl;
for(k=nyear+1;k<=upk;k++)
{
simdata << Cst_pred_fut(k)<<endl;
}
simdata << "#Captura a la edad arrastre centro"<<endl;
simdata << Cct << endl;
simdata << "#Captura a la edad arrastre centro Simulado"<<endl;
for(k=nyear+1;k<=upk;k++)
{
simdata << Cct_pred_fut(k)<<endl;
```

```
}
simdata << "#Captura a la edad crucero"<<endl;
simdata << Chb << endl;
simdata << "#Captura a la edad crucero Simulado"<<endl;
for(k=nyear+1;k<=upk;k++)
{
simdata << qacus*N_hb_fut(k)<<endl;
}
simdata << "#Peso medio a la edad"<<endl;
simdata << Wmed << endl;
simdata << "#Peso medio sim"<<endl;
for(k=nyear+1;k<=upk;k++)
{
simdata << Wmed_fut(k) << endl;
}
simdata << "#Peso inicial a la edad"<<endl;
simdata << Win << endl;
simdata << "#Peso inicial sim"<<endl;
for(k=nyear+1;k<=upk;k++)
{
simdata << Win_fut(k) << endl;
}
simdata << "#Peso cerco a la edad"<<endl;
simdata << Wps << endl;
simdata << "#Peso cerco sim"<<endl;
for(k=nyear+1;k<=upk;k++)
{
simdata << Wps_fut(k) << endl;
}
rv=system("./esmeco -nox -nohess");
ifstream eval_indices("indices.dat");
eval_indices >> eval_now;
eval_indices.close();
//Guarda los indices del estimador
keep_Btot(l,i)=eval_now(1);
keep_SSBt(l,i)=eval_now(2);
keep_Rt(l,i)=eval_now(3);
keep_mups(l,i)=eval_now(4);
keep_muct(l,i)=eval_now(5);
keep_must(l,i)=eval_now(6);
keep_mutot(l,i)=eval_now(7);
//Guarda los indices del Mop
fut_Btot(l,i)=Biomass_fut(i);
fut_SSBt(l,i)=SSB_fut(i);
fut_Rt(l,i)=N_fut(i,1);
fut_mups(l,i)=max(mu_ps_fut(i));
fut_muct(l,i)=max(mu_ct_fut(i));
fut_must(l,i)=max(mu_st_fut(i));
fut_mutot(l,i)=fut_mups(l,i)+fut_muct(l,i)+fut_must(l,i);
```

```
//cout << "==========fut_Btot:======"<< " "
//<< fut_Btot<<endl;
//cout << "keep_Btot:"<<keep_Btot<<endl;
}
//Variables de desempeño
//razon desovante potencial dinamica
//RPDdin(i,l)=fut_SSBt(i,l)/BDvp(i,l);
}
//cout << "fut_Btot:"<<fut_Btot<<endl;
//cout << "keep_Btot:"<<keep_Btot<<endl;exit(1);
}

RPDdin=elem_div(fut_SSBt,BDvp);
//Biomasa total futura modelo operante
byr_out<< fut_Btot <<endl;
syr_out<< fut_SSBt <<endl;
ryr_out<< fut_Rt << endl;
mps_out<< fut_mups<<endl;
mct_out<< fut_muct<<endl;
mst_out<< fut_must<<endl;
mt_out<< fut_mutot<<endl;//mt_out.close();
yps_out << fut_Yps<<endl;//yps_out.close();
yct_out << fut_Yct<<endl;//yct_out.close();
yst_out << fut_Yst<<endl;//yst_out.close();
ytot_out << fut_Ytot<<endl;//ytot_out.close();

//Biomasa total futura estimador
ebyr_out<< keep_Btot <<endl;//ebyr_out.close();
esyr_out<< keep_SSBt <<endl;//esyr_out.close();
eryr_out<< keep_Rt << endl;//eryr_out.close();
emps_out<< keep_mups<<endl;//emps_out.close();
emct_out<< keep_muct<<endl;//emct_out.close();
emst_out<< keep_must<<endl;//emst_out.close();
emt_out<< keep_mutot<<endl;//emt_out.close();
eytot_out << catch_fut <<endl;//eytot_out.close();

//Razon de potencial reproductivo dinamico
rpr_out << RPDdin <<endl;//rpr_out.close();
//Razon de potencial reproductivo estatico
rpr2_out << fut_SSBt/So <<endl;//rpr2_out.close();
yrfav_out << yrfav << endl;

/*
FUNCTION CTP_cal

ofstream ctp_out("ctpmcol.dat");
ofstream ssb_out("ssbmcol.dat");
ofstream rpr1_out("rpr1mcol.dat");
for (int j=1; j<=nFt; j++) // ciclo de multiplicadores de F
```

```
{
Np = N(nyear); //Abundancia en el ultimo anio
Nvp = N(nyear); //Abundancia en el ultimo anio en ausencia de pesca
Rp = mean(Recruits(nyear-5,nyear)); // Supuesto: reclutamiento constante igual al promedio de los ultimos 5
a√±os
wp = Wmed(nyear); //Pesos medio ultimo anio
Selp = S_tot(nyear); //Selectividad total en el ultimo anio con datos
mu_ref = 0.18*mf(j)*Selp; //Tasa de explotacion por edad Hay q multiplicar por mu de referencia (mu40)!!

for (int i=nyear+1; i<=nyear+yr_sim; i++)
{
Nplus = Np(nages)*(1-mu_ref(nages))*exp(-1.0*M); //a utilizar en grupo plus
Np(2,nages) = ++elem_prod(Np(1,nages-1),(1-mu_ref(1,nages-1)))*exp(-1.0*M);
Np(nages) += Np(nages) + Nplus;// Grupo plus
Np(1) = Rp;
NDp = elem_prod(elem_prod(Np*exp(-0.67*M),(1-mu_ref)),matur); //Abundancia desovante proyectada
BDp(i,j) = sum(elem_prod(NDp,wp));
Ctp = elem_prod(mu_ref,Np)*exp(-0.5*M); //captura numero
Yp = sum(elem_prod(Ctp,wp)); //Captura en peso
Yproy(i,j) = Yp;
Nplus = Nvp(nages)*exp(-1.0*M); //Nplus es re-utilizado en el grupo plus de abundancia en ausencia de
pesca
Nvp(2,nages) = ++Nvp(1,nages-1)*exp(-1.0*M);
Nvp(nages) = Nvp(nages) + Nplus;// Grupo plus en ausencia de pesca
Nvp(1) = Rp;
NDvp = elem_prod(Nvp*exp(-0.67*M),matur); //Abundancia desovante proyectada en ausencia de pesca
BDop(i,j) = sum(elem_prod(NDvp,wp));
}
}

//biomasa desovante y razones (varias) de potencial desovante
mean_BDop = mean(BDop);
RPDdin = elem_div(BDp,BDop); //dinamica
RPDmed = BDp/mean_BDop; //media
//RPDeqp = BDp/So; //de BDo F40%
//RPDeqm = BDp/; //de equilibrio modelo
ctp_out << Yproy << endl; ctp_out.close();
ssb_out << BDp << endl;ssb_out.close();
rpr1_out<< RPDdin << endl; rpr1_out.close();
*/
//FUNCTION MCWrite
//
//report3 << Biomass_fut << endl;
//report4 << SSB_fut << endl;
//report6 << Yst_fut << endl;

FUNCTION Eval_selectivity
int i;
for (i=1;i<=nyear;i++)
```

```
{
//Purse_seine
S_ps(i)=mfexp(-0.5/square(exp(log_Sps(1)))*square(-1.*(ages-exp(log_A50ps))));
for (int j=1;j<=nages;j++){
if(ages(j)>mfexp(log_A50ps)){
S_ps(i,j)=mfexp(-0.5/square(exp(log_Sps(2)))*square(-1.*(ages(j)-exp(log_A50ps))));}
}

//Trawling southern area
//domme or asymptotic at the begining, depending on the penalties
S_st(i)=mfexp(-0.5/square(exp(log_Dst(1)))*square(-1.*(ages-exp(log_A50st(1)))));
for (int j=1;j<=nages;j++){
if(ages(j)>mfexp(log_A50st(1))){
S_st(i,j)=mfexp(-0.5/square(exp(log_Dst(2)))*square(-1.*(ages(j)-exp(log_A50st(1)))));}}

//by year-block (3)
if (years(i)>=indSt(1))
{S_st(i)=(elem_div(Ones_age,(1+exp(-1.0*log(19)*(ages-exp(log_A50st(2)))/exp(log_Dst(3))))));}
if (years(i)>=indSt(2))
{S_st(i)=(elem_div(Ones_age,(1+exp(-1.0*log(19)*(ages-exp(log_A50st(3)))/exp(log_Dst(4))))));}

//Trawling central area
S_ct(i)=(elem_div(Ones_age,(1+exp(-1.0*log(19)*(ages-exp(log_A50ct(1)))/exp(log_Dct(1))))));
//by year-block (3)
if (years(i)>=indCt(1))
{S_ct(i)=(elem_div(Ones_age,(1+exp(-1.0*log(19)*(ages-exp(log_A50ct(2)))/exp(log_Dct(2))))));}
if (years(i)>=indCt(2))
{S_ct(i)=(elem_div(Ones_age,(1+exp(-1.0*log(19)*(ages-exp(log_A50ct(3)))/exp(log_Dct(3))))));}

//Acoustic
S_hb(i)=(elem_div(Ones_age,(1+exp(-1.0*log(19)*(ages-exp(log_A50hb(1)))/exp(log_Dhb(1))))));
//by year-block (3)
if (years(i)>=indSrv(1))
{S_hb(i)=(elem_div(Ones_age,(1+exp(-1.0*log(19)*(ages-exp(log_A50hb(2)))/exp(log_Dhb(2))))));}
if (years(i)>=indSrv(2))
{S_hb(i)=(elem_div(Ones_age,(1+exp(-1.0*log(19)*(ages-exp(log_A50hb(3)))/exp(log_Dhb(3))))));}
}

//Swept-area
S_sa=mfexp(-0.5/square(exp(log_Ssa(1)))*square(-1.*(ages-exp(log_A50sa))));

for (int j=1;j<=nages;j++){
if(ages(j)>mfexp(log_A50sa)){
S_sa(j)=mfexp(-0.5/square(exp(log_Ssa(2)))*square(-1.*(ages(j)-exp(log_A50sa))));}}

FUNCTION Eval_mortality

if(phase11>0){M=mfexp(log_M);}
if(phase12>0){h=mfexp(log_h);}
```

```
FUNCTION Eval_abundance
int i, j;

Neq(1)=1;
//BPRo estimation

for (j=2;j<=nages;j++)
{Neq(j)=Neq(j-1)*mfexp(-1*M);} // steady-state condition per recruit
Neq(nages)=Neq(nages)/(1-exp(-1*M)); // plus group
BPRo=sum(elem_prod(Neq,Win(1)));

//Ro estimation
log_Ro=log_Bo-log(BPRo);
log_Rmed1=log_avgR1;
Prec=exp(log_PR2);
log_Rmed2=log_PR2+log_avgR1;

//Abundance at the first year by age
Neq=Neq*mfexp(log_Ro);// steady-state as reference

if (phase4<0){
N(1)=Neq;}
else{
N(1)=mfexp(log(Neq)+log_dev_No-0.5*square(cv_penal(2)));}

//Recruitments by year starting in t=1
for (i=2;i<=20;i++){
N(i,1)=mfexp(log_Rmed1+log_dev_Rt(i-1)-0.5*square(cv_penal(3)));
}
for (i=21;i<=nyear;i++){
N(i,1)=mfexp(log_Rmed2+log_dev_Rt(i-1)-0.5*square(cv_penal(3)));
}

N_sa=elem_prod(S_sa,N(1));

//Abundance by seson within year
dvariable fpen=0.0;

Biomass(1)=sum(elem_prod(N(1),Win(1)));
N2=N(1)*exp(-dt(1)*M);// central

Bio_ct(1)=sum(elem_prod(elem_prod(N2,S_ct(1)),Wmed(1))+1E-10);//central
mu_ct(1)=Yct(1)/Bio_ct(1)*S_ct(1);
Cct_pred(1)=elem_prod(N2,mu_ct(1));
N3=posfun(elem_prod(N2,1-mu_ct(1)),0.5,fpen);// central
f+=10000*fpen;

fpen=0.0;
```

```
Nj(1)=N3*exp(-0.25*M);// It will be use for total CPUE
N2=N3*exp(-dt(2)*M);// southern
Bio_st(1)=sum(elem_prod(elem_prod(N2,S_st(1)),Wmed(1))+1E-10);
mu_st(1)=Yst(1)/Bio_st(1)*S_st(1);
Cst_pred(1)=elem_prod(N2,mu_st(1));
N3=posfun(elem_prod(N2,1-mu_st(1)),0.5,fpen);//
N_hb(1)=elem_prod(N3,S_hb(1));//
Bio_hb(1)=sum(elem_prod(N_hb(1),Wmed(1))+1E-10);
SSB(1)=sum(elem_prod(elem_prod(N3,matur),Wmed(1))+1E-10);
f+=10000*fpen;

fpen=0.0;

N2=N3*exp(-dt(3)*M);// purse-seine
Bio_ps(1)=sum(elem_prod(elem_prod(N2,S_ps(1)),Wps(1))+1E-10);
mu_ps(1)=Yps(1)/Bio_ps(1)*S_ps(1);
Cps_pred(1)=elem_prod(N2,mu_ps(1));
N3=posfun(elem_prod(N2,1-mu_ps(1)),0.5,fpen);// central

N4=N3*exp(-(1.-sum(dt))*M);// final
N4(nages)=N4(nages)/(1-exp(-1.*M));

f+=10000*fpen;
//Survival by year
for (i=1;i<nyear;i++){
dvariable fpen=0.0;
N(i+1)(2,nages)=++N4(1,nages-1);//
//N(i+1)(nages)+=N4(nages);
Biomass(i+1)=sum(elem_prod(N(i+1),Win(i+1)));
N2=N(i+1)*exp(-dt(1)*M);// central
Bio_ct(i+1)=sum(elem_prod(elem_prod(N2,S_ct(i+1)),Wmed(i+1))+1E-10);//central
mu_ct(i+1)=Yct(i+1)/Bio_ct(i+1)*S_ct(i+1);
Cct_pred(i+1)=elem_prod(N2,mu_ct(i+1));
N3=posfun(elem_prod(N2,1-mu_ct(i+1)),0.5,fpen);// central
f+=10000*fpen;
fpen=0.0;
Nj(i+1)=N3*exp(-0.25*M);// It will be use for total CPUE (in July)
N2=N3*exp(-dt(2)*M);// southern
Bio_st(i+1)=sum(elem_prod(elem_prod(N2,S_st(i+1)),Wmed(i+1))+1E-10);
mu_st(i+1)=Yst(i+1)/Bio_st(i+1)*S_st(i+1);
Cst_pred(i+1)=elem_prod(N2,mu_st(i+1));
N3=posfun(elem_prod(N2,1-mu_st(i+1)),0.5,fpen);// central
N_hb(i+1)=elem_prod(N3,S_hb(i+1));//
Bio_hb(i+1)=sum(elem_prod(N_hb(i+1),Wmed(i+1))+1E-10);
SSB(i+1)=sum(elem_prod(elem_prod(N3,matur),Wmed(i+1))+1E-10);
f+=10000*fpen;
fpen=0.0;
N2=N3*exp(-dt(3)*M);// purse-seine
```

```
Bio_ps(i+1)=sum(elem_prod(elem_prod(N2,S_ps(i+1)),Wps(i+1))+1E-10);
mu_ps(i+1)=Yps(i+1)/Bio_ps(i+1)*S_ps(i+1);
Cps_pred(i+1)=elem_prod(N2,mu_ps(i+1));
N3=posfun(elem_prod(N2,1-mu_ps(i+1)),0.5,fpen);// central
f+=10000*fpen;
N4=N3*exp(-(1.-sum(dt))*M);// final
N4(nages)=N4(nages)/(1-exp(-1.*M));
f+=10000*fpen;
}
S_tot=mu_ct+mu_ps+mu_st+1e-10;
for (i=1;i<=nyear;i++){
S_tot(i)=S_tot(i)/max(S_tot(i));}

Bio_trw=rowsum(elem_prod(elem_prod(Nj,Wmed),S_tot));

FUNCTION Eval_age2length
//
int i, j;
mu_age(1)=Lo;
for (i=2;i<=nages;i++){
mu_age(i)=growth(1)*(1-exp(-growth(2)))+exp(-growth(2))*mu_age(i-1);
}
sigma_age=cv*mu_age;

for (i=1;i<=nages;i++){
P1(i)=(length2-mu_age(i))/sigma_age(i);

for (j=2;j<=nlength;j++){
P2(i,j)=cumd_norm(P1(i,j));}}

for (i=1;i<=nages;i++){
for (j=2;j<=nlength;j++){
P3(i,j)=P2(i,j)-P2(i,j-1);}}



p_age2length=elem_div(P3+1e-16,outer_prod(rowsum(P3+1e-16),Ones_length));

FUNCTION Eval_C_predicted

//pred=predicted, obs=observed

//Catch-at-age and length
Cpsl_pred=Cps_pred*p_age2length;

//landings
Yps_pred=rowsum(elem_prod(Cps_pred,Wps));
Yst_pred=rowsum(elem_prod(Cst_pred,Wmed));
Yct_pred=rowsum(elem_prod(Cct_pred,Wmed));
```

```
//proprotions
pobs_ps=elem_div(Cps,outer_prod(rowsum(Cps+1e-10),Ones_age));
pobs_st=elem_div(Cst,outer_prod(rowsum(Cst+1e-10),Ones_age));
pobs_ct=elem_div(Cct,outer_prod(rowsum(Cct+1e-10),Ones_age));
pobs_psl=elem_div(Cpsl,outer_prod(rowsum(Cpsl+1e-10),Ones_length));

ppred_ps=elem_div(Cps_pred,outer_prod(rowsum(Cps_pred+1e-10),Ones_age));
ppred_st=elem_div(Cst_pred,outer_prod(rowsum(Cst_pred+1e-10),Ones_age));
ppred_ct=elem_div(Cct_pred,outer_prod(rowsum(Cct_pred+1e-10),Ones_age));
ppred_psl=elem_div(Cpsl_pred,outer_prod(rowsum(Cpsl_pred+1e-10),Ones_length));

pobs_hb=elem_div(Chb,outer_prod(rowsum(Chb+1e-10),Ones_age));
ppred_hb=elem_div(N_hb,outer_prod(rowsum(N_hb+1e-10),Ones_age));

ppred_sa=(N_sa*p_age2length)/sum(N_sa);
pobs_sa=Csal/sum(Csal);

FUNCTION Eval_stock_recruit

Recruits=column(N,1);
So=sum(elem_prod(elem_prod(Neq*exp(-0.67*M),matur),Wmed(1)));
//alfa=4*h*mfexp(log_Ro)/(5*h-1);
//beta=So*(1-h)/(5*h-1);
alfa=(1-h)*(So/mfexp(log_Rmed1))/(4*h);
beta1=(5*h-1)/(4*h*mfexp(log_Rmed1));
beta2=(5*h-1)/(4*h*mfexp(log_Rmed2));
Rpred(1)=mfexp(log_Rmed1);
for(int i=2;i<=20;i++){
Rpred(i)=SSB(i-1)/(alfa+beta1*SSB(i-1));
}
for(int i=21;i<=nyear;i++){
Rpred(i)=SSB(i-1)/(alfa+beta2*SSB(i-1));
}
//Rpred=elem_div(alfa*SSB,beta+SSB);

FUNCTION Eval_indexes

int i;
qacus=mfexp(log_qacus);
qps=mfexp(log_qps);
qst=mfexp(log_qst);
qsa=mfexp(log_qsa);

pred_Acous=qacus*Bio_hb;
pred_CPUEps=qps*Bio_ps;
pred_CPUEst=qst(1)*Bio_trw;
Bio_sa=qsa*sum(elem_prod(N_sa,Win(1)));// Swept-area
```

```
for (i=1;i<=nyear;i++)
{
if (years(i)>=indq(1)){
pred_CPUEst(i)=qst(2)*Bio_trw(i);}

if (years(i)>=indq(2)){
pred_CPUEst(i)=qst(3)*Bio_trw(i);}
}

FUNCTION Eval_likelihood
int i;

suma1=0; suma2=0; suma3=0; suma4=0;

for (i=2;i<=nyear;i++)
{
if (Acous(i)>0){
suma1+=square((log(Acous(i))-log(pred_Acous(i)))/cv1(i));}
if (CPUEst(i)>0){
suma2+=square((log(CPUEst(i))-log(pred_CPUEst(i)))/cv2(i));}
if (CPUEps(i)>0){
suma3+=square((log(CPUEps(i))-log(pred_CPUEps(i)))/cv3(i));}
if(i>=Nyeq_ini){
suma4+=square(log(Rpred(i-1))-log(Recruits(i)));} // Recruits
}
likeval(1)=0.5*suma1;//survey
likeval(2)=0.5*suma2;//cpue_st
likeval(3)=0.5*suma3;//cpue_ps

//multinomial
likeval(7)=-nmus(1)*sum(elem_prod(pobs_ps,log(ppred_ps)));
likeval(8)=-nmus(2)*sum(elem_prod(pobs_st,log(ppred_st)));
likeval(9)=-nmus(3)*sum(elem_prod(pobs_ct,log(ppred_ct)));
likeval(10)=-nmus(4)*sum(elem_prod(pobs_hb,log(ppred_hb)));
likeval(11)=-nmus(5)*sum(elem_prod(pobs_psl,log(ppred_psl)));
likeval(12)=-nmus(6)*sum(elem_prod(pobs_sa,log(ppred_sa)));

//penalties
//lognormal Ninicial y Reclutas
penalty(1)=0.5*norm2(log_dev_No)/square(cv_penal(1));
penalty(2)=0.5*suma4/square(cv_penal(2)); // Rpred
penalty(3)=0.5*norm2(log_dev_Rt(1,Nyeq_ini))/square(cv_penal(3));
penalty(4)=0.5*square((log_M-log(Mandh_pars(1)))/cv_penal(4));
penalty(5)=0.5*square((log_h-log(Mandh_pars(2)))/cv_penal(5));
penalty(6)=0.5*square((log_Dst(2)-log(nages)-log_A50st(1))/cv_penal(6));

f+=sum(likeval)+sum(penalty); //+sprpen;

REPORT_SECTION
```

rep(years)
rep(Yst)
rep(Yst_pred)
rep(Yct)
rep(Yct_pred)
rep(Yps)
rep(Yps_pred)
rep(Acous)
rep(pred_Acous)
rep(CPUEst)
rep(pred_CPUEst)
rep(CPUEps)
rep(pred_CPUEps)
rep(SSB)
rep(Biomass)
rep(Recruits)
rep(Rpred)
rep(N)
rep(mu_ps)
rep(mu_st)
rep(mu_ct)
rep(pobs_st)
rep(ppred_st)
rep(pobs_ct)
rep(ppred_ct)
rep(pobs_ps)
rep(ppred_ps)
rep(pobs_hb)
rep(ppred_hb)
rep(Bio_sa)
rep(p_age2length)
rep(pobs_psl)
rep(ppred_psl)
rep(S_st)
rep(S_ct)
rep(S_ps)
rep(S_hb)
rep(S_sa)
rep(pobs_sa)
rep(ppred_sa)
rep(likeval)
rep(penalty)
rep(BPRo)
rep(h)
rep(M)
rep(alfa)
rep(beta1)
rep(beta2)

```
rep(exp(log_qacus))
rep(sum(likeval))
//rep(mu40)

GLOBALS_SECTION
//const double pi = 3.141592654;
#include <admodel.h>
#include <time.h>
#include <string.h>
adstring simname;

//ESCRIBE ARCHIVOS DE SALIDA DEL MOP
ofstream byr_out("byr_mcmc_op",ios::app);
ofstream syr_out("syr_mcmc_op",ios::app);
ofstream ryr_out("ryr_mcmc_op",ios::app);
ofstream mps_out("mps_mcmc_op",ios::app);
ofstream mct_out("mct_mcmc_op",ios::app);
ofstream mst_out("mst_mcmc_op",ios::app);
ofstream mt_out("mtot_mcmc_op",ios::app);
ofstream yps_out("yps_mcmc_op",ios::app);
ofstream yct_out("yct_mcmc_op",ios::app);
ofstream yst_out("yst_mcmc_op",ios::app);
ofstream ytot_out("ytot_mcmc_op",ios::app);

//ESCRIBE ARCHIVOS DE SALIDA DEL ESTIMADOR
ofstream ebyr_out("byr_mcmc_es",ios::app);
ofstream esyr_out("syr_mcmc_es",ios::app);
ofstream eryr_out("ryr_mcmc_es",ios::app);
ofstream emps_out("mps_mcmc_es",ios::app);
ofstream emct_out("mct_mcmc_es",ios::app);
ofstream emst_out("mst_mcmc_es",ios::app);
ofstream emt_out("mtot_mcmc_es",ios::app);
//ofstream eyps_out("myps_mcmc_es");
//ofstream eyct_out("myct_mcmc_es");
//ofstream eyst_out("myst_mcmc_es");
ofstream eytot_out("mytot_mcmc_es",ios::app);
//Razon de potencial reproductivo dinamico
ofstream rpr_out("rpr_mcmc",ios::app);
//Razon de potencial reproductivo estatico
ofstream rpr2_out("rpr2_mcmc",ios::app);
ofstream yrfav_out("yrfav_mcmc",ios::app);

#undef rep
#define rep(object) report << #object "\n" << object << endl;

#undef depur
#define depur(object) cout << #object "\n" << object << endl; exit(1);
```